VULNERABILITY OF URBAN PUBLIC SUPPLY WELLS IN FRACTURED SILICICLASTIC AQUIFER SYSTEMS

By

Christopher Allan Gellasch

A dissertation submitted in partial fulfillment of

the requirements for the degree of

Doctor of Philosophy

(Geology)

at the

UNIVERSITY OF WISCONSIN-MADISON

2012

Date of final oral examination: 8/7/12

The dissertation is approved by the following members of the Final Oral Committee:

Jean M. Bahr, Professor, Geoscience
Herbert F. Wang, Professor, Geoscience
Kenneth R. Bradbury, Professor, University of Wisconsin-Extension (WGNHS)
Gregory W. Harrington, Professor, Civil and Environmental Engineering
Steven P. Loheide II, Associate Professor, Civil and Environmental Engineering
Mary P. Anderson, Emeritus Professor, Geoscience

Abstract

Approximately one third of the U.S. population uses public supply wells (PSWs) as their drinking water source and recently a greater focus has been placed on assessing the risk of contaminants entering PSWs. Among the many contaminants of concern are chemical and microbiological indicators of wastewater contamination. This research project used a variety of field methods to better understand the primary mechanisms that control the transport of human enteric viruses and other wastewater contaminants in bedrock multi-aquifer systems and to develop effective methods for assessing the vulnerability of PSWs in such settings.

At a field site in Madison, WI, borehole investigations suggest that fractures in siliclastic bedrock are important transport pathways from the surface to the deep aquifer. Some fractured intervals have transmissivity values several orders of magnitude higher than non-fractured intervals. In a siliciclastic aquifer near a public supply well, fractures may have an important role in the transport of sewer-derived wastewater contaminants. Reverse water-level fluctuations (RWFs), a phenomenon in which water levels rise briefly in response to pumping, were detected in monitoring wells. Data from pressure transducers located at varying depths and distances from a PSW suggest that the RWFs propagate rapidly through fractures to influence wells hundreds of meters from the pumping well. The rate and cycling frequency of pumping is an important factor in the magnitude of RWFs. The pattern of RWF propagation can be used to better define fracture connectivity in an aquifer system.

Time sequenced sampling for geochemical wastewater indicators and human enteric viruses is a useful tool for characterizing transport within an aquifer system. There is an apparent connection between recharge events and increased flow in sanitary sewers and, based on limited data, these increased wastewater flows appear linked with virus detection in groundwater at short times after these events. In order to accurately assess the vulnerability of PSWs to near surface contaminants it is important to characterize fracture flow and the impact of PSW pumping. The use of RWFs to determine fracture connectivity is an important method to accomplish this goal.

Acknowledgements

I want to thank my advisor, Professor Jean Bahr, for all of her assistance. Her patience, wisdom, and mentorship have been invaluable. I am also grateful to the other members of my committee, Professors Ken Bradbury, Herb Wang, Steve Loheide, Mary Anderson, and Greg Harrington for their contributions to this endeavor. Their guidance during the planning, execution, and writing stages were critical to the success of this project. Among this group Ken Bradbury deserves special thanks for his guidance, assistance, and enthusiasm.

This research was funded by an Army Research Office Short Term Innovative Research (STIR) grant and an U.S. Environmental Protection Agency Science to Achieve Results (STAR) grant. The Rocky Mountain Association of Geologists provided additional research support through the Veterans Memorial Scholarship Fund. The U.S. Army Long Term Health and Education program allowed me to spend three years in graduate school while I remained on active duty.

Many other students were also instrumental in the completion of this project. Thank you to all of the members of Professor Bahr's 2011 Hydrogeology Field Methods course that took part in the pumping test at the field site. Thank you to all of my fellow graduate students in the Department of Geoscience that provided encouragement, advice, assistance and friendship. My undergraduate assistant, Lauren Lande, provided enthusiasm, hard work, and a willingness to learn while conducting some of the less glamorous tasks related to field work and data analysis. Thank you to the homeowners that allowed me to place pressure transducers in their basement wells.

The employees at the Wisconsin Geological and Natural History Survey played a substantial role in the completion of my project. Dr. David Hart and Madeline Gotkowitz provided advice and guidance regarding many aspects field work. Peter Chase was my all around resource for field methods and was critical in the design, construction, and deployment of the light weight straddle packer. Jacob Krause was a tireless field assistant during many rounds of sampling and I appreciated his suggestions to improve sampling methods.

Dr. Mark Borchardt and Susan Spencer of the U.S. Department of Agriculture laboratory in Marshfield, Wisconsin provided invaluable assistance on virus sampling procedures and quickly analyzed all virus samples. Professor E. Calvin Alexander of the University of Minnesota analyzed all water chemistry samples and provided useful feedback. Joe Demorett was my main point of contact at the Madison Water Utility and provided valuable data on Unit Well 7. David Taylor at the Madison Metropolitan Sewerage District was responsible for coordination for wastewater collection and providing data related to sewer flows and chemistry of wastewater.

My wife and best friend, Amy, was always there to take care of our son and me when I was wrapped up with field sampling, writing, or other portions of my research. She worked tirelessly to ensure I was able to focus on the task at hand and maintained a positive attitude. My son, Brian, was always understanding and gave me plenty of hugs when I was too busy working to play with him.

Table of Contents

Abstract i
Acknowledgements iii
Table of Contents v
List of Figures viii
List of Tables x
Accompanying Material xi
Chapter 1. Introduction 1
1. Background 1
    1.1. Public water supply vulnerability to contamination 1
    1.2. Sewer exfiltration as a source of contamination 3
    1.3. Human enteric virus sampling and detection 4
    1.4. Viral Decay Rates 6
    1.5. Transport pathways and velocities 10
2. Public supply well vulnerability in Madison, Wisconsin 13
    2.1. Viruses in Madison Public Supply Wells 14
    2.2. Source of contamination in the Madison area 16
3. Research Objectives 17
4. Introduction to the Dissertation 21
Chapter 2. Characterization of fracture connectivity in a siliciclastic bedrock aquifer near a public supply well 23
1. Introduction 23
2. Background 26
    2.1. Location 26
    2.2. Stratigraphy and geologic setting 27
    2.3. Installation of monitoring wells 29
    2.4. Motivation and initial work 32
3. Methods and Results 34

3.1. Borehole logging and fracture identification 34
3.2. Packer slug tests 37
3.3. Borehole pumping test 40
3.4. Vertical Flow Assessment 41
3.5. Conceptual model for fracture connectivity 43
3.6. Evaluation of hydrogeological properties 47
3.7. Comparison of groundwater chemistry between fractures 52
4. Discussion 58
5. Conclusion 61
Chapter 3. Pumping induced reverse water-level fluctuations in a fractured siliciclastic aquifer system 64
1. Introduction 64
2. Methods and Results 70
2.1. Initial RWF observations 70
2.2. Subsequent site changes 72
3. Discussion 76
3.1. Mechanisms for RWF propagation 76
3.2. Water level changes prior to RWFs 83
3.3. Evaluation of unit well annulus as a preferential flow pathway 85
3.4. Effect of pumping rate and amplitude on RWF magnitude and duration 86
4. Summary and Conclusion 88
Chapter 4. Use of groundwater geochemistry and human enteric virus detection to characterize transport in a fractured siliciclastic aquifer 90
1. Introduction 90
2. Methods 93
2.1. Strategy 93
2.2. Sampling methods 95
2.3. Initial 2010 and 2011 sampling 97
2.4. 2012 sampling 100
3. Results 101

3.1. Virus results 101
3.2. Water chemistry results 105
3.3. Coliform bacteria and E. coli results 110
4. Discussion 111
4.1. Precipitation, sewer flow, and virus detection 111
4.2. 2010 data comparison 111
4.3. 2011 snowmelt 113
4.4. 2012 data comparison 114
4.5. Trends in virus detection (spatial and temporal) 115
4.6. Water chemistry trends 118
4.7. Link between water chemistry and virus detection 120
4.8. Geochemical evidence for connection between aquifers 121
4.9. Conceptual model 125
5. Conclusions 128
Chapter 5. Conclusions 131
1. Conclusions 131
2. Significance 137
3. Future Research Needs 141
3.1. Unsaturated zone transport 141
3.2. Evaluation of RWF duration 141
3.3. Numerical fracture flow modeling 142
3.4. Long term virus sampling 143
References 144
Appendix A: Well drilling logs 152
Appendix B: Standard operating procedure for the light weight straddle packer 157
Appendix C: Pumping test data 161
Appendix D: Groundwater sampling standard operating procedures 168
Appendix E: Geochemistry data 173

List of Figures

Figure 1.1. Virus decay rates from reviewed studies, averaged by temperature group... 9

Figure 1.2. Microscopic flow paths in an aquifer can significantly increase average flow path length and flow velocity. 11

Figure 1.3. Normal distribution of groundwater flow velocities in a homogeneous aquifer highlighting the existence of rapid, statistically extreme velocities 12

Figure 1.4. Predicted capture zone for flow in the Mount Simon aquifer at Madison Unit Well 7. 19

Figure 2.1. Study area location. 27

Figure 2.2. Study area stratigraphy 29

Figure 2.3. Cross section of field site with location of monitoring wells with respect to the unit well. 31

Figure 2.4. Selected borehole logging data from MW-C..... 35

Figure 2.5. Summary of downhole logging methods that indicated potential fractures in borehole MW-C. 37

Figure 2.6. Flow characterization results from borehole MW-C..... 39

Figure 2.7. Conceptual model of fracture connectivity at Unit Well 7 based on a FracMan model projected onto a north-south plane viewed from the east..... 46

Figure 2.8. Results of borehole flow logging including data from both ambient and pumping conditions 51

Figure 2.9. Water chemistry data from straddle packer intervals 53

Figure 2.10. Water chemistry data from 2010 sampling (Table 2.2) with the addition of data from Fracture 2 straddle packer interval..... 55

Figure 3.1. Cross section including Unit Well 7, monitoring wells, and house wells..... 68

Figure 3.2. Location map of Unit Well 7 with monitoring well nest and instrumented house wells in Madison, Wisconsin. 69

Figure 3.3. Monitoring well water elevation data from a 24 hour period in June 2010 showing both MW-A and MW-B.. 71

Figure 3.4. Water level data from monitored wells during August 2011 and February 2012 75

Figure 3.5. Comparison of MW-B and MW-C RWF effects after the MW-C borehole was grouted during December 2011 and June 2012..... 84

Figure 4.1. Schematic of standard monitoring well virus sampling using glass wool filtration..... 97

Figure 4.2. Piper diagram plot of average values from 2010 monitoring well, Unit Well 7, and sanitary sewer samples..... 107

Figure 4.3. Average values for selected constituents from ten samples collected during 2010 with error bars indicating one standard deviation from the mean. 108

Figure 4.4. Piper diagram plot of average values from 2012 monitoring well, Unit Well 7, and sanitary sewer samples..... 109

Figure 4.5. Average values for selected constituents from ten samples collected during 2012 with error bars indicating one standard deviation from the mean. 110

Figure 4.6. Daily flow data for both the Nine Springs Wastewater Treatment Plant (WWTP) and wastewater pumping station #1 from May 1st to July 27th, 2010. 112

Figure 4.7. Daily precipitation and wastewater pumping station data for Madison, WI from May 1st to July 27th, 2010. 113

Figure 4.8. Comparison of flow into the Nine Springs Wastewater Treatment Plant (WWTP) with depth of snow on the ground in Madison, WI for February 2011..... 114

Figure 4.9. Daily precipitation and wastewater pumping station data for Madison, WI from January 1st to May 17th, 2012..... 115

Figure 4.10. Geophysical logs from Unit Well 7 for enlarged interval in which the pump was seated 124

Figure 4.11. Conceptual model of Unit Well 7 based on Figure 2.7 126

List of Tables

Table 2.1. Construction data for monitoring wells adjacent to Unit Well 7 31

Table 2.2. Wastewater indicator concentrations from 2010 sampling locations. 33

Table 2.3. Orientation of selected fractures in borehole MW-C based on WellCAD analysis of fracture log.. 43

Table 2.4. Transmissivity data from the FLASH computer program for layers in borehole MW-C. 51

Table 2.5. Conductivity measurements of groundwater from selected MW-C straddle packer intervals and MW-B well screen interval. 56

Table 3.1. Construction data for monitoring and house wells in the study..... 69

Table 3.2. Comparison of Noordbergum and Rhade responses and Unit Well 7 discharge in MW-B for 5 periods during the study. 73

Table 3.3. Ratio of reverse water-level fluctuation magnitude and duration in instrumented wells for several periods compared with MW-B. 74

Table 3.4. Aquifer matrix and fracture properties based on straddle packer slug test data and pumping test data. 80

Table 3.5. Estimated travel time (in seconds) between the base of the Wonewoc Formation at borehole MW-C and other instrumented locations. 81

Table 4.1. Information on sampling rounds described in this study. 95

Table 4.2. Results of 2010 and 2011 virus sampling reported as log concentration. . 102

Table 4.3. Results of 2012 virus sampling reported as log concentration 104

Table 4.4. Average field parameter measurements at each location from 2010 sampling rounds. 106

Accompanying Material

The accompanying CD contains the following information, listed by folder:

1. **Slug Test** – Contains data and analyses from straddle packer slug tests.

2. **Pumping Test** - Complete pumping test data summarized in Appendix C.

3. **Water Level** - Pressure transducer data files for the five time periods discussed in the dissertation.

Chapter 1. Introduction

1. Background

1.1. Public water supply vulnerability to contamination

Approximately one third of the U.S. population uses public supply wells (PSWs) as their drinking water source (Eberts et al. 2005). The presence of contaminants in these wells has been variable and unpredictable (U.S. Environmental Protection Agency 1999). During the past decade a greater focus has been placed on assessing the risk of contaminants entering PSWs. Among the many contaminants of concern are chemical and microbiological indicators of wastewater contamination. The U.S. Geological Survey's National Water-Quality Assessment (NAWQA) program has conducted research related to PSW vulnerability as one of its five focus areas. The NAWQA Transport of Anthropogenic and Natural Contaminants to Supply Wells (TANC) study strives to better understand the transport pathways and geochemical processes related to selected contaminants that may be found in groundwater captured by PSWs in a variety of hydrogeological settings (Landon et al. 2010). Sampling of monitoring wells at multiple depths within an aquifer in conjunction with PSW sampling has allowed for increased understanding of contaminant transport and associated health risks. Although the TANC program evaluated many representative aquifer systems throughout the U.S., not every hydrogeological setting has been covered.

Human impacts on groundwater used as drinking water sources have been evaluated using many different methods to quantify contamination levels and associated health risks. Indicator organisms have been utilized for more than 100 years to assess

the microbiological quality of water supplies with coliform bacteria serving as the primary indicator (Yates 2007). However, coliform bacteria are not ideal indicators of all pathogenic organisms in water. This is especially true in groundwater environments where the smaller sizes of viruses (23-80 nm) compared with bacteria (0.5-3 μm) and protozoans (4-15 μm) result in significantly different transport behavior (Abbaszadegan et al. 2003). The direct evaluation of virus concentrations in the groundwater environment poses several challenges but also holds promise as a tool for improving the understanding of groundwater flow between the surface and confined aquifers.

Human enteric viruses in drinking water pose a substantial public health risk. There are more than 100 enteric viruses that are known to cause illness in humans (Bosch 1998; Abbaszadegan et al. 2003). More than 50% of the waterborne outbreaks in the U.S. are attributed to contaminated groundwater, with approximately 65% of those cases caused by enteric viruses (Yates et al. 1985). Half of waterborne outbreaks involving acute gastrointestinal illness have an unknown origin but viruses are suspected in most of these cases (Lambertini et al. 2008; Yeh et al. 2009). In the developed world, human enteric viruses have been responsible for causing thousands of people to become ill each year (Dongdem et al. 2009) and gastroenteritis is responsible for killing millions world-wide (Bosch 1998). It has been demonstrated that water meeting regulatory standards for coliform bacteria still may contain human enteric viruses (Dongdem et al. 2009). In one outbreak study involving treated drinking water, the level of chlorine disinfection in the distribution system was high enough to inactivate coliform bacteria but human enteric viruses were still present (Bosch 1998). Recent

research on non-disinfected groundwater systems serving small communities suggests that viruses in the groundwater pose an increased risk of acute gastrointestinal illness (Borchardt et al. 2012).

Recognizing the threat of microbial contamination in groundwater, the U.S. Environmental Protection Agency (U.S. EPA) finalized the Ground Water Rule in October 2006 to address the risk of microbial contamination in drinking water supplied from groundwater sources (U.S. Environmental Protection Agency 2006). The U.S. EPA has added four human enteric viruses (adenovirus, calciviruses, enterovirus, and hepatitis A virus) to the Drinking Water Contaminant Candidate List 3 (U.S. Environmental Protection Agency 2009), which indicates their study in drinking water sources is a priority. The direct monitoring of enteric viruses may be the best method of determining if they are present in water supplies (Bosch 1998).

1.2. Sewer exfiltration as a source of contamination

Unlike other viruses, human enteric viruses have only one source: human waste. There are many potential sources of human enteric viruses but all are linked to human waste. The most common sources of viruses in groundwater are leaking sanitary sewers, sewage treatment plant effluent/biosolids, onsite septic systems, and sanitary landfill effluent (Yates et al. 1985; Bosch 1998; Abbaszadegan et al. 2003; Hunt et al. 2010). Sewers are the most likely source of viruses and other wastewater contaminants that enter groundwater in urban environments and may contaminate PSWs. In order to evaluate the potential volume of wastewater entering an aquifer it is important to quantify sewer exfiltration. Many urban areas have miles of aging clay pipe sanitary

sewers that are not well maintained. Estimates of sanitary sewer leakage in the U.S. are as high as 50% of the total flow, with exfiltration rates on the order of 0.01 L/sec/km (Hunt et al. 2010). An review of several reports indicated a range of exfiltration rates between 1 and 9 L/sec/km with a controlled experiment of exfiltration yielding a rate of 2 L/sec/km (Blackwood et al. 2005). A study in Nottingham, UK determined that average exfiltration rates in the UK range from 0.01 to 0.1 L/sec/km (Chisala and Lerner 2008) and another UK study estimated that 10% of the flow in sanitary sewer leaked and was recharging the aquifer (Rueedi et al. 2009).

Sewer exfiltration in significant quantities has been documented in urban areas in the U.S. and Europe. Urban areas typically use sewers instead of private, onsite septic systems for wastewater disposal due to high population density. The aging, leaking sewer pipes in many urban areas are a likely distributed source of wastewater contamination to groundwater that may be used as municipal drinking water. Due to the high concentration of pathogenic and chemical contaminants in wastewater, only a small volume of sewage is required to measurably contaminate a large volume of groundwater.

1.3. Human enteric virus sampling and detection

Recent advances in sampling and analytical methods have made it feasible to conduct broad scale monitoring for viruses in groundwater. Environmental virology as a scientific field has been evolving for more than 60 years (Yeh et al. 2009). Initial virus detection methods relied on cell cultures and those are still in widespread use today. Newer, polymerase chain reaction (PCR)-based molecular methods have been

developed to increase the sensitivity of virus detection in the environment. A recent decrease in the high cost of conducting environmental virus sampling has made it feasible to apply this method to larger projects. Each of these methods has advantages and disadvantages.

Most methods for detection and quantification of waterborne viruses from environmental samples require concentration from large volumes (100 to 1,000 L) of water. The ideal method of virus concentration would be inexpensive, simple, fast, and be capable of recovering a high percentage of viruses, be useful for a wide range of enteric viruses, and produce a small volume of concentrate; no one method meets all of these criteria (Bosch et al. 2008). Lambertini et al. (2008) summarized the concentration methods that have been successfully used during the past 20 years. The most popular concentration method is adsorption by the use of a 1MDS electropositive cartridge, which is approved by the U.S. EPA for enteric virus analysis. Another method of concentrating virus samples by adsorption is use of electropositive glass wool filters. The efficacy of glass wool filters was demonstrated by several recent studies (Cronin et al. 2003; Powell et al. 2003; Lambertini et al. 2008; Albinana-Gimenez et al. 2009; Borchardt et al. 2010) and the $10 cost of a glass wool filter is significantly less than a $300 1MDS filter.

Polymerase chain reaction methods rely on amplification of DNA or RNA from the target organism and are able to detect very low concentrations of genetic material. Bosch (2008) calls PCR the current gold standard for virus detection. Most enteric viruses of concern contain RNA, which must be converted to DNA using reverse

transcription PCR (RT-PCR) methods for analysis. The PCR methods are rapid (1-4 hours), are 100 times more sensitive than cell culture methods (Abbaszadegan et al. 2003) with detection limits of less than one genomic copy of virus per liter of sample, are highly specific, and can detect non-culturable viruses. There are, however, some disadvantages with PCR techniques. There is a high potential for contamination of samples, a potential for amplification of non-target sequences, and limitations due to the fact that only a small portion of the concentrated sample is analyzed. Furthermore, there is no way to distinguish between infective and non-infective viruses. This inability to detect infectiveness with PCR hampers efforts to determine the human health risk from virus genomes found in the sample. Nevertheless, PCR still can provide information about virus transport (Abbaszadegan et al. 1993; Abbaszadegan et al. 1999; Bosch 1998; Mattison and Bidawid 2009; Yeh et al. 2009).

1.4. Viral Decay Rates

Determining the survival rate of viruses in the subsurface is important because, unlike many chemical contaminants, enteric viruses pose a health risk for only a relatively short time. If the travel time for a virus genome to reach a target well or spring is greater than the time the virus can remain infectious, the public health risk is low. Viruses will survive longer in the environment than pathogenic bacteria so it is important to understand that the absence of indicator bacteria may not correlate with an absence of pathogenic viruses. Some of the factors that influence viral decay in groundwater include the virus type, temperature, dissolved oxygen, pH, electrical conductivity, and presence of native micro-organisms (Gordon and Toze 2003). Most viruses are thought

to lose infectivity after one to two years (Hunt et al. 2010) and several researchers have investigated what impact the above factors have on the decay rate of virus genomes in groundwater.

Virus genome decay can be described in terms of reduction of virus concentration per unit of time and can be calculated using the following first order decay formula.

$$\frac{dC}{dt} = -k\,C \qquad (1)$$

where C is the concentration, genomic copies per liter (gc/L) for PCR, and k is the decay constant [day^{-1}]. Equation 1 can be integrated and rewritten as

$$C(t) = C_0\, e^{-kt} \qquad (2)$$

Where C_0 is the initial virus genome concentration. Equation 2 can be rewritten as

$$k = -\left(\frac{1}{t}\right)\ln\left(\frac{C}{C_0}\right) \qquad (3)$$

to solve for the decay constant.

Field and laboratory studies have evaluated virus genome decay over time and determined decay constants for several virus groups. A study of virus genome decay over long time periods determined that an initial concentration of 10^4 Adenovirus was detectable by PCR for 364 days in groundwater and had a decay constant of 0.01 d^{-1} while an initial concentration of 10^4 enterovirus was detectable for 140 days and had a decay constant of 0.073 d^{-1} (Charles et al. 2009). Many researchers report the decay constant as a $\log_{10}$ reduction in virus genome concentration per day (log/d) to match the

virus inactivation nomenclature typically used in drinking water treatment. Using that nomenclature, the above-mentioned rates would be reported as 0.004 log/d and 0.03 log/d.

Work by Yates et al. (1985) indicated that temperature was the most important factor in determining virus persistence in groundwater. Samples were collected from locations across the U.S. and seeded with bacteriophage MS-2, poliovirus 1, and echovirus 1 before decay rates were determined at different temperatures. There was a strong correlation between virus decay rates and temperatures and it was noted that decay rates were much lower in groundwater than for other water types (e.g. marine, river, lake, and tap) at the same temperature.

A more recent review of microbial survival in groundwater (John and Rose 2005) compiled data from many studies on this topic. Temperature was cited as a major controlling factor in virus decay rates from the reviewed studies (Figure 1.1) but it was recognized that predicting virus decay based solely on groundwater temperature and virus type will lead to inaccurate rates. Native microorganisms, dissolved oxygen, soil media and attachment were all determined to have an impact on decay rates. Most studies only observed microbial survival in a water column without considering the role of the aquifer material. It was also noted that most of these studies only lasted 30 days and were unable to determine if rates were constant over a 3 log reduction in virus concentrations. Decay rates below 0.01 log/d may not be accurately measured unless data are collected for periods of a year or longer. A longer study of virus survival in an

aquifer determined that viruses persist much longer in situ than would be predicted on the basis of bench-scale experiments (DeBorde et al. 1998).

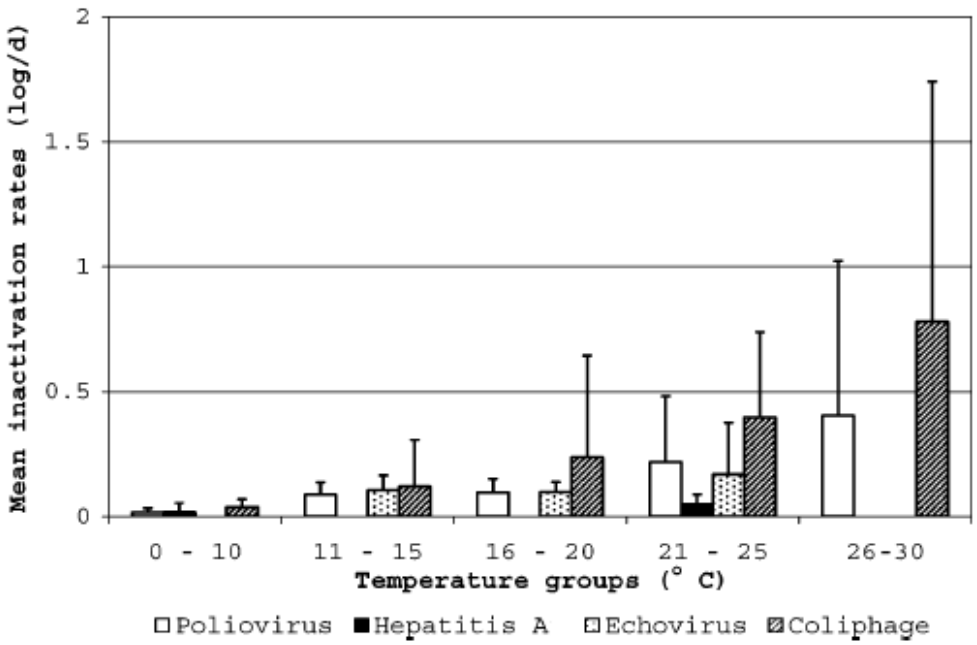

Figure 1.1. Virus decay rates from reviewed studies, averaged by temperature group (from John and Rose, 2005).

Given the above data on virus decay rates, it is possible to determine approximate times that virus genomes may remain viable in groundwater. A typical concentration of a virus genomes in wastewater may be between 10^4 to 10^5 gc/l and PCR can detect viruses genomes at 10^{-2} gc/l in groundwater; therefore a 6 to 7 log reduction must occur before the virus genome is no longer detectable. Although PCR specifically detects the RNA or DNA of viruses and does not directly indicate infectivity, previous research has indicated that virus genomes detected in PSWs using PCR are likely to be infectious and have negative health impacts on the local community (Borchardt et al. 2012). For most enteric virus genomes detected in groundwater at a temperature below 15°C the decay constant varies between 0.01 log/d and 0.1 log/d

(John and Rose 2005). A 6 to 7 log reduction in virus genome concentration would take only 60 to 70 days with a 0.1 log/d decay constant but 600 to 700 days with a 0.01 log/d decay constant. The dilution of wastewater mixing with groundwater in an aquifer may further result in a 1 to 2 log reduction in virus genome concentration. Based on this information it is reasonable to assume most viruses in groundwater at these temperatures will be detectable for no more than two years and might be infectious for a shorter period. Because decay constants increase with groundwater temperature, the survival time is reduced as temperature increases.

1.5. Transport pathways and velocities

A key assumption made when siting new drinking water wells is that if sources of contamination are not present within a set distance from the well (wellhead protection area) then the water source has a low risk of contamination because of natural attenuation and filtering processes (Hunt et al. 2010). This assumption does not account for actual groundwater flow paths and velocities involved in the transport of human enteric viruses and other microbial pathogens (DeBorde et al. 1999; Taylor et al. 2004). Aquitards have lower hydraulic conductivities and are assumed to reduce vertical contaminant transport through them. Viruses have been documented to travel up to 67 m vertically and over 400 m laterally in aquifers (Keswick and Gerba 1980).

Groundwater velocities are typically reported as an average linear velocity but the tortuosity of pore scale flow pathways results in a distribution of velocities around the mean (Figure 1.2). Rapid, statistically extreme groundwater velocities may involve only a small portion of the total flow volume but it is possible for water moving at these

extreme velocities to transport small numbers of viruses (Figure 1.3). While the longer, smaller diameter pathways through the matrix are more likely to attenuate viruses by filtration or sorption, viruses can remain mobile in the larger, more direct, higher velocity pathways. Increasing heterogeneity of the aquifer material may lead to the preferential transport of microbial pathogens at velocities that greatly exceed the average velocities of conservative ionic tracers such as chloride or bromide.

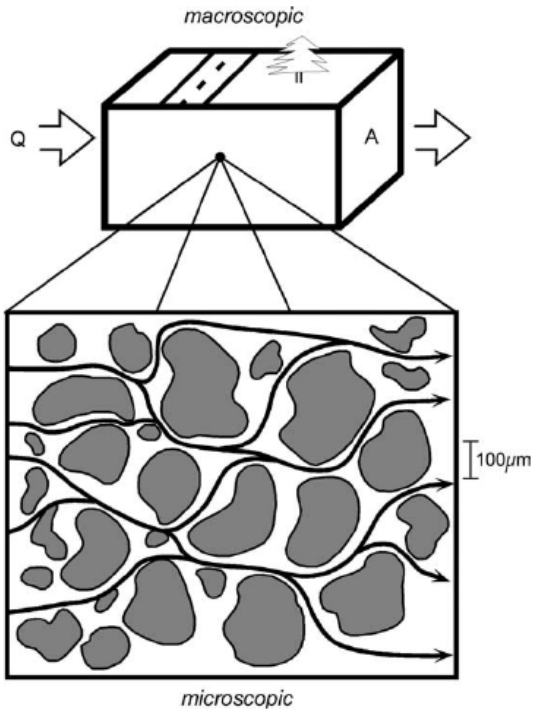

Figure 1.2. Microscopic flow paths in an aquifer can significantly increase average flow path length and flow velocity (from Taylor et al., 2004).

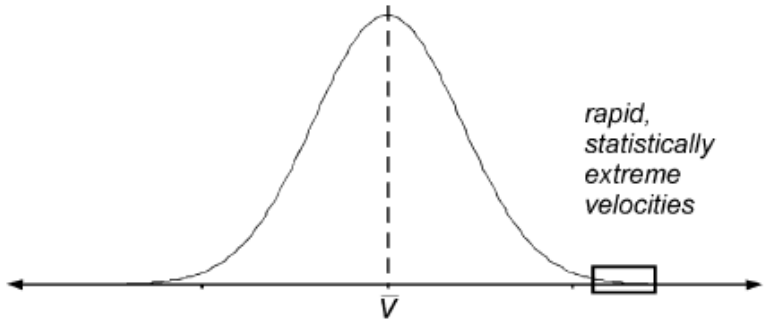

Figure 1.3. Normal distribution of groundwater flow velocities in a homogeneous aquifer highlighting the existence of rapid, statistically extreme velocities (from Taylor et al., 2004).

While it is important to recognize the effects of pore scale flow, it is also important to understand larger scale flow pathways that allow viruses to travel over distances of hundreds of meters in the subsurface. Studies in the United Kingdom of sandstone aquifers with sanitary sewer microbial contamination have identified possible mechanisms for increased macroscopic flow (Cronin et al. 2003; Powell et al. 2003). Vadose zone transport was linked to rainfall levels (recharge) and saturated zone transport included (1) short circuiting the well annulus, (2) bulk flow through the aquifer, and (3) bulk flow along preferential pathways (e.g. fractures).

The most likely route for wastewater from leaking sewers to rapidly reach a deep, confined aquifer is through macroscopic preferential flow pathways. These are the least well understood mechanism for transport of viruses into deep aquifer systems. As noted previously, only a small amount of sewer effluent is required to contaminate a drinking water well with viruses. Therefore, the fastest pathway with the shortest travel time to a well is the primary concern (Hunt et al. 2010). Unlike chemical contaminants in groundwater, and as discussed in the preceeding section on virus decay, viruses are

only infectious for a relatively short period of time. For that reason, only pathways that allow for travel times of less than two years to PSWs are of concern.

There are several potential routes for rapid transport of enteric viruses into aquifers. In the case of wastewater contamination in deep confined aquifer wells, the bedrock geology may lead to hydrostratigraphic conditions that promote preferential flow. Highly transmissive fractures are likely preferential flow pathways in sedimentary units (Runkel et al. 2006). Natural groundwater velocities in porous sandstone units with high hydraulic conductivity may experience increased flow rates when public supply wells are pumping, thereby increasing the head gradient. The installation of public supply wells may create new preferential flow pathways if the well annulus is not properly sealed and grouted to prevent vertical flow of groundwater (Lacombe et al. 1995). Open boreholes in fractured bedrock may also act to “short circuit” flow and increase downward migration (Williams and Conger 1990). All of these preferential flow pathways are possible and must be evaluated to find which are responsible for the travel times that will result in the arrival of infectious viruses in a PSW.

2. Public supply well vulnerability in Madison, Wisconsin

The Madison, Wisconsin area is an excellent location for investigating preferential flow pathways that may lead to virus contamination of PSWs. Madison is a medium-size (population 220,000), Midwestern city that relies on groundwater from 27 deep high-capacity production wells for its drinking water (Borchardt et al. 2007; Bradbury et al. 2010). The principal aquifer used for drinking water supply is the confined Cambrian Mount Simon aquifer, which is approximately 75 m below the

surface and overlain by the Eau Claire aquitard. The upper aquifer consists of Paleozoic siliciclastic and carbonate units overlain by 30 to 100 feet of glacially-deposited sediments. The Madison area has a temperate continental climate averaging 78 cm of precipitation per year with cold winters and warm summers. It is similar to many other cities of its size in terms of the age of water and wastewater infrastructure and it has extensive, but separate, storm and sanitary sewer networks across the city.

2.1. Viruses in Madison Public Supply Wells

Virus genomes have been detected in Madison area PSWs during research conducted by the Wisconsin Geological and Natural History Survey (WGNHS) on the confined Mount Simon aquifer, the drinking water source for the City of Madison. Historically, it was thought that deep, confined aquifers were protected from microbial contamination by natural attenuation and filtering. The WGHNS set out to test the validity of this assumption. Initial work in 2003 and 2004 detected human enteric virus genomes in 2 of 3 deep public supply wells sampled (Borchardt et al. 2007). The virus positive wells are hundreds of meters deep and cased through the regional aquitard (Eau Claire aquitard). This work utilized 1MDS filters to concentrate an average of 1,450 L of groundwater at the wellheads before water was treated with chlorination. Samples were analyzed by RT-PCR for enterovirus, rotavirus, hepatitis A virus, and norovirus genogroups I and II. Seven of the 30 samples (23%) were positive for enteroviruses, but no samples were positive for other virus groups. The seven enterovirus positive samples were evaluated for infectivity using established cell culture methods; none of the positive samples were infective.

A subsequent study (Bradbury et al. 2008; Bradbury et al. 2010) conducted from 2007 to 2009 sampled a larger number of Madison PSWs for viruses on a monthly basis. Due to lower costs for glass wool filters compared with 1MDS filters, sample concentration was accomplished using glass wool filtration (Lambertini et al. 2008) with acid pH adjustment to between 6.5 and 7.0 before filtration if groundwater pH exceeded 7.5. Sample volumes ranged from 700 to 1,000 liters with flow rates below 4 L/min to maximize virus adsorption to the glass wool. Samples were analyzed by RT-PCR for enterovirus, rotavirus, adenovirus, hepatitis A virus, and norovirus genogroups I and II. Enterovirus positive samples were evaluated for infectivity by cell culture. During the 13 months of the study, the percentage of wells with virus genomes positive results each month varied from zero to 80%, with an overall average of 43% positive samples. Both adenoviruses and enteroviruses were detected. Infectious enteroviruses were found in 3 of the wells sampled. Although not all wells were virus positive during the same month, each of the 6 wells that were continuously sampled were virus positive at some point during the study.

It was necessary to sample over many months to accurately determine levels of virus contamination in each well. Virus presence appeared to follow high recharge events (i.e. high rainfall or snow melt), which could facilitate virus transport. Preferential flow pathways were not investigated in those studies, but would be required to explain the presence of infective viruses in the PSWs. These studies suggested several potential mechanisms by which viruses could reach the Mount Simon aquifer including (1) transport through the aquitard by porous-media flow, (2) transport through “windows”

or areas where the aquitard is not present, (3) fracture flow, and (4) leaks associated with poorly constructed wells (Bradbury et al. 2008).

2.2. Source of contamination in the Madison area

The WGNHS study evaluated sources of virus contamination. Surface water was considered as a potential source of the viruses but no correlations were found between samples from local lakes and from PSWs for the virus serotypes, $^{18}O/^{2}H$ ratios, or virus genome concentrations. The sanitary sewer was, therefore, suggested as the most likely source of the viruses detected in the Madison wells. A study at LaCrosse, Wisconsin (Borchardt et al. 2004) found the highest virus genome concentrations in a PSW that is located near a pressurized lift station. Madison sanitary sewer lines are primarily gravity mains that are not pressurized but that flow into pressurized mains operated by the Madison Metropolitan Sewerage District (MMSD), which serves Madison and surrounding communities. During a period of heavy rainfall in south-central Wisconsin during June 2008 it was observed that inflow to the MMSD operated Nine Springs Wastewater Treatment Plant (WWTP) rose from an average flow of 150 million liters per day (MLD) to a high of 460 MLD, with a flow of 300 MLD for several days afterward (Bradbury et al. 2008). The additional water in the sanitary sewer pipes most likely caused some gravity mains to fill with effluent and become pressurized, resulting in increased leakage into the subsurface and eventually into the aquifer. In urban environments like Madison, leaking sanitary sewers are in close proximity to public supply wells and could act as a distributed source of virus contamination.

In summary, the Madison area has many kilometers of old, leaking sewers that provide a source of viruses. The average groundwater temperature in Madison is approximately 11°C, which is favorable for relatively long virus survival times. The hydrostratigraphy of the area is suitable for the development of fracture flow and defective PSWs may serve as preferential flow pathways. The physical and hydrogeologic setting in Madison is representative of other areas not only in the upper Midwest, but also in other areas around the world. This makes a study of Madison public supply well vulnerability relevant to other locations. The least understood part of this setting is the mechanism of transport by preferential flow pathways that allows effluent to travel at relatively high velocities and contaminate public supply wells.

3. Research Objectives

The overall goals of this research were to better understand the primary mechanisms that control the transport of human enteric viruses and other wastewater contaminants in bedrock multi-aquifer systems and to develop effective methods for assessing the vulnerability of public water supply wells in such settings. A thorough study of one PSW was chosen as the best approach for achieving these goals, with the expectation that results of this work will be applicable across the hydrogeologic region and other areas with similar hydrostratigraphy characteristics.

One of the Madison PSWs in which viruses had been detected in previous work, Unit Well 7, was selected as the site for field studies. The Madison Sewer Utility conducted video logging of the sanitary sewers in the neighborhood surrounding Unit Well 7. These logs indicated that most sections of the 70 year old vitrified clay pipes

contain multiple cracks and holes that may lead to exfiltration. Simulations using porous-media assumptions indicate that transport of viruses by porous media flow alone is very unlikely. The WGNHS had used the Dane County hydrogeological model (Krohleski et al. 2000) to predict capture zones based on porous media flow in the Mount Simon Sandstone for many PSWs, including Unit Well 7 (Figure 1.4). The Dane County model utilized a MODFLOW finite difference grid with a 400 m horizontal spacing and three layers. The predicted 5 year capture zone in the Mount Simon aquifer extended only to a radius of 300 m from the unit well. Preliminary work as part of this dissertation included creating a telescopic mesh refinement of the Dane County model for the area surrounding Unit Well 7. This more detailed model (not shown) contained 6 layers and a central grid spacing of 2.4 m. Particle tracking using MODPath indicated that under porous media flow, particles at the water table at a radial distance of 30 m from the well would not enter the unit well after 600 days of pumping. In fact the model predicted that pumping of the lower aquifer for 10,000 days had no noticeable effect on transport at the top of the upper aquifer.

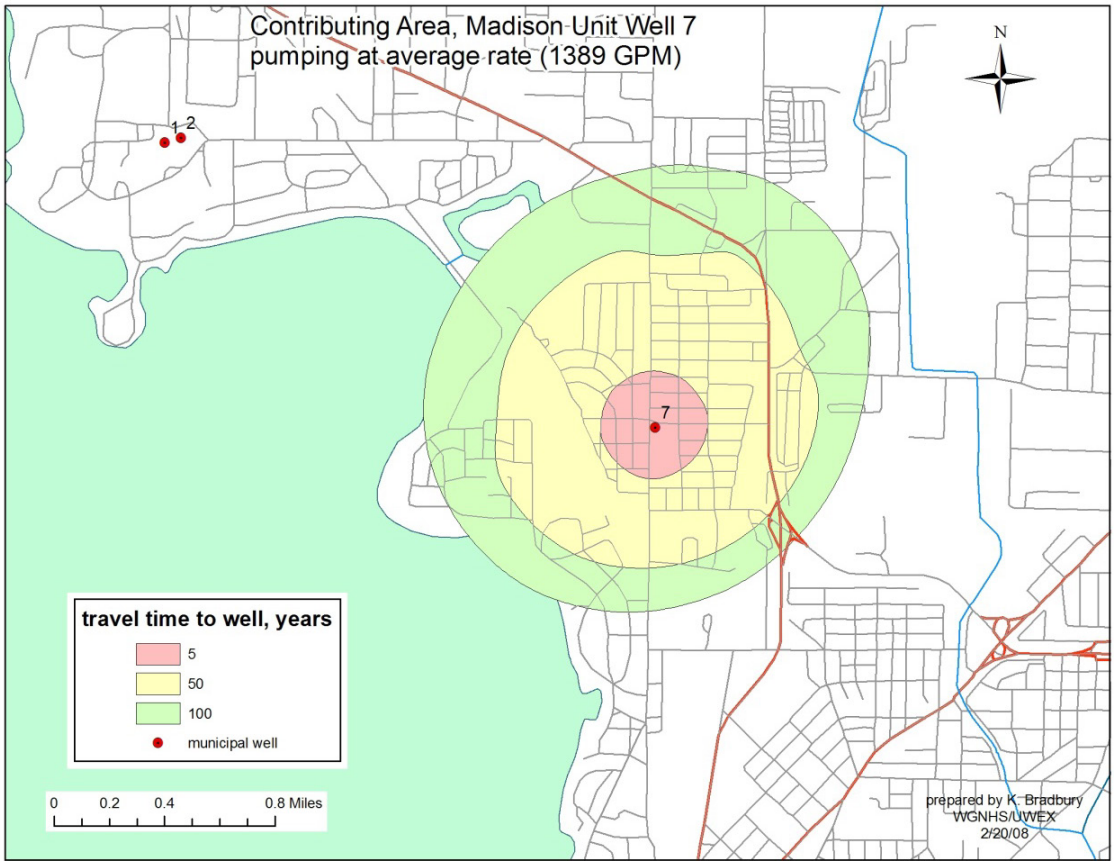

Figure 1.4. Predicted capture zone for flow in the Mount Simon aquifer at Madison Unit Well 7 (Ken Bradbury, personal communication).

Based on groundwater flow modeling with porous media assumptions, it appeared that contaminants at the water table would not enter the deep confined PSW in time frames appropriate for virus survival. The most likely explanation for the virus detects in Unit Well 7 and other PSWs in Madison was the existence of preferential flow pathways. Stratigraphically controlled preferential flow paths have been identified in the same Cambrian age siliciclastic units in south-central Wisconsin (Anderson 2002; Swanson 2007; Swanson et al. 2006) and also in equivalent units found in southeastern Minnesota (Runkel et al. 2006).

Field investigations at Unit Well 7 in Madison, Wisconsin were undertaken to address the following hypotheses and related questions:

1. Preferential flow pathways associated with leaky aquitards, fracture flow and/or defective well casings promote rapid downward transport of wastewater contaminants into the subsurface. What are the dominant transport pathways and how might one distinguish among these? What is the contribution of fracture flow in a siliciclastic aquifer?
2. The cycling frequency and discharge of high capacity public supply wells affects the rate of transport for sewer effluent in a multi-aquifer system. What is the mechanism responsible for reverse water-level fluctuations that are observed in the upper aquifer during pumping of the lower aquifer? How do RWFs rapidly propagate through the upper aquifer and what might these indicate about connectivity of fractures or other preferential flow paths?
3. Because they are detectable even after significant dilution and decay, human enteric viruses are a useful spatial and temporal tracer of sewage contaminant transport in the subsurface. Can virus data provide constraints on preferential pathways and processes that contribute to rapid contaminant migration? Is there a correlation between large recharge events, high rates of sewer flow, and detection of virus genomes at various depths in the subsurface?
4. Because the cost and effort of virus genome sampling may not be practical for routine monitoring, other chemical and physical parameters may be more useful for identifying preferential flow pathways in a multi-aquifer system subject to wastewater

contamination. Which chemical constituents are the most appropriate indicators of wastewater effluent in these settings? Which chemical or physical parameters correlate with virus genome detection in groundwater?

4. Introduction to the Dissertation

As stated previously the purpose of this research was to better understand the primary mechanisms that control the transport of human enteric viruses and other wastewater contaminants in bedrock multi-aquifer systems and to develop effective methods for assessing the vulnerability of public water supply wells in such settings. The first step in this study was to evaluate physical flow in the upper aquifer. Chapter 2 describes the use of several methods to assess the hydrogeological properties of the upper aquifer and the contribution of fracture flow. The use of borehole geophysics, a straddle packer, and a pumping test allowed for the collection of data that indicate fracture flow is substantial and that horizontal and vertical fractures may be connected to form transport pathways.

Water level data collected from several wells in the upper aquifer provided insight into the effects of pumping on the aquifer system. Chapter 3 provides an analysis of poroelastically generated reverse water-level fluctuations (RWFs) observed in several monitoring wells in the study area. The water level data were collected over a two year period and under a variety of pumping rates. These data indicate that public supply well pumping rate and cycling frequency impact the magnitude of RWFs in the upper aquifer. The RWFs also appear to propagate rapidly through the upper aquifer via fractures and may play a role in enhancing contaminant transport.

The presence of human enteric viruses and other wastewater contaminants provide the most direct evidence of public supply well vulnerability. Chapter 4 presents results of time sequenced microbiological and chemical sampling of groundwater at the site. Factors that may influence the transport of wastewater contaminants temporally and spatially through the system are evaluated. Chapter 5 provides a summary of the research, conclusions, overall significance of the work, and suggests future related research.

Chapter 2. Characterization of fracture connectivity in a siliciclastic bedrock aquifer near a public supply well

1. Introduction

In order to protect public water supply wells from a wide range of contaminants, it is imperative to understand physical flow and transport mechanisms in an aquifer system. With regard to microbiological contamination, determining the travel time between source and target has increased importance due to limited timespan of viability for these organisms. Human enteric viruses may only be viable for 1-2 years in a groundwater environment depending on factors such as water temperature (Yates et al. 1987; John and Rose 2005). If the time of transport to a well exceeds the viability period of the microorganism in groundwater, the risk of infection is low.

Many recent studies have highlighted the impact of microbiological contaminants on aquifer systems. Research in the United Kingdom by Powell et al. (2003) has identified microbial contaminants in urban sandstone aquifers at depths up to 90 m below ground surface. Hunt et al. (2010) have detected viruses in public supply wells that access a variety of aquifer types and are located in several Wisconsin communities. Previous work by the Wisconsin Geological and Natural History Survey (WGNHS) has revealed the presence of infectious human enteric viruses in public supply wells in Madison, Wisconsin, USA that draw groundwater from a deep (75+ m), confined siliciclastic aquifer system (Borchardt et al. 2007; Bradbury et al. 2010).

It has been challenging to identify specific pathways for viruses and other contaminants to rapidly reach public supply wells in these settings. Standard

calculations of porous media transport in siliciclastic aquifer systems are made using the advective transport equation

$$v = -(K/n_e)(dh/dl) \quad (1)$$

where v is the average linear velocity (L/T), K is the hydraulic conductivity (L/T), n_e is the effective porosity (dimensionless), and dh/dl is the hydraulic gradient (dimensionless). Using equation 1, it does not seem likely that microbiological contaminants could travel these distances quickly enough to remain viable upon entering a public water supply well. One hypothesis to explain the presence of infectious viruses at depth is that a small quantity of groundwater can travel along the most direct pathways through porous media at rapid, statistically extreme velocities, which enable a portion of the microbiological contamination to reach the target well (Taylor et al. 2004). However, only a very small fraction of the initial contaminant would be able to reach the target well in this scenario. Another transport mechanism that could explain rapid transport in these aquifer systems is groundwater flowing through fractures.

Fracture patterns and fracture flow in carbonate sedimentary rocks have been the focus of many studies (Bradbury and Muldoon 1994; Muldoon et al. 2001; Rayne et al. 2001; Underwood et al. 2003) and carbonate rocks can have a wide range of hydraulic conductivity values that result in the unit acting either as an aquifer or aquitard (Brahana et al. 1988). Although flow through fractures has typically been associated with crystalline and carbonate rocks, there is growing evidence it is also important to flow in relatively shallow sandstone aquifers. Research by Runkel et al. (2006) on fractures and fracture flow in the Cambrian siliciclastic sedimentary rocks of the North

American craton concluded that fracture flow may dominate intergranular flow even in highly permeable coarse grained sandstone aquifers. These fractures were associated with certain lithostratigraphic intervals and even at great burial depths the fractures were hydraulically significant. Recent work on the Cambrian Tunnel City Group of southern Wisconsin (Swanson 2007; Swanson et al. 2006) has demonstrated the importance of bedding parallel fractures to spring flow and also a correlation between changes in lithofacies and the presence of these fractures. Detailed hydraulic head measurements at another site in southern Wisconsin delineated several distinct hydrogeological units within this formation based on large vertical variations in head related to the vertical connectivity and presence of fractures (Meyer et al. 2008). Thermal tracer tests in open boreholes near Madison, Wisconsin identified hydraulically significant fractures in the local Cambrian age formations (Leaf et al. 2012).

The purpose of this work is to test the hypothesis that fracture connectivity in siliciclastic aquifer systems is a likely mechanism for rapid transport of microbiological organisms and other wastewater contaminants. Urban areas with aging, leaky sanitary sewers in proximity to public water supply wells may be at increased risk of wastewater derived contaminants entering the municipal water supply. A detailed field investigation at a site near a public water supply well determined the distribution, orientation, and hydraulic properties of fractures; the response of the fracture system to pumping stress; and the presence of geochemical indicators in individual fractures. Fracture data were obtained from a single borehole, which resulted in limited spatial resolution. The data collected from both the overall aquifer and from individual fractures were utilized to

determine the role of fractures in the rapid transport of wastewater contaminants in the upper aquifer. The primary means to identify and characterize fracture connectivity in these settings involved the use of borehole methods, including a combination of geophysical logging, vertical flow assessment, and discrete interval evaluation of physical and chemical groundwater parameters. The construction and use of a custom made, light-weight straddle packer allowed for the isolation and evaluation of individual fractures.

2. Background

2.1. Location

The study area includes Madison Unit Well 7 (UW-7), a public water supply well where viruses have been detected previously, and the surrounding residential neighborhood in the City of Madison, Dane County, Wisconsin, USA (Figure 2.1). The UW-7 was drilled in 1939 and is one of 23 high capacity wells used by the City of Madison Water Utility as a potable water source. The well is cased and grouted through the Eau Claire aquitard and is a 41 cm open borehole through the full thickness of the Mount Simon aquifer. Unit Well 7 has a maximum discharge of 8,300 liters (2,200 gallons) per minute that fills an adjacent 568,000 liter (150,000 gallon) reservoir, which supplies the distribution system. The well had historically been used as a seasonal well (May to November) but more recently it supplied water year-round and produced approximately 950 million liters (250 million gallons) during 2010 (Madison Water Utility 2011). Sanitary sewers in the neighborhood were installed in the late 1940s and consist primarily of vitrified clay pipe. Video logging of the sanitary sewer by the Madison

Sewer Utility indicates that some sewer pipe has cracked sections that may allow wastewater to leak out. Madison has separate sanitary sewer and storm sewer systems.

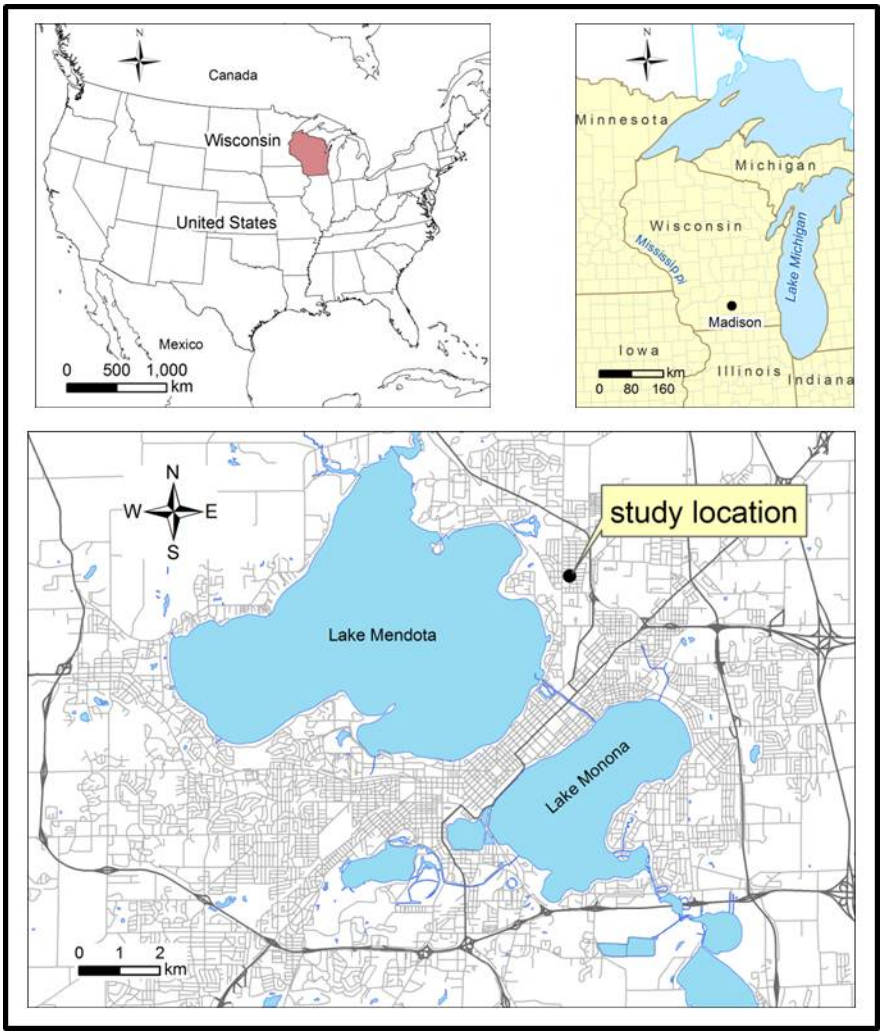

Figure 2.1. Study area location.

2.2. Stratigraphy and geologic setting

The site is underlain by approximately 10 m of unlithified till and more than 200 m of Cambrian age sandstone, siltstone, and shale units as depicted in Figure 2.2. Bedding within these units is primarily horizontal, with only a slight regional dip of 2-3 m per kilometer southeast away from the Wisconsin Arch (Cline 1965). The Cambrian units

are underlain by Precambrian age granite that is considered a barrier to groundwater flow. The Mount Simon Formation, a sandstone unit that forms the confined lower bedrock aquifer, is used as a primary water source by the City of Madison and surrounding Dane County. The shale and siltstone intervals of the overlying Eau Claire Formation act as a regional aquitard (Aswasereelert et al. 2008). The Wonewoc Formation and Tunnel City Group form a semi-confined upper bedrock aquifer at this location. The Tunnel City Group consists of several lithofacies that contain either glauconitic layers or thin silt and clay drapes (Swanson 2007). These fine grained layers act as a leaky confining unit. Public supply wells pump tens of millions of gallons per day from the Mount Simon aquifer beneath Madison, resulting in a substantial cone of depression across the area. Hydraulic gradients due to this cone of depression result in downward vertical flow from the upper aquifer to the lower aquifer in Madison (Bradbury et al. 1999).

Age		Stratigraphic Units		Thickness (m)	Hydrostratigraphy	Description
Cenozoic	Pleistocene	Holy Hill Fm. (Horicon Mbr.)		10	Unsaturated	Unconsolidated till consisting of gravelly, clayey, silty sand [a]
Paleozoic	Cambrian	Tunnel City Group	Lone Rock Fm. Mazomanie Fm.	20	Upper Aquifer	Yellowish brown to brown, very fine to fine grained silty sandstone with some dolomite cement and glauconitic layers [b]
		Elk Mound Group	Wonewoc Fm.	32		Very pale brown to orange brown, medium to coarse grained sandstone with minor glauconite and some iron oxide coated intervals [b]
			Eau Claire Fm.	11	Aquitard	Very pale yellow brown fine sand interbedded with gray green shale [b]
			Mount Simon Fm.	150	Lower Aquifer	White, yellow, and brown clean, well sorted, fine- and medium-grained sandstone, quite friable in some sections [a]

Figure 2.2. Study area stratigraphy. [a] Ostrom 1978 [b] Description from MW-C geological log based on drilling cuttings (Roger Peters, WGNHS)

2.3. Installation of monitoring wells

Three monitoring wells were installed at the site in order to investigate the upper aquifer. Figure 2.3 illustrates the position of the monitoring wells in relation to the public supply well and the geological units. A rotary drill rig was used to complete boreholes on site with an air rotary technique and a 15 cm (6 inch) tricone bit. The boreholes are located approximately 6 m from UW-7 and approximately 2 m from each other. Table 2.1 summarizes the construction details of each borehole and monitoring well. Cuttings were collected at 1.5 meter intervals from MW-B and MW-C and used to create geologic logs (Appendix A). The two shallower wells (MW-A and MW-B) were drilled in April 2010 and 5 cm (2 inch) diameter schedule 40 PVC monitoring wells were installed the

same day. The shallowest well (MW-A) is screened across the water table and the intermediate well (MW-B) is screened across the Tunnel City – Wonewoc contact. The deepest well, MW-C, was drilled a year later, in April 2011, to the top of the Eau Claire aquitard as an open borehole with a 15 cm (6 inch) steel casing driven approximately 10 m to the top of bedrock. This open borehole was utilized for most of the subsurface characterization at the site. When the MW-C borehole was not in use, a blank FLUTe™ flexible liner system was installed to minimize vertical circulation of groundwater in the borehole. The MW-C 5 cm (2 inch) diameter schedule 80 PVC monitoring well was completed in December 2011.

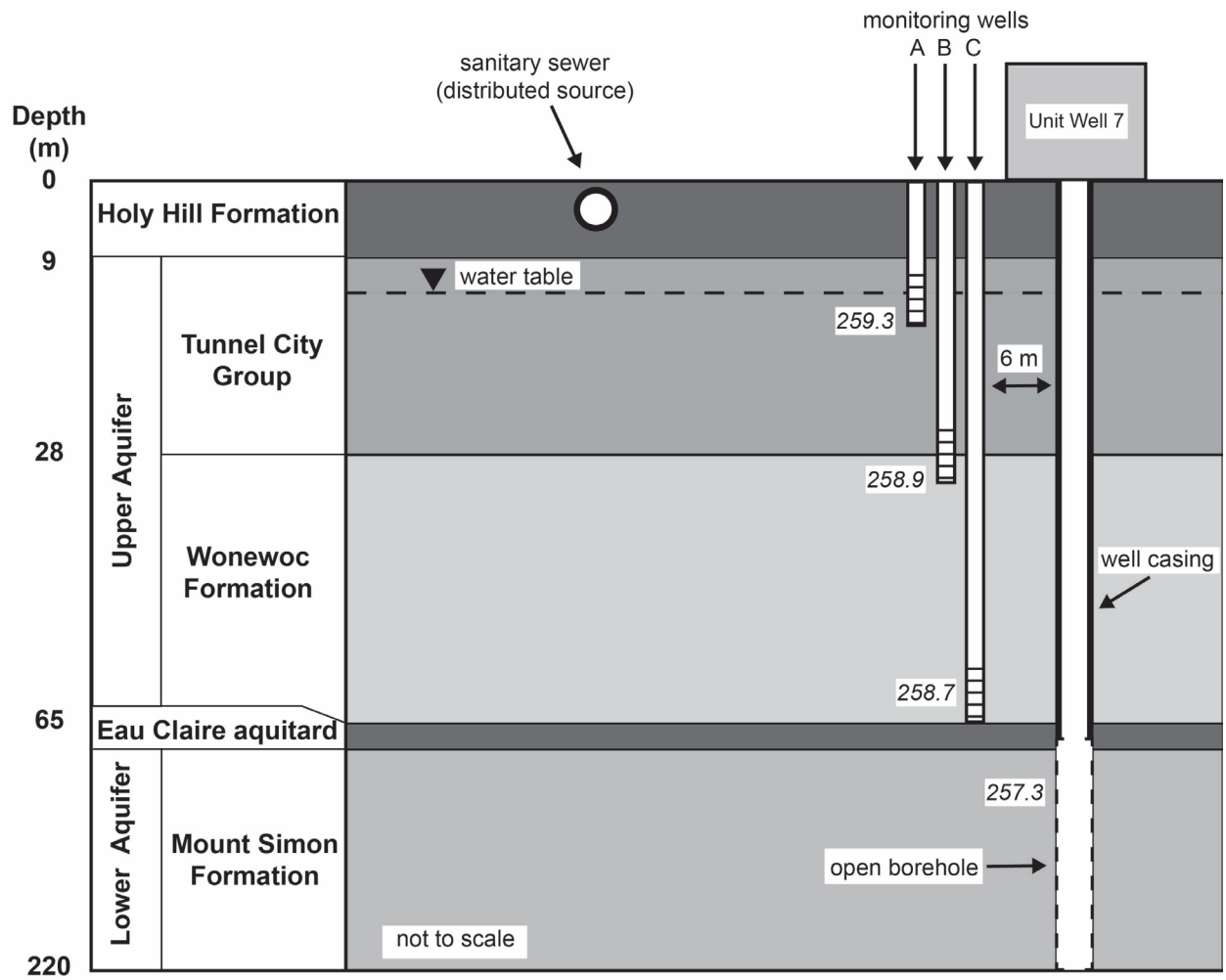

Figure 2.3. Cross section of field site with location of monitoring wells with respect to the unit well. Numbers next to each monitoring well screen and the Unit Well 7 borehole are hydraulic head elevations (in meters) from May 2012 while the aquifer system was at steady state during well maintenance.

Table 2.1. Construction data for monitoring wells adjacent to Unit Well 7

Well Name	Date Drilled	Borehole Diameter (cm)	Borehole Depth (m)	PVC Well Casing Diameter (cm)	MW Screen Interval (m)	Screen Length (m)
MW-A	13 April, 2010	15	14.6	5	10.0 – 14.6	4.6
MW-B	13 April, 2010	15	30.5	5	27.5 – 30.5	3
MW-C	20 April, 2011	15	66.4	5	62.5 – 65.5	3

2.4. Motivation and initial work

Results of previous work that detected human enteric viruses in Madison public supply wells were the motivation for this study (Bradbury et al. 2010; Borchardt et al. 2007). Two previous rounds of time sequenced sampling detected viruses in both the sanitary sewer and at several public supply wells in Madison. The temporal pattern of virus detections in the sewers and the public supply wells indicated that the viruses reached the wells on a time scale (days to weeks) much faster than expected for porous media flow (years to tens of years). Preferential flow pathways between the sewers and the deeper monitoring well appeared necessary to explain these apparently rapid transport rates. The earlier studies did not investigate the upper aquifer or the specific pathways responsible for virus transport to the public supply wells.

The sanitary sewer, Unit Well 7, MW-A, and MW-B were sampled six times over a 12 week period during the summer of 2010. Each sample was evaluated for the presence of human enteric viruses and major ions. Virus sampling required pumping 1,000 liters of groundwater through electropositive glass wool filters at less than 5 L/min. As expected, the sanitary sewer chemistry samples contained high levels of typical wastewater indicators including nitrate, chloride, and bromide. In addition, most homes in Madison use water softening devices that require sodium chloride salt. Backflushing these systems discharges high levels of chloride and sodium into the sanitary sewer. The deeper groundwater samples from MW-B contained significantly higher levels of wastewater indicators than samples from the water table well MW-A. Data provided in Table 2.2 demonstrate that wastewater indicators are higher at 29 m below ground surface (MW-B) than at the water table (MW-A) or in the confined

aquifer (UW-7). It is important to note that the relatively low levels of nitrate in the sanitary sewer are due to reducing conditions under which the primary nitrogen species in wastewater is ammonia, which then oxidizes to nitrate in groundwater. Ammonia was not analyzed in these samples. The distinct pattern of wastewater indicators at depth suggested that a preferential flow pathway exists that allows sewer effluent to rapidly migrate to discrete intervals within the upper aquifer.

Table 2.2. Wastewater indicator concentrations from 2010 sampling locations.

Sample Location					
Depth (m)	Name	Sodium (mg/L)	Chloride (mg/L)	Nitrate as N (mg/L)	Bromide (µg/L)
2.0	Sanitary Sewer	183	263	0.024	138
12.3	MW-A	45	105	0.72	29
29.0	MW-B	194	488	6.1	228
75+	Unit Well	8	14	0.026	29

In May 2010, pressure transducers were placed in the monitoring wells to continuously record water level readings at 5 minute intervals. The shallower monitoring well (MW-A) did not respond noticeably to pumping but the deeper monitoring well (MW-B) responded almost immediately each time Unit Well 7 began pumping. The MW-B water level dropped by approximately 50 cm after three UW-7 pumping/recovery cycles over a 12 hour period. Between MW-B and the Unit Well, the Eau Claire Formation acts as a regional aquitard (Figure 2.3). The strong hydraulic connection between MW-B and the Unit Well suggested fracture flow between 30 m below ground surface (bgs) and the Mount Simon aquifer may be influencing the water level response in MW-B. Well construction records indicate UW-7 is cased and grouted through the upper part of the Eau Claire Formation and this was confirmed by recent

geophysical logging of the Unit Well. This portion of the upper Eau Claire Formation includes a silty shale interval approximately 3 m thick, while the rest of the formation consists mainly of fine to medium grained sandstone. Other possible explanations for a hydraulic connection between the upper and lower aquifers are that the casing and/or grouting has failed, or the drilling of the well may have compromised the integrity of the aquitard near the borehole.

3. Methods and Results

3.1. Borehole logging and fracture identification

The MW-C borehole was geophysically logged with several downhole tools during the spring and summer of 2011 in order to characterize the aquifer system and identify fractures. Several of the borehole logs are presented in Figure 2.4. An Advanced Logic Technology (ALT) OBI-40 optical borehole imager captured an oriented 360 degree visual image of the borehole at 3 mm intervals and the ALT ABI-40 acoustic borehole imager transmitted ultrasonic pulses at 3 mm intervals to collect data on the diameter of the borehole. The OBI-40 images were used to identify potential fractures, bedding planes, and color changes. The ABI-40 data identified changes in borehole diameter that may indicate fractures. Gamma logging measured background levels of gamma radiation at 1.5 cm intervals that reflect differing percentages of potassium feldspar clasts, glauconite layers, and clay drapes in siliciclastic units (Swanson 2007). At this site the Tunnel City Group and Eau Claire Formation have higher gamma readings while the clean, quartz sandstone of the Wonewoc Formation has a relatively low gamma signature (Figure 2.4). Fluid temperature and conductivity of the

groundwater in the borehole were measured at 3 cm intervals and a mechanical caliper determined borehole diameter at 3 cm intervals.

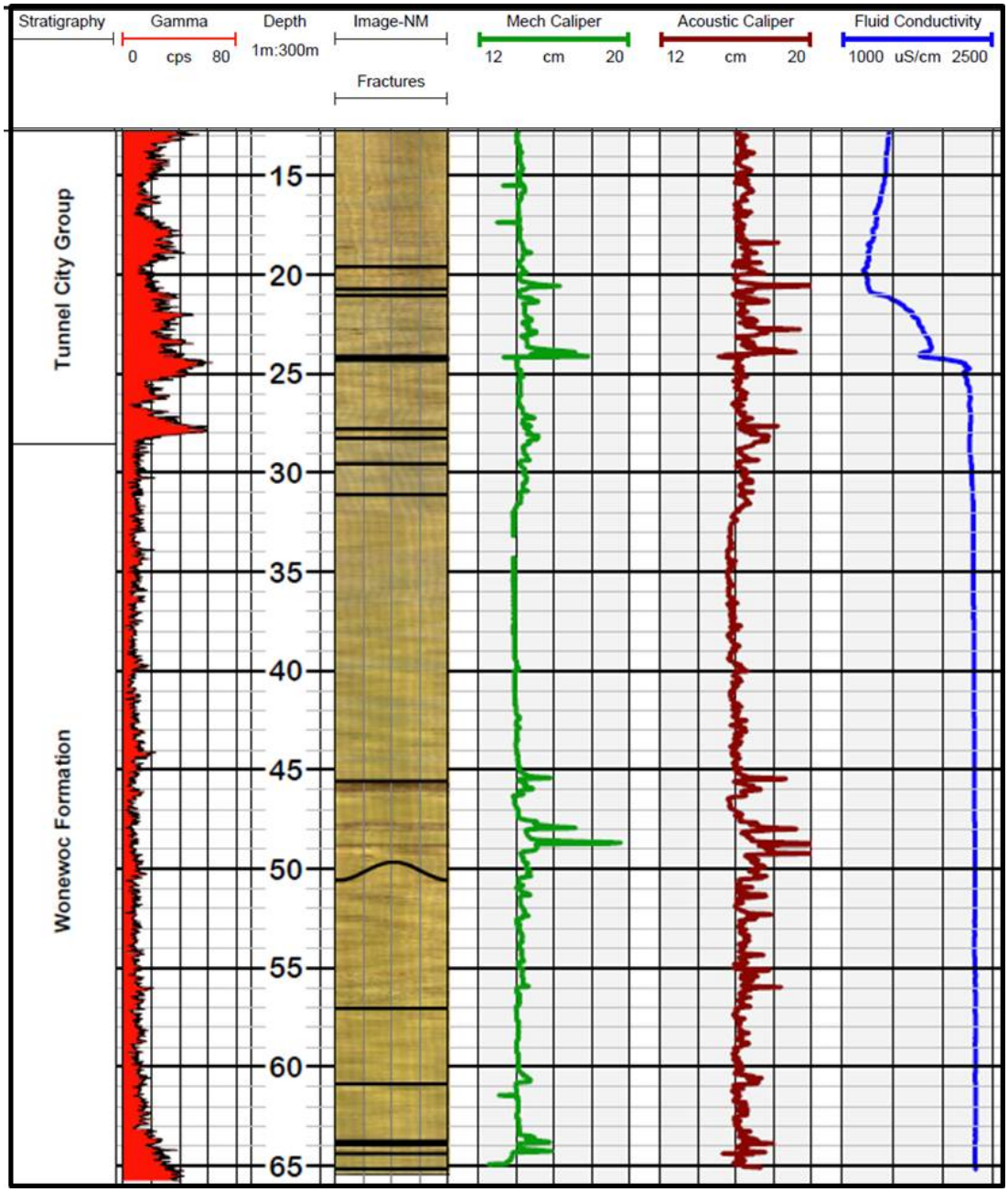

Figure 2.4. Selected borehole logging data from MW-C. The "Image-NIM" log was generated using the Optical Borehole Imager (OBI) and the "Acoustic Caliper" log was generated using the Acoustic Borehole Imager (ABI).

Fracture identification in borehole MW-3 was accomplished with a combination of logs from the mechanical caliper, ABI, and OBI tools. One or more of these methods identified a total of 12 potential hydraulically significant fractures (Figure 2.5). The OBI log identified all fractures but that method was subjective and based on a visual examination of the log for sections that appeared to be fractures. The OBI produces a “virtual core” that can be examined as a three dimensional cylinder or “unrolled” and viewed as a flat, oriented surface as depicted in Figure 2.4. Fractures are typically bedding plane parallel with an extremely narrow apparent aperture, and some surface oxidation or staining. A log of fracture position and orientation was created from the OBI data and is superimposed on the OBI log (Figure 2.4). The mechanical caliper and ABI both were more quantitative and measured the diameter of the borehole, with sharp increases of more than 1.5 cm taken as an indication of a potential fracture. Some intervals were likely enlarged during drilling based on the width of the interval and lack of fracture evidence in the OBI log. The mechanical caliper log identified the fewest fractures (6) and was the least sensitive of the three methods used.

Fracture Number	Depth (m)	Fracture Identification Method: Mechanical Caliper	Acoustic Borehole Imager	Optical Borehole Imager	Straddle Packer Hydraulic Conductivity (cm/sec)
1	19.5		X	X	
2	20.9	X	X	X	
3	24.1	X	X	X	
4	27.7		X	X	
5	28.0		X	X	
6	29.0		X	X	
7	30.8		X	X	
8	45.4	X	X	X	
9	50.0		X	high angle	
10	57.0			X	
11	60.7			X	
12	64.3	X	X	X	

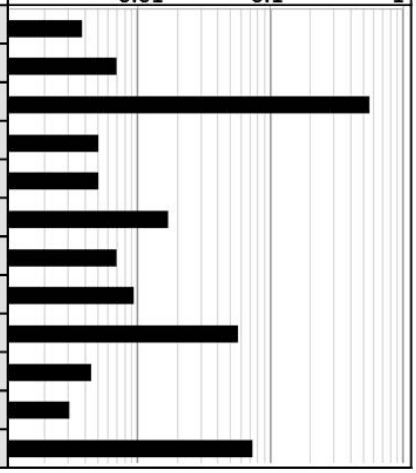

Figure 2.5. Summary of downhole logging methods that indicated potential fractures in borehole MW-C. Hydraulic conductivity values based on straddle packer slug tests for selected intervals reveal which fractures are hydraulically important. Fractures 4 and 5 have the same hydraulic conductivity value because they were in the same packer interval.

3.2. Packer slug tests

The MW-C borehole was evaluated at discrete intervals with an inflatable straddle packer assembly. The straddle packer was constructed using customized flow through packers designed for use in isolating sections of sewer pipe. These devices are lightweight but only suitable in settings with less than 10 m of head difference across the packer. When used with 5 cm (2 inch) PVC riser pipe, the packer assembly has the advantage of being light enough that it can be deployed down a borehole with a hand winch. Construction and operation details are given in Appendix B. The straddle packer was deployed at a total of 16 intervals in the borehole with 11 of those containing fractures. The open interval between the packers was 70 cm, which, in most cases, allowed the isolation of single fractures for physical testing and water chemistry sampling.

At each interval the packer was inflated and the water level in the riser pipe was monitored with a pressure transducer using a direct read cable to ensure equilibrium with the packed interval hydraulic head. After the head measurement was recorded, the transducer was set to record water levels at one second intervals. A 2.5 cm diameter and 1.5 m long solid slug was rapidly inserted fully below the water level in the riser pipe for the “slug-in” test. After the water level stabilized, the slug was rapidly removed from the water column as a “slug-out” test. Two sets of “slug-in” and “slug-out” tests were conducted at most intervals. The results of the head measurements and hydraulic conductivity values calculated from slug tests analysis for the straddle packer intervals are shown in Figure 2.6.

Hydraulic conductivities for many packer intervals were evaluated using the KGS, Hvorslev, and Bower-Rice methods for unconfined aquifers (Butler 1998). Some intervals with particularly rapid responses and/or oscillation in the recovery data required utilization of the Springer-Gelhar method (Butler 1998) instead of the KGS method. Although there is some variation in values obtained by the three different methods at each interval, most vary by less than 15%. The unit well was inactive for the majority of the testing but was pumped intermittently based on requirements of the Madison Water Utility. This pumping of the lower aquifer influenced water levels in the isolated zones of the upper aquifer. Changes in water levels due to pumping drawdown or recovery after pumping ceased were accounted for during slug test data analysis by using a trend removal function in the software.

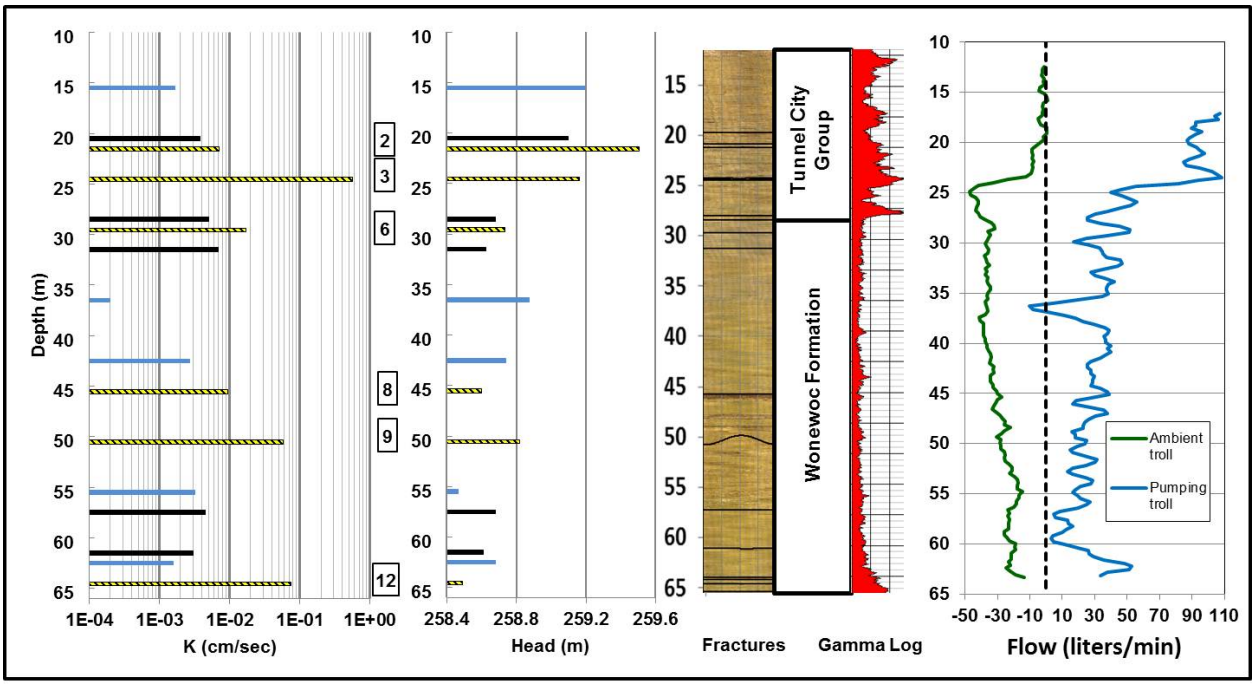

Figure 2.6. Flow characterization results from borehole MW-C. Head and hydraulic conductivity and measurements from straddle packer testing. Lighter bars are measurements from unfractured intevals, solid bars are fractured intervals, and striped bars are key fractures highlighted in this paper and indicated by fracture numbers in boxes. Fractures are shown by lines on OBI log with the gamma log used to show changes in lithology. Flow logging data presented under ambient and pumping conditions with negative flow in the downward direction.

Interval hydraulic conductivity values from the slug tests (Figure 2.6) vary by more than three orders of magnitude. The highest value was from a fractured interval in the Tunnel City Group while the lowest value was from an unfractured interval in the Wonewoc Formation. Although some fractured intervals had higher hydraulic conductivities, other fractured intervals had values similar to those of unfractured intervals. An interval with fractures was considered to be matrix dominated if the hydraulic conductivity was similar to unfractured intervals. Fractured dominated interval values range from

9.4×10^{-3} cm/sec to 5.5×10^{-1} cm/sec with a geometric mean of 5.2×10^{-2} cm/sec. Values for the matrix dominated intervals range from 2.0×10^{-4} cm/sec to 7.0×10^{-3}

cm/sec with a geometric mean of 2.7 x 10^{-3} cm/sec. Changes in hydraulic conductivity do not appear to be related to depth or lithology.

In addition to identifying fractures, it is important to determine which methods are best for identifying the most hydraulically significant fractures. The results of straddle packer slug test hydraulic conductivity values for 12 of the fractured intervals identified in the borehole are listed in Figure 2.5. The hydraulic conductivity values range from 3.1 x 10^{-3} cm/sec to 5.5 x 10^{-1} cm/sec but only four of the values exceed 10^{-2} cm/sec. The two fractured intervals with the highest hydraulic conductivity values were detected by all three logs, while the third and fourth highest values were only detected by the OBI and ABI logs. In order to locate the most hydraulically significant fractures for rapid transport of contaminants, a combination of all three methods is ideal. However, the ABI and OBI tools appear to be superior to using only the mechanical caliper tool for identification of the most hydraulically significant fractures. The potential fractures were considered confirmed when they were detected by both the OBI log and either the mechanical caliper or the ABI log.

3.3. Borehole pumping test

A pumping test in the MW-C borehole was conducted in May 2011 to evaluate aquifer properties. The borehole was pumped for approximately 20 hours at a discharge of approximately 95 liters per minute. Water levels from the shallower monitoring wells and the pumped borehole were analyzed using the Moench (1984) solution for a fractured aquifer with slab blocks. Pumping test data and analyses are included in Appendix C. The bulk transmissivity of the borehole was calculated as 49.9

cm^2/sec with a fracture system value of 28.8 cm^2/sec and a matrix system value of 21.1 cm^2/sec based on a saturated borehole thickness of 54.25 m.

3.4. Vertical Flow Assessment

Vertical groundwater flow in the borehole was measured with two devices: an impeller flow meter for higher flows and a heat pulse flow meter for flows below 3.8 liters per minute. Data were recorded while trolling the tools both upward and downward in the borehole. Flow meter logging was conducted initially under ambient conditions and with the unit well inactive, followed by dynamic flow meter logging by pumping the borehole to stress the system. Logging under ambient conditions initially used the heat pulse flow meter. This instrument was not useful due to high vertical flow in the borehole and the impeller flow meter was required for ambient and dynamic flow logging. The first iteration of dynamic logging utilized a submersible pump with a maximum discharge of approximately 15 liters per minute but this did not adequately stress the system. The second iteration used a larger submersible pump with a discharge of approximately 95 liters per minute. The pumps were placed at the top of the water column and the flow meter logged from the bottom of the borehole upward and then from near the top of the water column downward.

The vertical flow assessment allowed for characterization of the flow in the borehole and identified locations that substantially contributed to changes in flow. Figure 2.6 shows the results of the ambient and pumping flow logging in the borehole using the impeller flowmeter. The ambient flow data are from upward trolling only because at some points during downward logging the tool was moving at nearly the

same velocity as the flow in the borehole. This resulted in relative flow velocities too low to accurately measure with the impeller. Flow at the top of the ambient log is initially downward at approximately 1 liter per minute, then increases to approximately 5 L/min at 23 m bgs before rapidly increasing to greater than 40 L/min after 24 m bgs. This rapid increase in downward flow corresponds to the large fracture at 24.1 m (Fracture 3). The flow decreases steadily between 24 m and 55 m and then remains relatively stable until a sharp decrease at the bottom of the borehole. The reduction in downward flow is probably due to a loss of water into Fractures 8 and 9, although some loss into the matrix of the Wonewoc Formation is possible. Due to a concern of fouling the impeller at the bottom of the borehole, logging was not conducted below 63 m. Because the downward flow has to exit the borehole in order to balance the inflow (i.e. there is no increase in well bore storage) it is assumed that remaining flow exits the borehole from the lowest fractures near 64 m. The pumping flow log data were highly variable and a 3 point moving average is shown in Figure 2.6 to reduce the signal noise. Even with this attempt to smooth the data, two data points near 37 m bgs deviate enough to indicate an apparent reversal of flow in an unfractured, relatively low hydraulic conductivity zone of the Wonewoc Formation. The apparent flow reversal is likely due to an error with the flow meter, possibly due to sediment becoming temporarily lodged in the impeller. It is unlikely that flow reversed in this section of the borehole. Even with the variability in the data it is still possible to see the same sudden shift in flow as was observed in the ambient flow log at Fracture 3.

3.5. Conceptual model for fracture connectivity

Analysis of the shapes of the fracture traces from the OBI log implemented in the software package WellCAD version 4.3 (Advanced Logic Technologies Inc 2009) yielded the orientation of each fracture. Many of the fractures in the OBI log have dip angles between 3 and 11 degrees from the horizontal. The true dip angle may be several degrees different than the measured values due to errors in manually drawn fracture traces on the OBI log. Table 2.3 lists the orientation of the six most important fractures discussed in this paper. The Tunnel City Group and Wonewoc Formation are nearly horizontal at the regional scale but locally some beds may dip at higher angles (Swanson 2007). It is possible that many of the low angle fractures listed in Table 2.3 are bedding plane controlled and detailed analysis of the OBI log indicates these fractures do not cross bedding planes within the MW-C borehole.

Table 2.3. Orientation of selected fractures in borehole MW-C based on WellCAD analysis of fracture log. Transmissivity and head data are from straddle packer slug testing of those intervals.

Fracture Number	Depth (m)	Azimuth (deg)	Dip (deg)	Transmissivity (cm^2/sec)	Head (m)
2	20.9	183	5	0.5	259.5
3	24.1	178	9	39.0	259.2
6	29.0	148	5	1.2	258.7
8	45.5	168	4	0.7	258.6
9	50.0	12	84	4.0	258.8
12	64.3	126	3	5.2	258.5

High angle fractures are difficult to detect in vertical boreholes but are important to understanding fracture connectivity. One high angle fracture was discovered in the borehole at 50.0 m (Fracture 9). This fracture has a dip azimuth of 12 degrees (strike of

102 degrees) and dips to the north at 84 degrees from the horizontal. At this dip angle and direction, if the fracture continues downward, it would intersect the Eau Claire aquitard between the monitoring wells and the unit well with the potential of intersecting Unit Well 7 in the Mount Simon Formation open borehole. Projecting Fracture 9 upward, it would not intersect the other two monitoring wells but would intersect other fractures within a few meters of the MW-A and MW-B well screens.

Work by Runkel et al. (2006) and Swanson (2007) used several methods to identify bedding parallel fractures in these same Cambrian-age siliclastic units based on lithological controls. These methods sought to associate fractures with either stratigraphic position or physical properties of the bedrock in order to facilitate identification of connected fractures between locations. Those methods are useful for fractures that run parallel to bedding planes in a stratigraphic section that does not vary laterally. However, fractures that are not parallel to bedding or not controlled by changes in lithology may be difficult to identify with those methods. Work by Meyer et al. (2008) described the presence of many low angle, bedding plane fractures in these units in addition to some vertical and oblique fractures present in the Tunnel City Group. Data from Table 2.3 indicate some fractures are not horizontal and may not be associated with bedding planes. This is especially true for Fracture 9, which is nearly vertical.

To best visualize the relationships among the fractures, monitoring wells, and the unit well, a conceptual model was created from data obtained from the site. The fractures, monitoring wells, and the unit well were incorporated into a 3D visualization

with the software package FracMan version 7.3 (Golder Associates Inc. 2010). The visualization was then projected onto a north-south oriented 2D plane viewed from the east similar to Figure 2.3. This conceptual model of fracture connectivity (Figure 2.7) was completed by including information about the stratigraphy and fracture hydraulic heads. The data on the orientation and position of the fractures in the upper aquifer are from the MW-C borehole OBI log but the model assumes the fractures extend far enough to connect with each other.

During May 2012 the Madison Water Utility removed the pump from Unit Well 7 in order to perform maintenance. The unit well is cased to 72 m bgs, which is the middle of the Eau Claire Formation, and beneath a 3 m thick shale layer. Geophysical logging data from the UW-7 borehole revealed fractures in the lower portion of the Eau Claire Formation and the Mount Simon Formation. The UW-7 borehole has a much larger diameter than MW-C, ranging from 41 cm to more than 1.0 m in several open voids. This greater diameter reduced the resolution of the OBI and ABI tools. The OBI log indicated a vertical fracture along most of the Unit Well 7. This fracture is likely to be related to blasting of the borehole during well construction to increase production. The fracture in UW-7 is probably not the same high angle fracture (Fracture 9) discovered in MW-C. It is possible a high angle fracture may connect the upper and lower aquifers, but in Figure 2.7 the extension of Fracture 9 in these formations is displayed as a dotted line due to the amount of uncertainty.

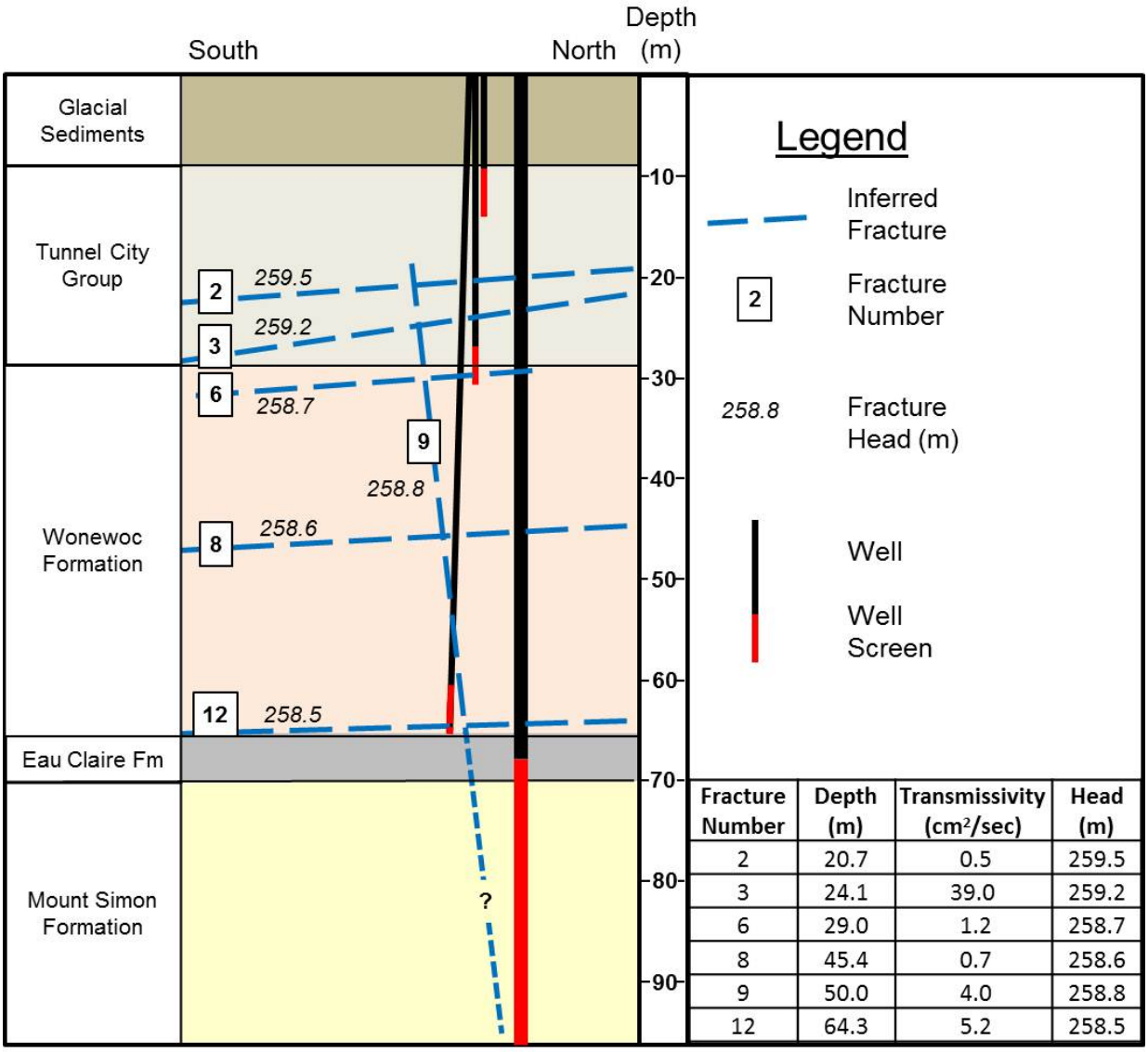

Fracture Number	Depth (m)	Transmissivity (cm^2/sec)	Head (m)
2	20.7	0.5	259.5
3	24.1	39.0	259.2
6	29.0	1.2	258.7
8	45.4	0.7	258.6
9	50.0	4.0	258.8
12	64.3	5.2	258.5

Figure 2.7. Conceptual model of fracture connectivity at Unit Well 7 based on a FracMan model projected onto a north-south plane viewed from the east. The deepest monitoring well (MW-C) deviates approximately 3 m to the south at the bottom of the hole and fracture orientations were adjusted to account for the deviation. Hydraulic head data for each fracture is based on straddle packer testing in the MW-C borehole. The lower 100+ m of the Mount Simon Formation and Unit Well 7 are not shown.

When placed in their proper spatial orientations, the fracture hydraulic heads provide a good match to the expected vertical hydraulic gradient in the upper aquifer that would generate downward flow. In Figure 2.7, the fracture heads in the near horizontal fractures steadily drop with depth from 259.5 m to 258.5 m. The head in

Fracture 9 is 258.8 m, which is close to the 258.9 m average value of the other five fractures and supports the view that this high angle fracture is connected to the others. If Fracture 9 were either not connected to other fractures or terminated before reaching Fractures 8 and 12, the expected head would be between 258.5 m and 258.6 m based on the vertical gradient in this section of the upper aquifer. The head in UW-7, which is open to the Mount Simon Formation, was measured after the well had not been pumped for more than week. In this approximately static condition the head in the lower aquifer was 1.4 m less than the head measured at the base of the upper aquifer in MW-C (Figure 2.3). This is approximately the head difference between the Mount Simon aquifer and the upper aquifer simulated using the numerical groundwater flow model for Dane County, Wisconsin (Krohleski et al. 2000) under similar conditions. Based on head data, it appears that if Fracture 9 extends through the Eau Claire Formation, it is not well connected to the Mount Simon Formation while UW-7 is not pumping. During pumping, the head in the UW-7 borehole can drop up to 49 m from static levels. It is possible that based on the head drop in both MW-B and MW-C that the head in Fracture 9 might drop substantially when UW-7 is pumping and reflect a hydraulic connection with the lower aquifer as the head difference increases substantially.

3.6. Evaluation of hydrogeological properties

As described in previous sections, three methods were used to evaluate hydrogeologic properties of flow in the MW-C borehole: pumping test, straddle packer slug tests, and flow logging. The pumping test investigated bulk properties of the entire saturated thickness of the borehole while the straddle packer determined properties of

distinct intervals, many of those containing fractures. The pumping test data indicate that approximately 60% of the borehole transmissivity is from fractures. Since the fractures are assumed to be responsible for the much higher interval hydraulic conductivities determined from analysis of packer slug tests, the effective hydraulic conductivity value for each packed-off interval containing a fracture was attributed entirely to flow through the fracture. The hydraulic conductivity was multiplied by the 70 cm straddle packer open interval to determine the fracture transmissivity (T_{fi}) [L^2/T] for each fracture using the following formula

$$T_{fi} = K_{fi} \times b_{fi} \qquad (2)$$

where K_{fi} is the hydraulic conductivity [L/T] of packed interval i and b_{fi} is the length of packed interval i [L]. (Note that the slug tests actually measured transmissivity for the intervals but each T had been converted to effective K by dividing by the interval length of 70 cm during the initial data analysis.)

The five fractured intervals accounting for 96% of the fractured transmissivity (Fractures 3, 6, 8, 9, and 12) were added together to calculate the total T_f value of 50.1 cm^2/sec. The other fractured interval data were similar to unfractured intervals and assumed to be dominated by matrix flow. Each of the five fractures was estimated to have a negligible aperture. Therefore, the total matrix thickness (b_m) was assumed to be equal to the saturated thickness of 54.25 m. The matrix hydraulic conductivity (K_m) values of the five unfractured packer intervals had an geometric mean of 1.4 $\times 10^{-3}$ cm/sec and T_m was determined by the formula

$$T_m = K_m \times b_m \qquad (3)$$

as 7.6 cm^2/sec. The total transmissivity of 57.7 cm^2/sec is the sum of the matrix and fracture transmissivity values. Based on packer data, these five fractures represent more than 80% of the total transmissivity in the borehole.

The borehole flow logging provided data for analyzing the contributions of different zones to overall flow. The vertical flow assessment (Figure 2.6) revealed several important pieces of information about flow in the borehole and the importance of fractures. The ambient flow log inflow data from 12 m to 23 m account for approximately 20% of the maximum flow and may be due to a combination of inflow from fractures and aquifer matrix. The remaining 80% of maximum inflow can be attributed to Fracture 3, which had the highest transmissivity value (Table 2.3). Below 25 m the flow decreases, but not uniformly. Approximately 20% of the flow is lost in the vicinity of Fracture 6. Approximately 50% of flow is lost in the next 27 m interval, which contains Fractures 8 and 9, both with high transmissivity values. One of these is the high angle Fracture 9 at 50 m that had the third highest straddle packer transmissivity value. The remainder of the flow (approximately 30% of maximum flow) exits the borehole via Fracture 12, which had the second highest straddle packer transmissivity value.

A more quantitative approach to analyzing borehole flow logging data involves the use of a numerical model to determine transmissivity values of fractured intervals (Paillet 1998; Paillet 2000). The computer program FLASH (Flow-Log Analysis of Single Holes) provides an easy to use interface for modeling flow in boreholes using a multi-layer Thiem solution based on data from ambient and steady state pumping

conditions (Day-Lewis et al. 2011). The FLASH program was used in “Fracture” mode instead of “Layer” mode because even with a combination of fracture and porous media flow in the data, it appeared fracture flow dominated the system. The left side of Figure 2.8 contains the flow logging data overlain with an interpreted profile required by the FLASH program to determine each layer. Interpreted profiles were used as a best fit to the field data and highlighted substantial changes in borehole flow. The greatest inflections in the interpreted data were used as the depths of fracture zones. The right side of the figure is the FLASH output, which includes field data (circles), user defined fracture zone boundaries (dashed lines), and a program simultaneously generated a best fit solution (solid line) for both ambient and pumping data.

The FLASH solution is a good match to the fracture zone boundaries. The solution slightly overestimates the flow at the top of both ambient and pumping flow but closely matches all other sections of the graphs. The transmissivity results of the analysis are presented in Table 2.4. The majority of the transmissivity in the model is from Zones D and C, which approximate the positions of Fractures 12 and 9, respectively. Zones B and A also contain hydraulically significant Fractures 6 and 3, respectively, which account for a substantial portion of the overall transmissivity. Only four layers with substantial borehole flow changes were evaluated with the FLASH program and consequently not all of the transmissivity was accounted for in this analysis. The transmissivity of these four layers associated with fracture flow was calculated at 39.3 cm^2/sec, which compared with straddle packer data is approximately 80% of the fracture T and 65% of the total T.

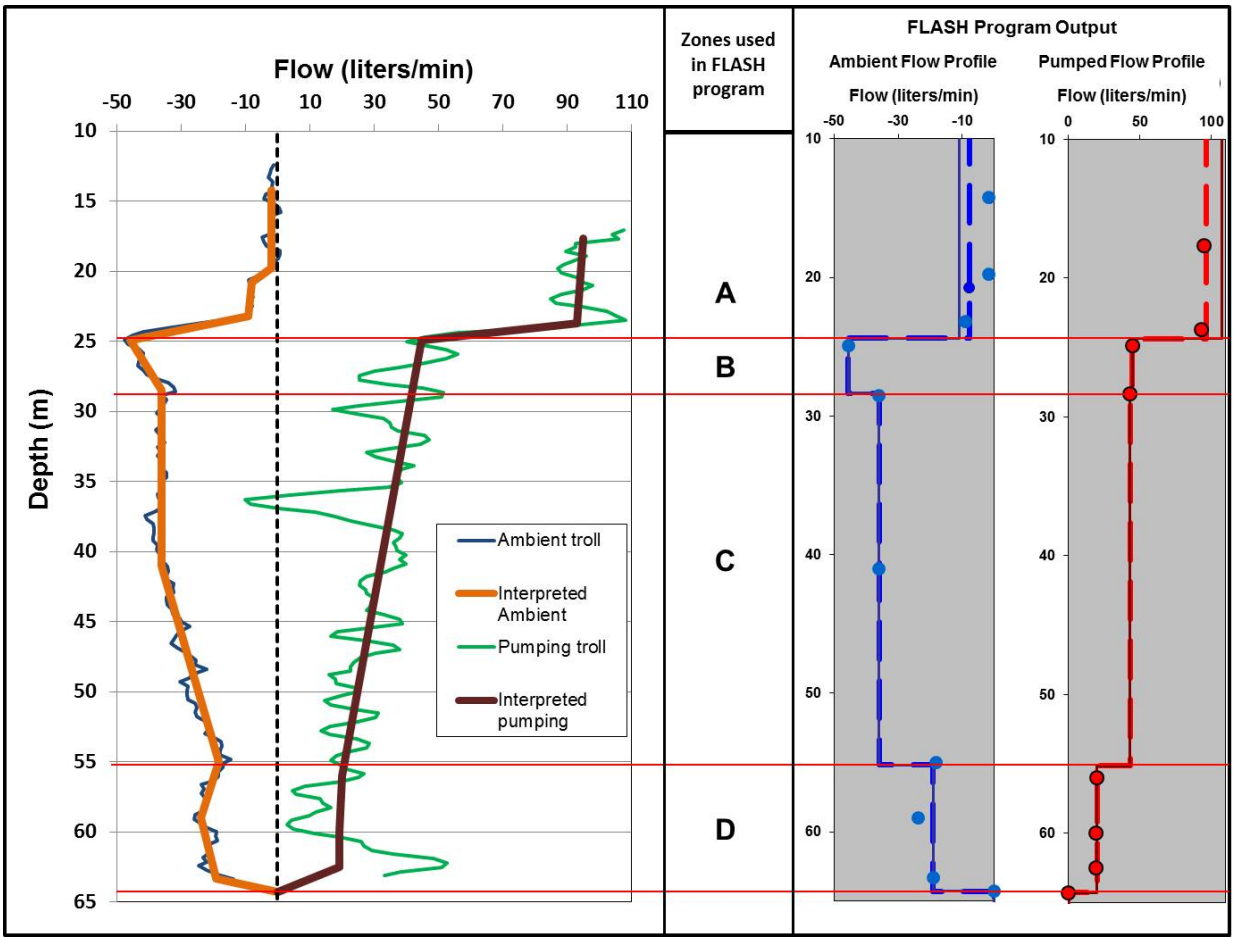

Figure 2.8. Results of borehole flow logging including data from both ambient and pumping conditions. Interpretated lines and layer numbers were used for determining transmissivity values in the FLASH computer program.

Table 2.4. Transmissivity data from the FLASH computer program for layers in borehole MW-C.

FLASH Layer	Fracture Number	Depth [m]	Layer T [cm^2/sec]	Fraction of total transmissivity
A	3	24.9	9.2	0.23
B	6	28.3	3.7	0.10
C	9	55.2	13.3	0.34
D	12	64.3	13.0	0.33

The three methods used to evaluate the aquifer provide similar information about the nature of fracture contribution to flow in the upper aquifer. The total T value for the

pumping test data was 49.9 cm^2/sec with 60% (29.9 cm^2/sec) of the contribution from fractures. The straddle packer data indicate a total T of 57.7 cm^2/sec with 80% (46.2 cm^2/sec) of the contribution from fractures. The flow logging analysis with the FLASH computer program only evaluated the four intervals with the greatest change in flow. Those fractured intervals had a T value of 39.9 cm^2/sec, which is comparable to the fracture values of the other methods. Based on these methods, the majority of transmissivity in the MW-C borehole can be attributed to fractures.

3.7. Comparison of groundwater chemistry between fractures

During August and September 2011 water chemistry samples were collected from 12 of the 16 packed intervals. A submersible pump was used to purge three well volumes from the 5 cm (2 inch) riser pipe before collecting a 1 liter grab sample. Each sample was sent to a laboratory and analyzed for major anions, major cations, and alkalinity. Field measurements of pH, temperature, and conductivity were also recorded from the pumped water at the time of sampling. Plots of selected water chemistry parameters are shown in Figure 2.9. For reference, the position of fractured intervals and monitoring well screens are given on the right side of the figure.

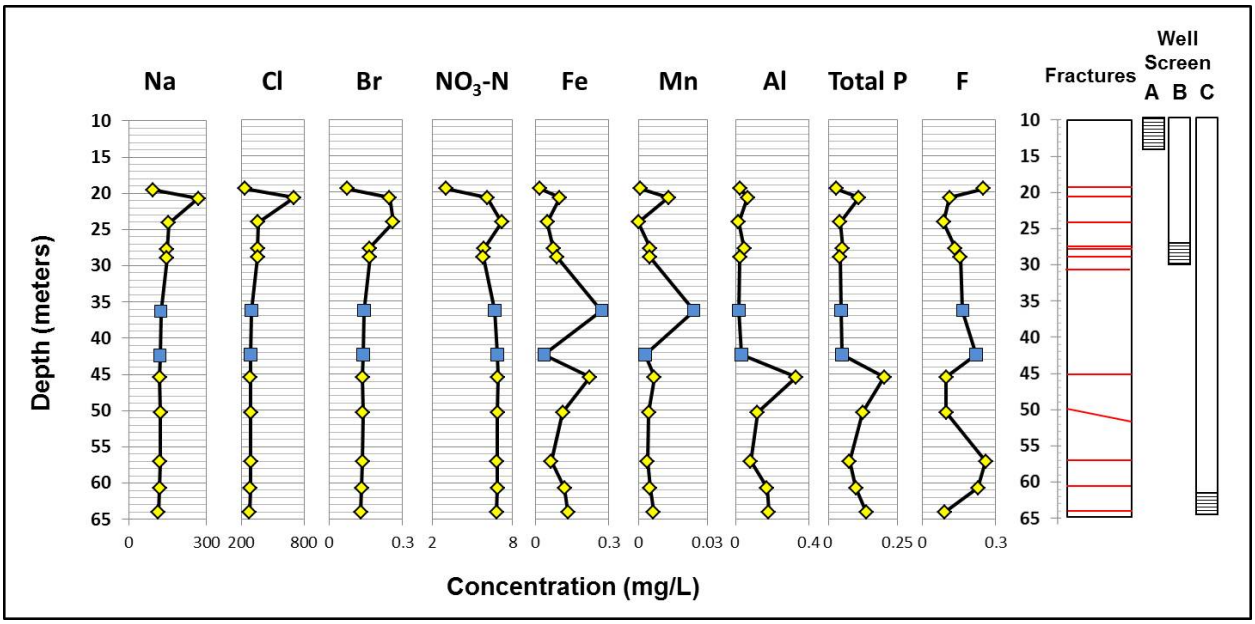

Figure 2.9. Water chemistry data from straddle packer intervals. Diamond data points are fractured intervals and square data points are matrix intervals. Fractured intervals and position of monitoring well screens are included for reference.

The water chemistry data from the summer 2010 preliminary sampling (Table 2.2) revealed higher concentrations of sodium, chloride, bromide, and nitrate in the deeper monitoring well (MW-B) compared with the water table monitoring well. The straddle packer was used in borehole MW-C to sample groundwater with greater spatial resolution than possible using the monitoring wells. The focus was primarily on isolating fractures for sampling, but unfractured intervals were also sampled for comparison. Intervals with fractures were evaluated to determine if they contained high levels of wastewater indicators similar to those found in MW-B. It proved impossible to sample an interval at the same depth as the MW-A well screen because the interval pumped dry during purging and the recovery period following purging was very long.

A comparison of chemical parameters at each interval sampled in the borehole MW-C (Figure 2.9) highlights several interesting relationships. Specific intervals had

concentrations that were either significantly above or below the average values for all straddle packer samples. Fracture 2 contained elevated levels of several constituents also found in MW-B samples. However, the screened interval of MW-B is from 27.5 – 30.5 m and none of the fractures (4, 5, and 6) in that zone that were sampled with the straddle packer contained similar levels of chloride, bromide, or sodium. The wastewater indicator values from Table 2.2 are compared with the addition of data from Fracture 2 in Figure 2.10. The concentrations of chloride, bromide, and sodium in both MW-B and Fracture 2 were higher than other intervals. Conductivity values for Fracture 2 and MW-B (2900 μS/cm and 2428 μS/cm respectively) were approximately twice the values from other sampling locations at the site. The concentration of nitrate was elevated in all packer samples below 20 m and not correlated with other potential wastewater indicators. The source of these wastewater indicators was most likely not groundwater from fractures that intersect the MW-B well screen, but from Fracture 2 that is located at a shallower depth in the aquifer.

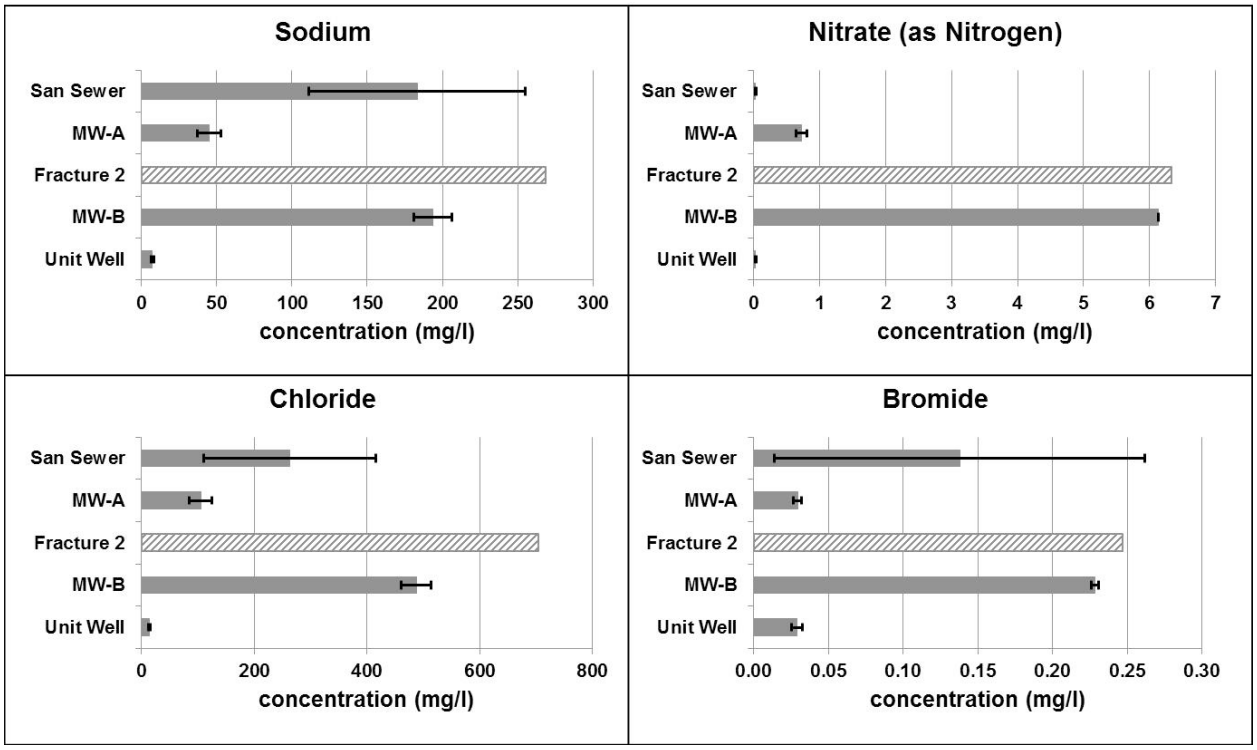

Figure 2.10. Water chemistry data from 2010 sampling (Table 2.2) with the addition of data from Fracture 2 straddle packer interval. Error bars indicate one standard deviation from 6 sampling events.

A preferential flow pathway is the most probable mechanism to allow the groundwater in Fracture 2 to reach the MW-B well screen during sampling. Based on the fracture conceptual model (Figure 2.7), it is likely that the pumping of 1,000 liters of groundwater from MW-B over several hours during virus sampling lowered the head in Fracture 6 and likely the high angle Fracture 9. This enabled the groundwater from Fracture 2 to travel though these other fractures to reach MW-B. The head in Fracture 2 is higher than that for any of the other intervals tested although the T value is lower than that of other fractures in the conceptual model. The reduction in head in Fractures 6 and 9 near the MW-B well screen during sampling may have generated a head difference that was great enough to allow groundwater to rapidly travel to the MW-B well screen.

Electrical conductivity measurements (Table 2.5) taken from several packer intervals in MW-C and the adjacent MW-B well screen under a variety of conditions provide additional evidence of fracture connectivity. Water conductivity measurements during static conditions within the straddle packer were collected with a combination pressure/conductivity logger lowered into the screened interval after heads reached equilibrium with the packed interval. Conductivity measurements from a shallow fracture (Fracture 2) and fractures at the same depth as the MW-B screen (Fractures 4, 5, and 6) during static (non-sampling) conditions were much lower than during sampling conditions. Conductivity measurements collected during geophysical logging of MW-C (Figure 2.4) also show distinct changes near fractured intervals.

Table 2.5. Conductivity measurements of groundwater from selected MW-C straddle packer intervals and MW-B well screen interval.

		Conductivity Measurements (μS/cm)		
		MW-C Straddle Packer Data		MW-B Well Screen
Fracture Number	Fracture Depth (m)	Static Conditions	1 Liter chemistry grab sample (Unit Well off)	1,000 liter Virus sampling at ~4 L/min (Unit Well pumping)
2	20.9	1125	2900	--
4 - 5	27.7 - 28.0	1250	1760	2220 – 2630 (6 samples)
6	29.0	1240	1773	

Changes in conductivity values from static to pumping conditions are useful in analyzing the transient nature of transport through fractures. Beside static conditions, two other types of measurements are listed in Table 2.5. During straddle packer sampling in MW-C, the Unit Well was inactive and the packed interval was pumped with a submersible pump at a rate of 8-10 L/min for approximately 10 minutes to purge the temporary piezometer and collect water chemistry samples. Conductivity readings in all intervals taken after sample collection were somewhat elevated compared with the

static readings, but the conductivity in the Fracture 2 interval was substantially higher than those in the intervals at the same depth as the MW-B screen. During six virus sampling rounds of the monitoring wells in 2010, the Unit Well was pumping due to the need to collect virus samples from that well. A submersible pump sampled MW-B at a low rate (4 L/min) for several hours in order to obtain the required volume of 1,000 liters for the virus sample. Conductivity readings were usually taken from MW-B near the beginning and at the end of sampling and readings were significantly higher than either static levels in MW-B or in the other sampled wells. As mentioned earlier, pressure transducer data indicate pumping of the Unit Well causes a head change in MW-B on the order of tens of centimeters. Sampling of MW-B likely allowed water with higher conductivity and wastewater indicators to reach the MW-B screened interval. Under conditions where sampling is conducted at a higher discharge but for a shorter period of time, the conductivity and wastewater indicator values were much lower.

The data in Figure 2.9 indicate that some fractures in the MW-C borehole contain groundwater with a distinctive chemical composition characterized by either above average or below average concentrations of major ions compared with other sampled intervals. The sample from Fracture 2 contained groundwater with elevated levels of chloride, bromide, and sodium while the sample from Fracture 8 contained high levels of aluminum, iron, and total phosphorus. Although some fractures may have a distinct chemical signature, many other fractures share a similar profile of major ions. These fractures are likely to be more hydraulically connected to each other than fractures with a different major ion profile. Based on the head data from Figure 2.6, there appears to

be no uniform hydraulic gradient in the upper aquifer. However, only looking at fracture head data (Figure 2.7) there appears to be a uniform vertical gradient indicating downward flow. Comparison of fractured interval water chemistry revealed correlations that may indicate they are part of the same flow pathway. The high angle fracture (Fracture 9) and Fracture 6 have similar concentrations of major ions and have similar head values. Fractures that have similar groundwater chemistry and similar head measurements are more likely to be connected to each other.

4. Discussion

Recognition of fractures in an aquifer system may alter the way in which the hydrostratigraphy of the system is evaluated. Although hydrostratigraphic units have been in use for several decades, the general trend is to define units based on the ability of lithologic units to transmit and store groundwater (Maxey 1964; Seaber 1988). More recent work by Meyer et al. (2008) divided the bedrock aquifer system at a site near Madison, Wisconsin using a hydrogeological unit (HGU) concept, which is based on changes in detailed head measurements with depth in a borehole. A head loss of between 2 and 35 percent of the total head in the borehole was used as a basis for delineating distinct HGUs and head values showed a progressive decrease with depth. The boundaries between HGUs are explained by Meyer et al. as poorly connected bedding parallel fractures which limit vertical flow. However, at locations near an active public supply well these changes in head may be dynamic and reflect differences in responses to pumping.

Hydraulic heads measured using a straddle packer in borehole MW-C varied substantially between individual fractures (Figure 2.6) and did not decrease uniformly with depth. In most cases heads increased or decreased between individual intervals with a range of 5 and 46 percent of the total head loss. The unit well was pumping during shallow interval testing but not during periods when data were collected below 30 m. The unit well was pumped each night during the several days of straddle packer testing. This dynamic system likely resulted in fractured intervals achieving steady state heads quickly while the matrix heads took longer to respond. If analyzed separately from other data, the heads in the low angle, high T fractures (Fractures 2, 3, 6, 8, and 12 in Figure 2.6) show a uniform decrease with depth.

In general, straddle packer tests yielded greater interval hydraulic conductivities for intervals containing fractures (Figure 2.6). Both straddle packer and vertical flow logging data indicate the majority of transmissivity in the borehole is related to flow from a small number of fractures. When considering contaminant transport in settings similar to Unit Well 7, the individual fractures may be considered the actual “aquifers” due to much higher transmissivity and contribution to overall flow. The siliciclastic bedrock (mostly sandstone) may therefore act as a “relative aquitard” (especially in the vertical direction) due to transmissivity values several orders of magnitude lower than those of adjacent fractures. This is especially relevant for issues of transport related to viruses and other contaminants that are an acute health threat at very low levels. Fractured sandstone may act as a dual porosity system horizontally and vertically, with certain fractures containing wastewater contaminants under static conditions. Other fractures

may function as vertical and horizontal pathways through which those contaminants migrate under the influence of pumping and the resulting change in hydraulic gradients within the fracture network.

High angle and/or vertical fractures are important for connectivity in a system where the majority of fractures have low dip angles. Logs from the MW-C borehole revealed only one high angle fracture in the Wonewoc Formation that may serve as a near vertical conduit of contaminants. The OBI-40 tool revealed a vertical fracture along most of the Unit Well 7 borehole. The vertical fracture in UW-7 is possibly related to blasting during well construction. Detecting vertical or high angle fractures can be problematic in a vertical borehole due to relative orientations. In addition, high angle fractures may terminate at lithologic boundaries making it difficult to determine if a single fracture extends vertically through the aquifer system to connect several important fractures. It is likely that the high angle fracture (Fracture 9) in MW-C extends upward and connects to the other important fractures previously mentioned. It is also possible Fracture 9 extends downward through the Eau Claire and Mount Simon Formations and connects directly with Unit Well 7. Other boreholes in the Madison area logged by the Wisconsin Geological and Natural History Survey using the same methods as this study have intersected multiple high angle fractures in the same bedrock units involved in this study, specifically high angle fractures in both the Eau Claire and Mount Simon Formations.

5. Conclusion

Microbiological contamination of deep, confined public supply wells in siliciclastic bedrock has generally been considered to be minimal due to assumed travel times that exceed the periods for which viruses remain infective. Advective flow calculations based on porous media assumptions indicate that viruses from sanitary sewers will not reach Madison Unit Well 7 during the 1-2 year period in which the viruses are able to infect humans. However, infectious human enteric viruses have been detected in Unit Well 7 and other deep, confined public supply wells in Madison. Rapid travel times required for infectious viruses to reach public supply wells suggests a preferential flow pathway is the most likely mechanism.

The results of this study support the hypothesis that fractures play an important role in movement of groundwater and transport of sewer derived wastewater contaminants near a public supply well. Based on the work reported here, fracture flow can serve as the primary mechanism of horizontal and vertical contaminant transport in a siliciclastic aquifer system. We have shown that fractures are present and have individual transmissivities several orders of magnitude higher than the remainder of the aquifer system. Most fractures at the study site dip less than 10 degrees from the horizontal and could allow long range, shallow transport of near surface contaminants. Groundwater chemistry is variable among fractures on spatial and temporal scales. The presence of wastewater indicators in Fracture 2 make it the likely source of contaminants detected in MW-B. These contaminants may also reach Unit Well 7, although dilution minimizes the level of major ions to near background levels. Viruses, with their much lower detection limit, can be detected in a public supply well even after

large amounts of dilution. This work has demonstrated a combination of geophysical logging, straddle packer, pumping test, and flow logging data that can be used to quantify the amount of transmissivity attributed to fractures. Furthermore, these methods can be used to identify the most hydraulically important fractures, which is essential to development of a conceptual model of fracture connectivity.

The identification and characterization of fracture flow and its contribution to contaminant transport is an important component of assessing the vulnerability of public supply wells in these settings. In urban areas with sandstone aquifers and public supply wells, leaking sewer effluent may travel greater lateral distances more rapidly than previously considered. The presence of vertical or high angle fractures adjacent to a public supply well could allow contaminants to rapidly migrate downward and enter the well. In fractured aquifers at risk of groundwater contamination, the proximity of a high capacity well is a major factor in contaminant transport. The frequent pumping of a high capacity public supply well can cause rapid, substantial head changes that may propagate through a fracture network. These head changes may alter the flow through the fracture network and allow contaminants to migrate into wells on time scales much faster than under steady state conditions. Wellhead protection strategies for this and similar sites must account for the presence of fractures and their potential role in contaminant transport.

Even in sandstone aquifers it is important to identify fractures and characterize their role in groundwater flow to wells. Unlike traditional applications of hydrostratigraphy, in fractured siliciclastic aquifer systems a small number of individual

fractures with high transmissivity values may serve as the relative “aquifers” supplying the majority of flow to wells and serving as conduits for contaminant transport. The sandstone matrix that may normally be considered the aquifer (but with a much lower transmissivity than the fractures) may serve as a relative “aquitard” that inhibits the migration of viruses and other near surface contaminants on a time scale of several years.

Chapter 3. Pumping induced reverse water-level fluctuations in a fractured siliciclastic aquifer system

1. Introduction

Pumping a confined or semi-confined aquifer can affect hydraulic heads in overlying aquitards and aquifers. In some instances a “reverse water-level fluctuation” (RWF) is observed in which the initial head responses during pumping are the opposite of what is normally expected (Andreasen and Brookhart 1963); pumping of a well in one aquifer causes heads in adjacent units to temporarily rise before falling. Similarly, when pumping ceases, the heads rapidly decrease for a period of time before increasing. The increase in head at the initiation of pumping is termed the “Noordbergum effect” based on the location in the Netherlands where it was first described (Verruijt 1969). The initial decrease in head after the cessation of pumping is called the “Rhade effect” after the location in Germany where it was studied (Langguth and Treskatis 1989). The head changes associated with these RWFs may only be on the order of centimeters and last for a few minutes, which makes them difficult to detect unless the aquitard and/or unpumped aquifers are monitored closely. Anecdotal reports from well drillers and hydrogeologists indicate these phenomena may be more common than reported in the literature and, when observed, they are often ignored.

A RWF in a well is normally caused by poroelastic (also referred to as hydromechanical) coupling between the solid and fluid components in an aquifer system (Wang 2000). An increase in effective stress on the aquifer or aquitard skeleton results in a pore pressure increase. The change in pore pressure is temporary, as the increased pressure diffuses horizontally and vertically through the aquifer system.

Aquitards generally shows more pronounced RWFs than aquifers and play key roles in generating RWFs due to slower head changes and faster mechanical changes across aquitards (Kim and Parizek 1997, 2005). The terms “Noordbergum effect” and “Rhade effect” generally refer to poroelastically coupled responses in aquitards and aquifers at the start of pumping and the start of recovery, respectively. In this paper the more general terms “Noordbergum response” and “Rhade response” are used to apply both to RWFs directly attributed to poroelastic effects in aquitards and also to RWFs that may involve transmission of a poroelastically generated RWF through fractures.

Most documented poroelastic water level changes are caused by pumping, although loading of an aquifer skeleton may also be the cause of these events. A classic example of water fluctuations in a well caused by poroelastic loading was described by Jacob (1939). In Jacob’s study as a train entered a station, the additional weight compressed the aquifer and resulted in a temporary increase in water level in a nearby well. When the train left the station the load was removed from the aquifer and the water level decreased. The release of upstream dam water and resulting increase in stream stage has also been shown to increase poroelastic loading of an aquifer and generate water level changes in wells (Boutt 2010). Hsieh (1996) developed a model to simulate deformation-induced effects of pumping on a confined multi-aquifer system.

Understanding the mechanisms and consequences of RWFs might help explain contaminant transport processes near water-supply wells in bedrock aquifers. Work by the Wisconsin Geological and Natural History Survey (WGNHS) has detected human enteric viruses in multiple public supply wells in Madison, Wisconsin (Borchardt et al.

2007; Bradbury et al. 2010). The viruses likely originate in leaky sanitary sewers and travel through the aquifer system before entering the deep public supply well. The WGNHS work did not determine transport pathways or how the pumping rate, duration, and cycling frequency of the public supply wells may contribute to the rate of virus transport. Anecdotal reports from Madison water utility workers indicate that RWFs in observation wells occur commonly during pumping tests of many Madison wells, though these short-term effects are usually ignored. Another unresolved question is whether the cased and grouted portions of the public supply wells have failed and now act as preferential flow pathways for near surface contaminants to enter the well.

The purpose of the research described in this paper is to utilize water level changes and the presence of RWFs to assess the potential impact of public supply well pumping on contaminant transport in a fractured siliclastic aquifer system. Pressure transducers were placed in a number of wells in a shallow, semi-confined, fractured sandstone aquifer to assess the impact of pumping from a deeper confined aquifer. Monitored wells varied in depth and distance from the public supply well. Reverse water-level fluctuation data were analyzed to determine magnitude and duration of the fluctuations with respect to depth in the aquifer and distance from the pumping well. Parameters that may affect RWFs include pumping rate, pumping cycle duration, fracture connectivity, and the integrity of the public supply well casing. The combination of RWFs, fractures, and public supply well pumping may result in more rapid transport of contaminants through the system than previously considered. Hydromechanical modeling of a simulated layered aquifer system by Kim and Parizek (1997) suggested

that irregular pumping and associated poroelastic effects may increase vertical transport of solutes.

The study area is centered on Unit Well 7 (UW-7), a public supply well located in Madison, Wisconsin, that was constructed in 1939 and has a capacity of approximately 8,300 liters per minute. The well is fully cased and grouted through two Cambrian-age units: the Tunnel City Group and Wonewoc Formation, two sandstone units that form the upper aquifer, and partially cased through the Eau Claire Formation, a regional aquitard that includes a 3 m thick shale interval at the field site (Figure 3.1). The well is open to the primary sandstone aquifer in Madison, the Cambrian Mount Simon Formation, and well logs from the time of construction report a diameter of 41 cm within the uncased interval. Three 5 cm diameter PVC monitoring wells (MW-A, MW-B, and MW-C) were constructed near UW-7 to evaluate the upper aquifer.

Most of the neighborhood surrounding UW-7 consists of single family homes that predate the construction of the unit well. Many of these houses were built before public water supply was available in the area and, therefore, most houses had a private well that was open to the upper aquifer. Although the neighborhood eventually connected to the city water supply, not all private wells were properly abandoned. Some of these wells are still present in basements as open conduits to the subsurface, including three in the neighborhood that were recently identified by the Madison Water Utility. Instead of being immediately abandoned, these were temporarily left open and included in the study as additional monitoring wells. Details of these house wells are listed in Table 3.1

and the location of each is shown schematically in Figure 3.1 and in map view in Figure 3.2.

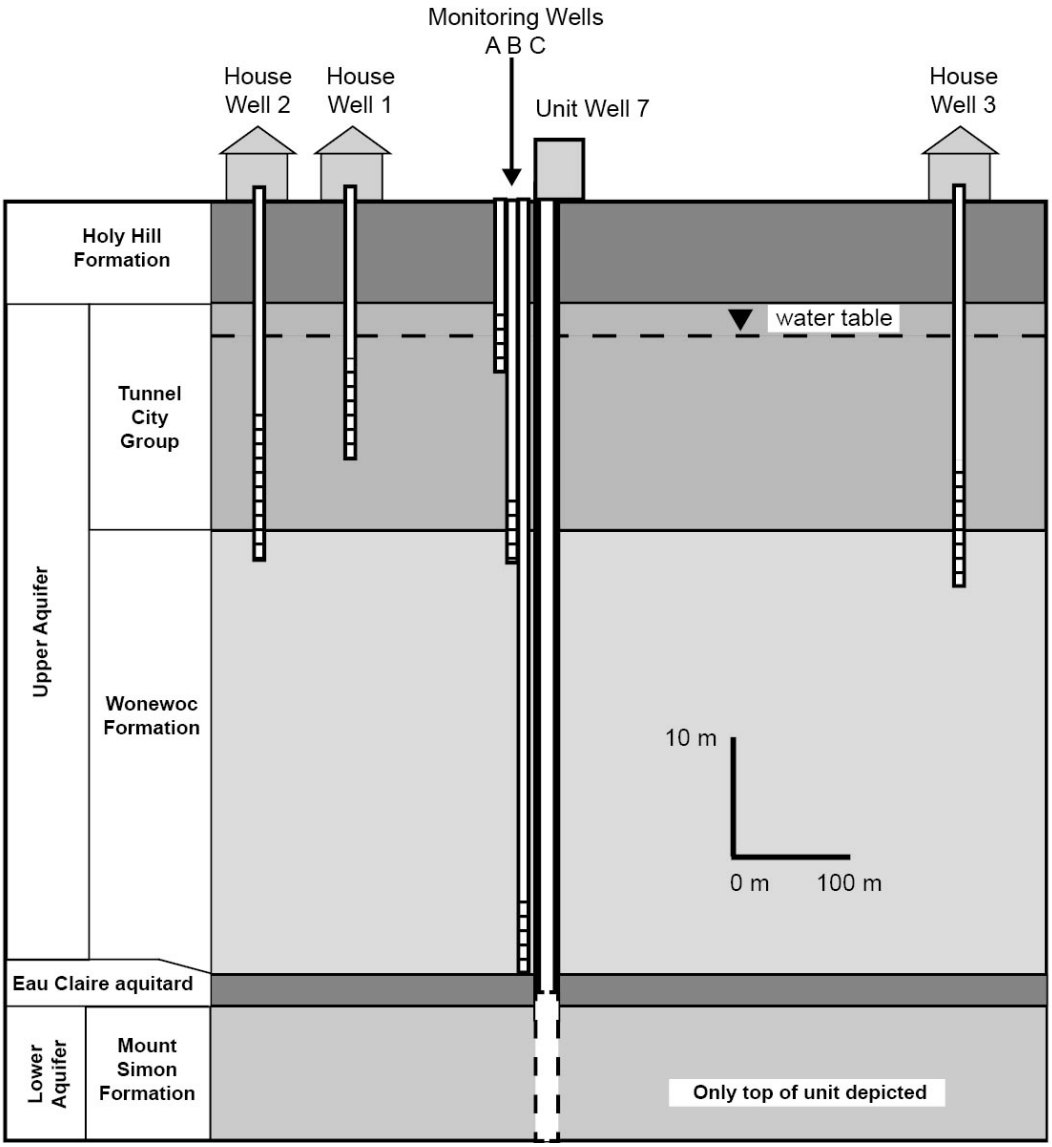

Figure 3.1. Cross section including Unit Well 7, monitoring wells, and house wells. The three monitoring wells are approximately 6 m from the unit well. The total thickness of the Mount Simon Formation is more than 150 m and the unit well is open to most of the Mount Simon Formation, but only the top portion is shown.

Table 3.1. Construction data for monitoring and house wells in the study. Open Interval refers to lengths of slotted screen for monitoring wells and of the open borehole for house wells.

Location	Diameter (cm)	Top of Casing Elevation (m)	Well Depth (m)	Open Interval (m)	Distance from UW-7 (m)
MW-A	5	271.2	14.6	4.6	6
MW-B	5	271.1	30.5	3	6
MW-C	5	271.2	65.5	3	6
House 1	13	267.2	20.4	Unknown	155
House 2	13	265.1	24.8	Unknown	235
House 3	13	268.6	32.0	10.7	345

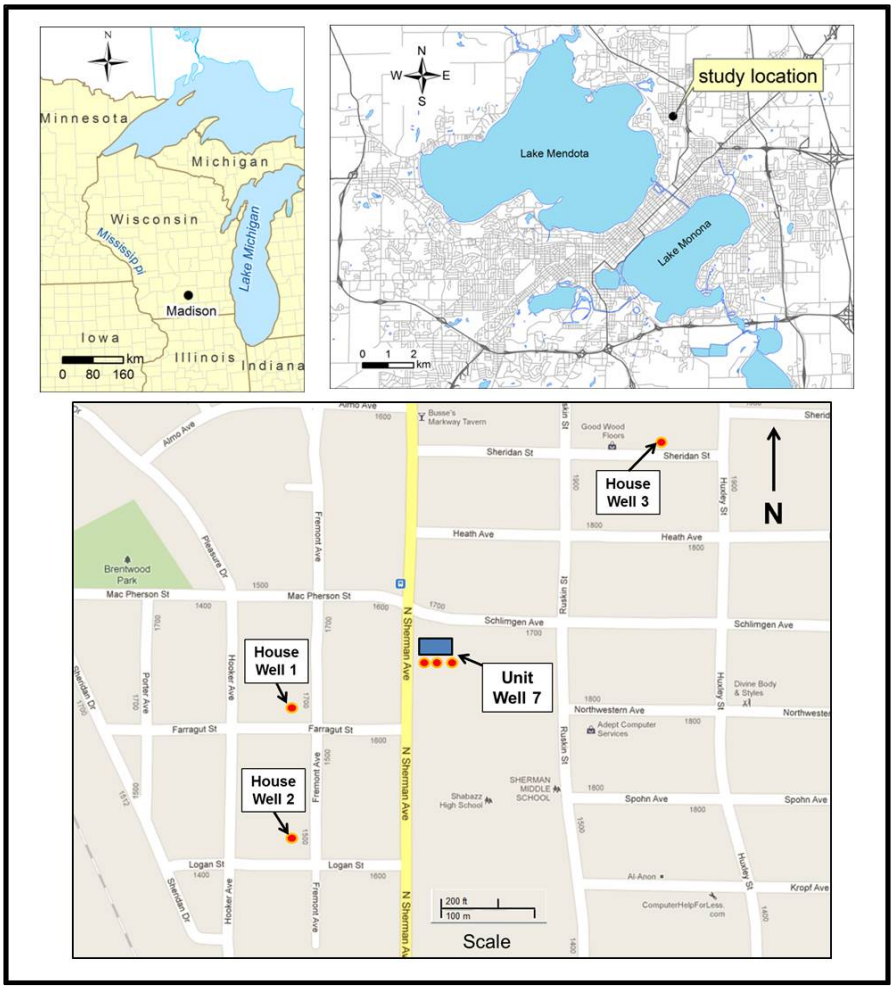

Figure 3.2. Location map of Unit Well 7 with monitoring well nest and instrumented house wells in Madison, Wisconsin.

In order to determine the impact of UW-7 pumping on the upper aquifer, the wells listed in Table 3.1 were each instrumented with a data logging pressure transducer. Both MW-A and MW-B were instrumented shortly after construction in April 2010; MW-C received a transducer in December 2011. The three house wells were instrumented during the summer of 2011, after they were identified by the Madison Water Utility and the home owners agreed to participate in the study. From April 2010 to April 2011 data were collected at 5 minute intervals; after April 2011 the sampling interval was decreased to 1 minute to allow for greater resolution.

2. Methods and Results

2.1. Initial RWF observations

The data collected during 2010 from MW-A and MW-B revealed RWFs in the upper aquifer. The hydraulic head in MW-A was 77 cm higher than in MW-B under the relative steady state conditions prior to UW-7 pumping on June 14, 2010 (Figure 3.3a). This head difference indicates that vertical flow was in the downward direction. Once UW-7 began pumping from the lower aquifer at approximately 7:00 AM (Figure 3.3b), the situation in the upper aquifer changed. The head in UW-7 declined on the order of 10 to 30 m during each pumping cycle. The water table (MW-A) remained relatively stable, but the water level in the deeper well (MW-B) experienced a sudden, substantial response to each of the three pumping cycles.

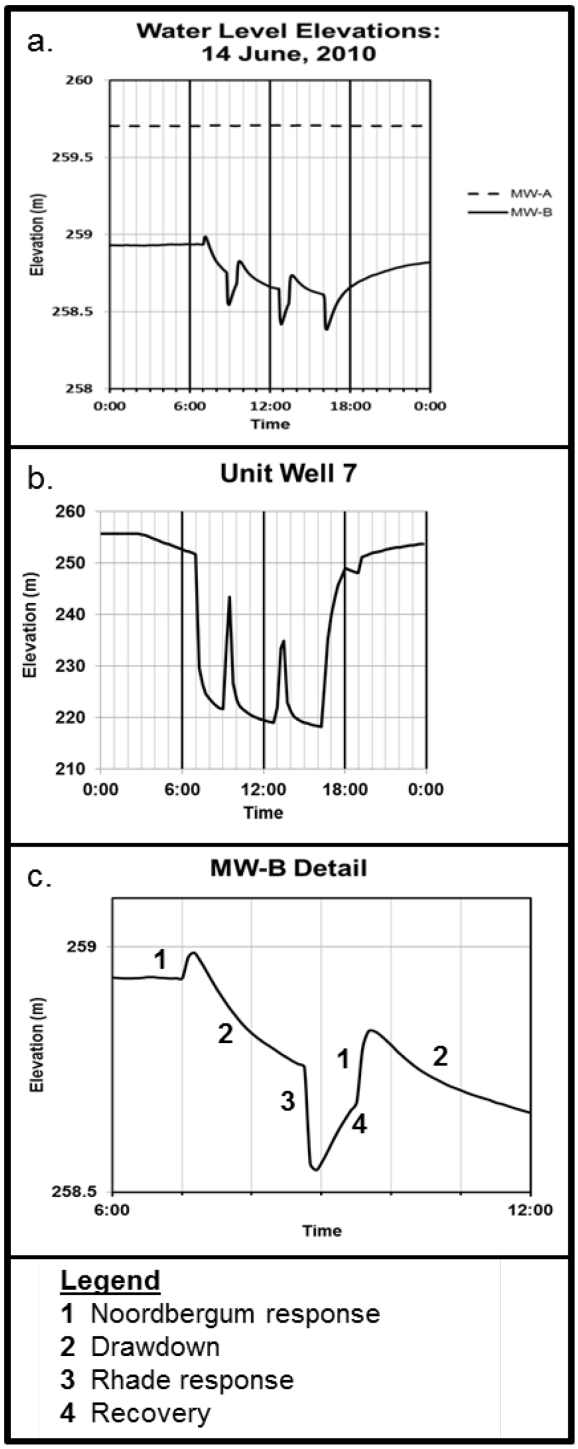

Figure 3.3. a. Monitoring well water elevation data from a 24 hour period in June 2010 showing both MW-A and MW-B. b. Unit well elevation for the same period with three pumping and recovery cycles during this time span c. The detailed figure of MW-B highlights the four responses related to pumping of the unit well over a 6 hour period.

Not only were the water level responses in MW-B substantial, they were unusual. A more detailed view of the MW-B responses (Figure 3.3c) displays four separate components, which are identified as (1) an initial Noordbergum response, (2) drawdown due to pumping, (3) a Rhade response as the well ceased pumping, and (4) recovery. These four components of response in MW-B were seen consistently each time the unit well was pumped. The presence of RWFs suggested, first, a poroelastic response in the Eau Claire formation and, second, a hydraulic connection between the upper and lower aquifer.

2.2. Subsequent site changes

Between June 2010 and June 2012, UW-7 pumping rates changed and a new monitoring well MW-C was installed at the site. During June 2010, UW-7 produced approximately 8,300 liters per minute (Table 3.2). From summer 2011 until May 2012, the UW-7 pump discharge steadily decreased, apparently due to a failing pump, and pumping duration was increased to compensate. During February 2012, with discharge at approximately 3,500 liters per minute and other unit wells offline for maintenance, pumping at UW-7 was almost continuous to meet demand. In June 2012 a new pump motor was installed, which allowed the well to again produce approximately 8,500 liters per minute.

Table 3.2. Comparison of Noordbergum and Rhade responses and Unit Well 7 discharge in MW-B for 5 periods during the study.

MW-B Comparison Data						
		Jun-10	**Aug-11**	**Dec-11**	**Feb-12**	**Jun-12**
Noordbergum	magnitude (cm)	12.42	10.14	1.53	3.08	21.94
	duration (mm:ss)	10:00	13:47	02:52	05:04	15:12
Rhade	magnitude (cm)	-20.24	-10.03	-3.80	-3.21	-24.29
	duration (mm:ss)	06:40	14:00	03:52	03:58	09:20
Unit Well Discharge (L/min)		8,300	5,400	4,400	3,500	8,500

In April 2011 the MW-C borehole was drilled to a depth of 65 m. This borehole was left open for approximately five months to allow for analysis of fracture connectivity in the upper aquifer using borehole geophysics, vertical flow logging, straddle packer slug testing, and pumping tests . While the borehole was not being logged or tested, a blank FLUTe ® flexible borehole liner was installed and pressurized by filling it with water to approximately 30 cm above the static water level. The liner was used in a manner similar to that described by Keller (2012) to seal the wall of the borehole and prevent vertical flow that may allow contaminants to migrate rapidly.

Well responses to pumping during the time periods listed in Table 3.2 were compared to determine what factors might contribute to the occurrence of RWFs in the upper aquifer. The relative magnitude and duration of RWFs in MW-B for each period are presented in Table 3.2. The responses of the other wells are presented as ratios with respect to MW-B in Table 3.3. Unexpected responses in MW-A, MW-B, and the three house wells were observed after the liner was installed in MW-C. These responses over a 48 hour period in August 2011, spanning two pumping cycles, are displayed in the left column of Figure 3.4. Unlike the initial responses from June 2010 (Figure 3.3), MW-A responses to UW-7 pumping included noticeable RWF events. The

three house wells also responded in a similar manner as MW-A. The responses in all wells were nearly simultaneous. For each pumping cycle the magnitudes of the corresponding Noordbergum and Rhade responses were roughly equal, as quantified by the magnitude ratios listed in Table 3.3.

Table 3.3. Ratio of reverse water-level fluctuation magnitude and duration in instrumented wells for several periods compared with MW-B.

			MW-A	MW-B	MW-C	House 1	House 2	House 3
Aug-11	Noordbergum	magnitude	0.12	1.00	No Data	0.06	0.35	0.30
		duration	4.41	1.00		1.38	2.58	3.51
	Rhade	magnitude	0.16	1.00		0.06	0.31	0.28
		duration	3.86	1.00		1.39	2.43	3.36
Dec-11	Noordbergum	magnitude	--	1.00	12.49	--	--	--
		duration	--	1.00	9.13	--	--	--
	Rhade	magnitude	--	1.00	3.18	--	--	--
		duration	--	1.00	8.86	--	--	--
Feb-12	Noordbergum	magnitude	--	1.00	4.13	--	0.74	0.61
		duration	--	1.00	4.99	--	6.30	9.22
	Rhade	magnitude	--	1.00	4.69	--	0.63	0.34
		duration	--	1.00	5.80	--	5.81	7.60
Jun-12	Noordbergum	magnitude	--	1.00	1.16	--	0.20	0.14
		duration	--	1.00	1.66	--	2.01	2.83
	Rhade	magnitude	--	1.00	1.21	--	0.21	0.11
		duration	--	1.00	2.13	--	2.05	1.74

-- No reverse wate-level fluctuation detected

It is important to note that although the arrival of RWFs occurred at similar times in all wells, the magnitudes of the RWFs were largest in MW-B (Table 3.3). The two farthest wells (Houses 2 and 3) had larger magnitude ratios than MW-A and House 1 but are also deeper than MW-A and House 1. Both MW-A and House 1 are completed entirely within the Tunnel City Group and are less likely to intersect the high transmissivity fractures detected in MW-C by geophysical logging. The RWF magnitudes are more closely correlated to well depth than to distance from the pumping well. The durations of RWFs in the house wells do appear to correlate with increasing

distance from the unit well. However, the longest durations are for MW-A, which is closest to the unit well.

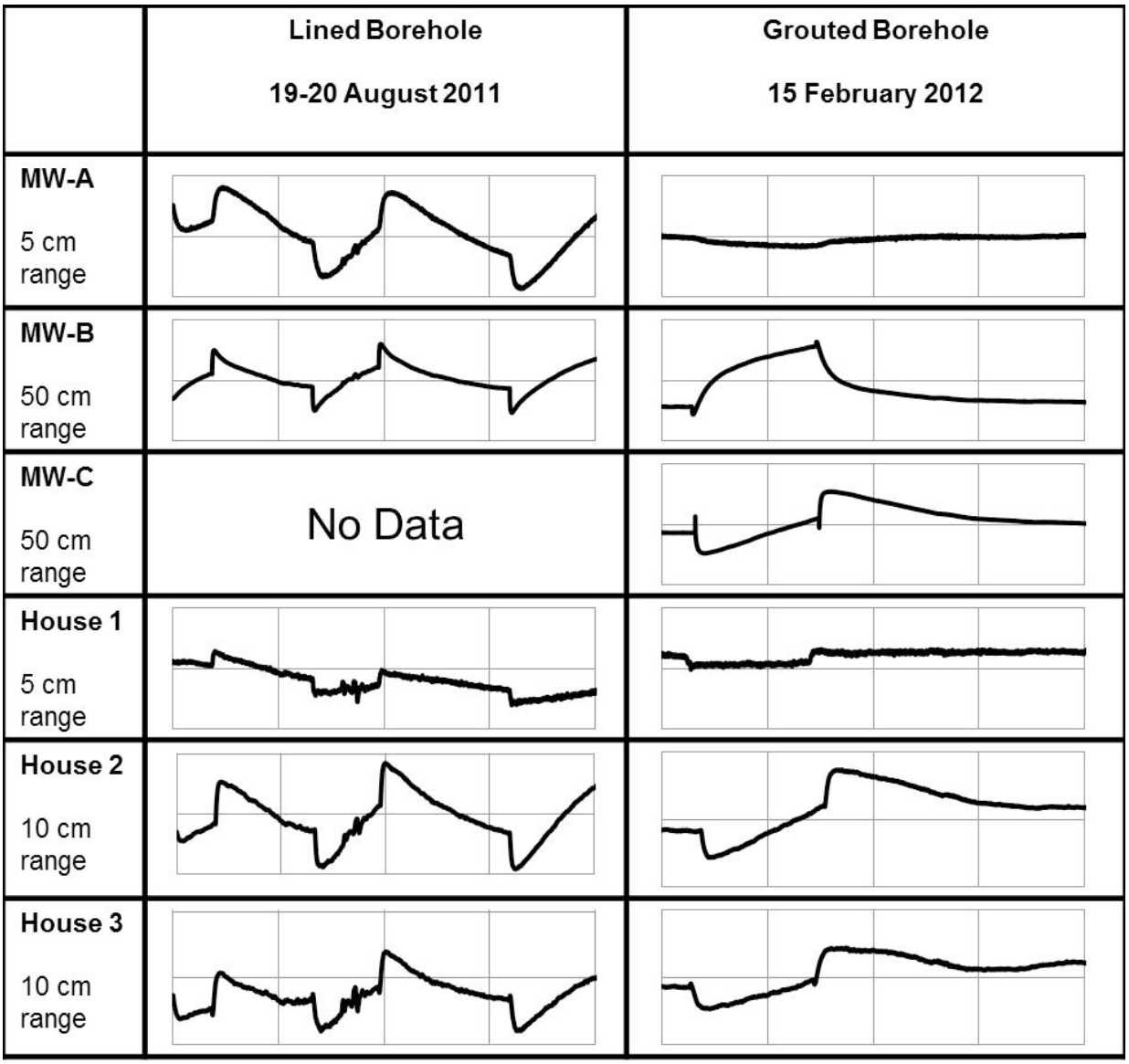

Figure 3.4. Water level data from monitored wells during August 2011 and February 2012. The vertical scale is different for each site with a range between 5 cm and 50 cm.

Once MW-C was installed and instrumented, with the annular space grouted in December 2011, another set of unexpected changes occurred in the instrumented wells. The right side of Figure 3.4 displays water levels in all instrumented wells over a

24 hour period in February 2012, which included a recovery cycle between two long pumping cycles. Wells MW-B, MW-C, House 2, and House 3 display RWFs (Table 3.3). The magnitudes of RWFs in MW-B were much lower with MW-C grouted than they had been when the borehole was lined with the FLUTe. The responses to pumping of the lower aquifer that were detected in the house wells and MW-A during August of 2011 appear to be enhanced by the presence of the borehole liner in MW-C.

3. Discussion

3.1. Mechanisms for RWF propagation

All the observation wells, except MW-C, are open in the upper aquifer tens of meters vertically and/or hundreds of meters laterally from the location of pumping in the lower aquifer. Inducing and sustaining a classic ”Noordbergum effect” as described originally by Verruijt (1969) is unlikely because a poroelastic mechanism at such distances requires high compressibility and low hydraulic conductivity, common in aquitards, but uncommon in aquifers. Alternatively, reduced heads in the lower aquifer may generate a poroelastic effect in the overlying aquitard, which then may subsequently affect the overlying aquifer. In a setting with RWFs at distances of more than 100 m radially from a pumping well, Burlingame (2008) used inverse hydromechanical modeling to match field data from the pumped aquifer and two overlying aquitards. However, the RWFs were observed only in aquitards, RWFs lasted for several hours, and there was a time lag between pumping and the observed RWFs. The modeling did not simulate any wells adjacent to the pumping well to evaluate RWF

propagation or radial head change. It does not appear that this scenario is the same as that at Unit Well 7.

It is unlikely that pumping of UW-7 caused simultaneous poroelastic effects in the Eau Claire aquitard both adjacent to the unit well and at a radial distance of more than 100 meters. Using hydrogeologic data for Dane County, Wisconsin (Bradbury et al. 1999) a Theis drawdown solution for the Mount Simon Formation was calculated for radial distances of 6 m and 150 m while UW-7 was pumping at 8,300 l/min. After one minute of pumping, the Theis solution predicted 8.2 m of drawdown at a radial distance of 6 m from UW-7. The same 8.2 m drawdown was not predicted at a distance of 150 m until after 10 hours of pumping and the solution predicted only 34 cm of drawdown after 5 minutes. Rapid head changes in the pumped aquifer are required to generate a poroelastic response in the overlying aquitard. The pumping rate also varied substantially over the two year study period and the reduced pumping rate during part of the study period would have increased the time for head changes to propagate radially and reduced the likelihood of a large poroelastic response.

It is also possible that surface loading may be responsible for the RWFs. Adjacent to the UW-7 pump house is a 568,000 liter above ground reservoir. As the reservoir fills and drains it changes the surface load similar to the trains described by Jacob (1939). If surface loading were the cause of the RWFs, the shallowest wells would experience the greatest magnitude fluctuations and the RWF magnitude would diminish rapidly with radial distance. The water table well (MW-A) close to UW-7 does not exhibit typical RWFs in most cases. It should also be noted that during the near

constant pumping of UW-7 in early 2012 the reservoir was not filling and draining but RWFs were still observed when the unit well briefly ceased pumping. Therefore, it is unlikely that surface loading at UW-7 is the mechanism for generating RWFs at this site.

After eliminating the above scenarios, the focus in this discussion is to examine how RWFs can occur tens of meters above and hundreds of meters radially outward from the open portion of the unit well. Each hypothesis is based on an initial poroelastic Noordbergum effect in the Eau Claire Formation near UW-7.

The first possibility examined is that the induced Noordbergum effect just below the bottom of the MW-C borehole (the top of the Eau Claire Formation) caused a change in pore pressure in the water filled borehole liner (FLUTe). This increased fluid pressure in the water filled liner would then cause mechanical loading outward from the borehole and influence the other wells. The Kirsch solution, developed in 1898 and commonly used in rock mechanics, describes the effect of stress acting on boreholes (Jaeger et al. 2007). The relevant portion of the solution is the pore pressure term, which indicates that the effect of a pore pressure change decreases away from the borehole as the ratio $(a/r)^2$, where a is equal to the borehole radius and r is equal to the radial distance from the borehole center to the observation point. Using this relationship, given a borehole with a diameter of 0.15 m and a radial distance of 100 m, the pore pressure effect in the observed well would be approximately 10^{-6} of the borehole change. However, the observed RWFs in the house wells during August 2011 were only one order of magnitude less than those in MW-B, which is adjacent to the unit

well. Although the Kirsch solution might explain a near instantaneous response in the house wells, the calculated magnitude is much lower than what was observed.

A more likely scenario is that the sudden poroelastic fluid pressure changes at the bottom of the borehole propagate through a thin layer of water between the borehole wall and the FLUTe liner. The hydraulic head inside the liner following installation was initially 30 cm greater than the head in the borehole, but measurements several weeks later indicated the internal head had fallen over time. The FLUTe used in MW-C had been used previously by the Madison Water Utility on other projects and may have developed a small leak. The Noordbergum response observed at the top of the Eau Claire could increase the hydraulic head at the bottom of the borehole enough to overcome this head difference and allow a pressure change to propagate along the outside of the liner.

This scenario offers a second potential mechanism for RWF propagation over large radial distances in the upper aquifer, namely that the fluid pressure change outside of the liner propagates outward as a pore pressure change based on hydraulic diffusivity. In order to test the feasibility of this mechanism, hydraulic diffusivity was calculated for the aquifer matrix as

$$C = {}^{K}/_{S_S} = {}^{T}/_{S} \qquad (1)$$

where C is hydraulic diffusivity, K is hydraulic conductivity, S_s is specific storage, T is transmissivity, and S is storativity. Slug tests of matrix intervals for the MW-C borehole yielded estimates of these parameters, which are listed in Table 3.4. Matrix S

values varied between 10^{-1} and 10^{-11} for KGS slug test analyses (Accompanying material CD) and ranged from 10^{-1} to 10^{-9} using the Moench (1984) solution for pumping test analyses (Appendix C). The highest matrix S value of 5.4×10^{-2} (Table 3.4) was used because it was within the range of expected values for the semi-confined upper aquifer.

Table 3.4. Aquifer matrix and fracture properties based on straddle packer slug test data and pumping test data.

	Transmissivity (cm^2/sec)	Storativity (dimensionless)	Hydraulic diffusivity (cm^2/sec)
Aquifer Matrix	7.6	5.4×10^{-2}	1.4×10^{2}
Horizontal Fracture (max T)	39	5.0×10^{-6}	7.8×10^{6}
Horizontal Fracture (base of Wonewoc)	5.2	5.0×10^{-6}	1.0×10^{6}
Vertical Fracture	4.0	5.0×10^{-6}	8.0×10^{5}

Once the hydraulic diffusivity, C, was estimated, the travel time of a pore pressure signal between points was calculated as

$$t = {x^2}/{4C} \qquad (2)$$

an equation derived from heat flow literature (Carslaw and Jaeger 1959) and adapted for poroelasticity (Wang 2000) where *t* is travel time and *x* is distance between points. Assuming the poroelastic effect originates near the bottom of the MW-C borehole, vertical and horizontal distances were calculated for the other monitoring wells and the house wells. The results of travel time calculations for each location are presented in Table 3.5. It would take hours to days for pore pressure changes to propagate outward by matrix diffusion. Therefore it is unlikely that a change in borehole pressure propagating outward by matrix diffusion is the cause of the house well RWFs.

Table 3.5. Estimated travel time (in seconds) between the base of the Wonewoc Formation at borehole MW-C and other instrumented locations.

	Vertical		Horizontal		
Name	MW-B	MW-A	House 1	House 2	House 3
Distance	35m	53m	155m	235m	345m
Aquifer Matrix	2×10^4	5×10^4	4×10^5	1×10^6	2×10^6
Horizontal Fracture (max)			8	18	38
Horizontal Fracture (base)			60	130	290
Vertical Fracture	4	9			

It is reasonable to assume that groundwater flows along preferential pathways within highly transmissive fractures. This has been demonstrated in other fractured systems to account for larger than expected responses in wells at early times (Schweisinger et al. 2011). While it would be desirable to conduct a set of calculations for propagation of a pressure pulse through fractures for comparison to the matrix travel times, estimating the appropriate parameters for fractures can be problematic because fracture pathways are not likely to have uniform apertures and the presence of asperities further complicates any estimates.

Nevertheless, preliminary calculations were conducted using available parameter estimates In order to provide an “order of magnitude” comparison between fracture and matrix travel times. Values of fracture T were taken from slug tests of fractured intervals in MW-C. Most fractures identified at the site are horizontal or have a dip of less than 5 degrees. Two values for horizontal fractures were used in these calculations and are listed in Table 3.4. One is the highest T measured for a horizontal fracture, located more than 40 m above the Eau Claire Formation (labeled “max” in the table); the other is for a fracture located at the base of the Wonewoc Formation (labeled “base” in the

table). Only one high angle, near vertical fracture was identified in the MW-C borehole and that T (4.0 cm^2/sec) was used for vertical calculations.

Slug tests for the fractured intervals yielded responses that were too rapid to allow estimates of fracture storativity. For that reason, a rough estimate of this parameter was obtained using results from the pumping test conducted on MW-C (Appendix C). The Moench (1984) double porosity solution for pumping tests provides a specific storage value for the entire “fracture system” that includes all fractures in the total saturated thickness of the aquifer. The “fracture system” Ss value of 1.1 x 10^{-8} was obtained from observations in MW-B, which have the best early time type curve fit of the three wells (Appendix C) and also approximated values based on similar research (Rutqvist et al. 1998). The average fracture S of 5.0 x 10^{-6} (Table 3.4) was obtained by multiplying the “fracture system” Ss by the saturated thickness of 54.25 m and then dividing by the total number of fractures (12) identified in the upper aquifer. Travel times to the house wells calculated for the fractures (listed in Table 3.5) range from 8 seconds to about 5 minutes, short enough to account for the rapid propagation of RWFs observed at these locations.

Based on these calculations, as well as the fact that RWFs continued to be observed in multiple wells following grouting of the annular space in MW-C, it appears likely that the RWFs propagate through fractures. The increased water pressure at the top of the Eau Claire Formation could propagate radially outward away from UW-7 through one of the several low angle, high transmissivity fractures identified in the MW-C borehole. The responses in wells indicate that the pressure pulse travels in both

vertical and horizontal directions. The high angle fracture is likely to also propagate the RWFs vertically, although less effectively than through the MW-C borehole liner annular space.

3.2. Water level changes prior to RWFs

While examining the data related to the RWFs, another effect was also detected in some wells. At the initiation of pumping, the water level suddenly dropped for one recording interval (between 15 seconds and 1 minute) before the Noordbergum response caused the water level to increase. The opposite occurred when pumping ceased and there was a brief increase in water level before the Rhade response caused levels to decrease. These effects are evident in the MW-C data from December and June in Figure 3.5 and had magnitudes approximately one tenth of the subsequent RWFs. They were normally detected in MW-C, House 2, and House 3; when the FLUTe liner was installed in August 2011 the effect was also observed in MW-B.

A likely mechanism for these short duration water-level fluctuations before the RWFs is a rapid response to pumping transmitted via fractures. When pumping begins, a head drop can propagate from the lower aquifer through a fracture network that includes the Eau Claire aquitard and the upper aquifer. This head drop can then be briefly detected in some wells before poroelasticity can generate a RWF. A short time later, the pumping creates a poroelastic effect in the Eau Claire aquitard and a Noordbergum response begins to propagate through the upper aquifer using the same fractures. As the Noordbergum response reaches each well, the much smaller initial

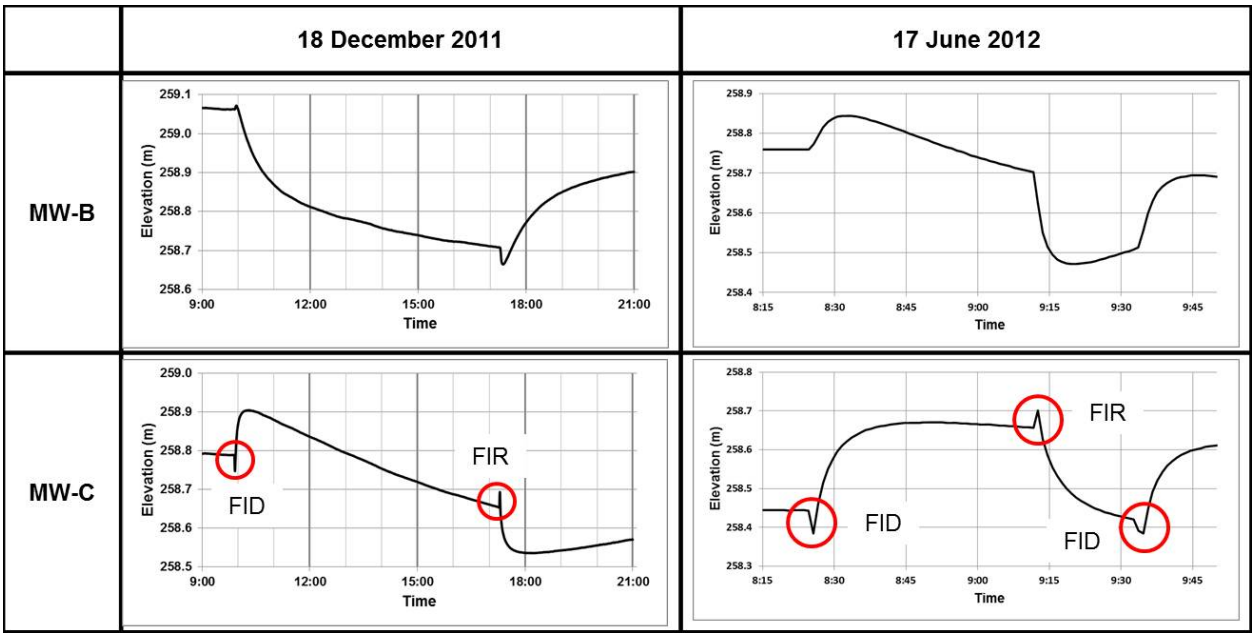

Figure 3.5. Comparison of MW-B and MW-C RWF effects after the MW-C borehole was grouted during December 2011 and June 2012. Each plot represents one pumping cycle although the time period in June is much shorter due to a higher pumping rate. The circled sections highlight FID and FIR.

drawdown is negated. The drop in water level at the beginning of pumping will be referred to as the Fracture Flow Initial Drawdown (FID) and the increase in water level as pumping ceases will be referred to as the Fracture Flow Initial Recovery (FIR).

The distribution of FID and FIR observations in the instrumented wells can be used to shed light on fracture connectivity in the upper aquifer. Only the deepest wells (MW-C, House 2, and House 3) consistently experience FIDs and FIRs. This indicates that these wells are likely the best connected by fractures to the lower aquifer. It is possible for both the fractures at the base of the Wonewoc Formation and a shallower, higher T fracture to be pathways for propagation of RWFs (Table 3.5). The higher T fracture is shallower than the screened interval of MW-B. Any FIDs or FIRs that travel along this fracture are likely to influence MW-B, but that well does not normally experience them. It is more likely that the fracture at the base of the Wonewoc is the

part of the preferred pathway connecting MW-C, House 2, and House 3. The FIDs and FIRs observed in MW-B while the MW-C borehole was lined indicate that during this time the pathway was altered to include the borehole. This temporary pathway allowed MW-B to be influenced by the fracture effects.

3.3. Evaluation of unit well annulus as a preferential flow pathway

Rapid transport of near surface contaminants into a deep, confined aquifer requires a preferential flow pathway. One hypothesis to explain the detection of viruses in UW-7 is that the grouting outside the UW-7 casing, which extends through the upper aquifer and Eau Claire Formation, had failed to the point where it created a highly transmissive conduit between the water table and well pump. In this scenario contaminants at the water table would migrate rapidly downward during unit well pumping and enter the water supply. It is possible to test this hypothesis with the data collected in this study.

The borehole liner installed in MW-C likely formed an imperfect seal along the borehole wall. During this time (August 2011 in Table 3.3) each of the five instrumented wells experienced RWFs in response to UW-7 pumping. The water table well (MW-A) adjacent to UW-7 experienced low magnitude, but distinctly visible, RWFs (August 2011 in Figure 3.4). After MW-C was grouted, MW-A no longer experienced distinct RWFs (February 2012 in Figure 3.4) even though it was closer to UW-7 than were House 2 and House 3. The absence of RWFs following grouting of MW-C suggests that RWFs in MW-A while the FLUTe was installed were caused by propagation of RWF head changes from the top of the Eau Claire Formation upward along the MW-C borehole

liner and then radially outward along shallow fractures. House 2 and House 3 must then intersect deeper fractures that are connected to a high angle fracture, as is also suggested by analysis of head data. When pumping discharge increased substantially in June 2012, and the RWFs in MW-B were the largest (Table 3.2), RWFs were still absent from the shallowest wells (Table 3.3).

The comparison of water level responses while the liner was installed and after its removal can be used to evaluate whether the UW-7 annulus is a preferential flow pathway. Although not intended, the borehole liner served as a proxy for a leaking public supply well annulus. The lack of RWFs in MW-A after the borehole liner was removed and MW-C grouted suggest that the borehole liner, and not a defective unit well, was responsible for those responses. If faulty UW-7 grout extended to shallow depths, the shallowest, closest well would be expected to respond to pumping at all times. A faulty annular seal would also allow rapid propagation of FID and FIR effects such that these would be observed in MW-A and MW-B at all times. Thus, it appears unlikely that a failure in the UW-7 grouting is the source of the preferential flow pathway responsible for rapid transport of contaminants between the water table and the UW-7 pump.

3.4. Effect of pumping rate and amplitude on RWF magnitude and duration

A comparison of head data from December 2011 and June 2012 for both MW-B and MW-C (Figure 3.5) highlights the impact of pumping on RWFs. The unit well pumping rate in December was 4,400 liters per minute. In June the pump was replaced and the well discharge increased to 8,300 liters per minute. The Noordbergum

response in MW-B increased substantially from 1.5 cm to 21.9 cm (Table 3.2). While MW-C also experienced an increase in RWF magnitude, the ratio of magnitudes in MW-C to MW-B decreased from more than 12:1 in December to nearly 1:1 in June. It is evident that higher pumping rates not only increase the magnitude of RWFs, they also expand the portion of the aquifer that experiences large RWFs. The lack of observable RWFs in the house wells during December is likely because they were too small to be detected as evidenced by the low magnitude of the RWFs in MW-B (Table 3.2).

In addition to a higher pumping rate in June, the unit well also began to cycle more frequently compared to the one cycle per day during December. The June cycles each lasted an hour or less, as the adjacent reservoir quickly filled and the well ceased pumping while the reservoir drained. The shortened pumping cycles resulted in the Noordbergum response persisting through a substantial portion of the period when the well was active. Instead of the pumping-induced head change in MW-C occurring over several hours during pumping and non-pumping periods, the majority of the head change occurred over tens of minutes and shifted to the initial portion of the RWFs at the beginning and end of each pumping cycle. The result was rapid changes in head during each of the ten daily cycles and these cyclic changes may serve as a mechanism for contaminant transport in a similar manner as barometric pumping may induce gas transport in fractured rocks (Nilson et al. 1991). First, the magnitudes and durations of RWFs are not equal for each pumping cycle (Table 3.2), with Rhade water level declines generally exceeding Noordbergum water level rises. This suggests that flow in the fractures might result in net transport towards the PSW. Second, the dual porosity

nature of the system might result in contaminants migrating from the fractures into the aquifer matrix during periods of higher head (Noordbergum response) and subsequently migrating back into the fractures during periods of lower head (Rhade response) and then travelling along the fracture toward the pumping well. Combined with high transmissivity fractures, these rapid fluctuations in head may promote rapid transport of contaminants through high T fractures in the upper aquifer.

4. Summary and Conclusion

Reverse water-level fluctuations may be more common than generally reported, and were studied in several wells in the vicinity of a public supply well, Unit Well 7, in Madison, Wisconsin. The RWF magnitude in instrumented wells was more closely related to well depth and to apparent connections to low angle fractures than to radial distance from UW-7. The lack of RWFs in the shallowest, closest well (MW-A) and the lack of FIDs and FIRs in both MW-A and MW-B suggest that the unit well casing is neither defective nor the source of the preferential flow pathway between the upper and lower aquifers.

The presence of RWFs in a well is commonly attributed to poroelastic effects in an aquitard due to pumping of an adjacent aquifer. The initial RWFs observed in MW-C at the top of the Eau Claire Formation are likely generated by such poroelastic effects. However, it is suggested here that RWFs observed in the other wells originate near MW-C and propagate by pressure changes transmitted rapidly through fractures over 300 meters radially from the pumping well. This behavior allows RWFs to appear in wells more quickly and much farther from the pumping well than expected. The link

between RWFs and fractures is important for the evaluation of pumping impacts on transport in the aquifer. The pattern of RWF propagation can be used to better define fracture connectivity in an aquifer system.

The unit well pumping discharge and the duration of pumping cycles affected not only the drawdown in the upper aquifer but also the short term head changes due to RWFs. A combination of rapid, pumping induced head changes and fracture flow are a potential mechanism for rapid transport of contaminants into UW-7. Analysis of RWF magnitude data for several time periods under a variety of pumping conditions indicates that pumping UW-7 at a lower discharge but for longer periods of time will result in RWFs that occur less often and with a smaller magnitude. Pumping at high rates with multiple pumping cycles per day will maximize the number and magnitude of RWFs in the upper aquifer and might lead to more rapid transport of contaminants into the unit well. By developing a better understanding of how public supply well pumping in a fractured aquifer system influences contaminant transport, it may be possible to identify strategies such as modified pumping schedules and the use of variable frequency drive well pumps to minimize risk of near surface contaminants entering the public water supply.

Chapter 4. Use of groundwater geochemistry and human enteric virus detection to characterize transport in a fractured siliciclastic aquifer

1. Introduction

The presence of microbial and chemical wastewater indicators is the most direct evidence of public supply well (PSW) vulnerability to near surface contaminants. As discussed in Chapter 1, there are substantial public health risks associated with virus contamination of drinking water supplies and recent research has demonstrated a link between viruses in non-disinfected PSWs and the incidence of acute gastrointestinal illness (Borchardt et al. 2012). Human enteric viruses originate from human waste and are therefore a specific indicator of wastewater contamination. In urban environments sanitary sewers are the most likely source of human waste containing infectious viruses that may enter groundwater. Precipitation might play a role in introducing viruses into an aquifer through direct recharge to groundwater and increased flow in leaky sanitary sewers.

Over time the population sheds different human enteric viruses into the sanitary sewer system, which may subsequently leak into the underlying aquifer. This means that viruses have the potential to be used as both spatial and temporal tracers. Although virus genomes have advantages in terms of detection limits and temporal variability compared with chemical tracers, previous virus sampling projects (Borchardt et al. 2007; Borchardt et al. 2004; Bradbury et al. 2008; Bradbury et al. 2010; Hunt et al. 2010) have shown that virus genomes in groundwater may not be detected consistently during individual sampling rounds, thus necessitating sampling over long time periods.

Travel times to deep PSWs are important because virus genomes are only detectable in the groundwater environment for 1-2 years (Hunt et al. 2010). In siliciclastic aquifer systems there are several potential pathways for near surface contamination to reach deep confined wells while the viruses are still infective. Porous media flow is normally associated with transport in sandstone aquifers and small volumes of wastewater might travel along the fastest pathways at statistically extreme velocities (Taylor et al. 2004). High transmissivity fractures have the potential to rapidly transport contaminants substantial distances over short periods of time. A defective PSW casing or grouting of the annular space could allow rapid vertical transport into the public water supply (Lacombe et al. 1995). These pathways need to be identified and travel times quantified to determine if infectious viruses are able to reach a PSW.

In addition to the immediate and direct health risks that viruses in PSWs represent, viruses might serve as tracers to help identify the most likely preferential flow pathway between the wastewater source and the PSW. Chemical wastewater constituents may also provide an indication of the route taken between assumed sources and PSW. Although viruses can be detected at lower concentrations (individual viruses per liter of water) than major ions (mg/l), the chemical constituents have the potential to be present more continuously over time. However, one drawback to using major ions as indicators of wastewater is that some of these may have other sources such as road salt or fertilizer (Panno et al. 2006).

1.1. Site description

The research described in this chapter was conducted from 2010 to 2012 at the Unit Well 7 (UW-7) site in Madison, Wisconsin (Figure 2.1). Unit Well 7 is a public supply well constructed in 1939 and pumps approximately 8,300 liters per minute. The well is cased and grouted through the upper aquifer and Eau Claire aquitard and draws water from the confined Mount Simon Sandstone. The site is surrounded by a residential neighborhood and the sanitary sewer is constructed mostly of vitrified clay pipe that was installed in the 1940s. Before installation of the sewers, homes in the area used septic systems or cesspools for wastewater disposal but none of these have been in use for decades and can be ruled out as a source of infectious viruses in groundwater. Previous studies in Madison have detected infective human enteric viruses in UW-7 (Bradbury et al. 2010). The Nine Springs Wastewater Treatment Plant (WWTP), which is operated by the Madison Metropolitan Sewerage District, collects all wastewater, approximately 120 million liters per day (MLD), from the Madison metropolitan area.

1.2. Purpose and approach

The analyses described in this chapter are intended to demonstrate the combined use of chemical and microbiological indicators of wastewater contaminants to identify the most likely preferential flow pathways in a fractured siliciclastic aquifer system near a public supply well. The amounts of recharge and sanitary sewer flow were compared for specific time periods in order to determine the role large recharge events have on increased sewer flow and subsequent loading of the aquifer. Spatial

and temporal patterns in both water chemistry and human enteric virus genome detection were used to evaluate transport pathways. Samples were collected at regular time intervals from the unit well, three monitoring wells, a sanitary sewer adjacent to the site, and the intake to the WWTP. Groundwater sampling was not conducted in the Eau Claire aquitard. The nature of the connection between the upper and lower aquifers across the aquitard was investigated by examining physical and chemical parameters of the UW-7 borehole. The chemical and microbial data were then used to construct a conceptual model to evaluate preferential flow.

2. Methods

2.1. Strategy

The constituents sampled included human enteric virus genomes detected in earlier Madison projects (Borchardt et al. 2007; Bradbury et al. 2010), coliform bacteria, E. coli, and chemical wastewater indicators. Potential chemical indicators included major ions, alkalinity, trace metals, and optical brighteners. In order to address the questions related to rapid transport of wastewater contaminants from the near surface to a PSW, a sampling strategy that involved both spatial and temporal aspects of the problem was required. Spatial resolution was achieved by sampling at multiple points between the most likely source (sewer) and UW-7. Characterization of the likely virus source was conducted by sampling wastewater from the sanitary sewer near UW-7 and also influent to the WWTP. The upper aquifer was sampled from three nested monitoring wells (Figure 2.3) that were open to the water table (MW-A), to a short interval at a depth approximately halfway between the water table and the bottom of the

upper aquifer (MW-B), and at the bottom of the upper aquifer (MW-C). The lower aquifer was sampled directly from UW-7 during normal pumping.

Although there is some variation in water quality among the 22 PSWs in Madison, UW-7 has concentrations of major inorganic constituents similar to those measured in other wells (Madison Water Utility 2011). Upper aquifer water quality at UW-7 is similar to that in other areas in Madison. Nitrate, sulfate, potassium, and alkalinity concentrations from upper aquifer wells in the Nine Springs Watershed (Swanson 2001), a wetland area located on the southern edge of the Madison metropolitan area, are similar to those in the upper aquifer at UW-7. These data indicate that the upper aquifer groundwater has a geochemical signature similar to other portions of Madison. However, the upper aquifer sodium and chloride concentrations in the Nine Springs Watershed wells are one to two orders of magnitude lower than those at UW-7, which suggests that these two ions are related to urbanization. Sodium, chloride, and chloride/bromide ratio have been identified as wastewater indicators in previous research (Eiswirth et al. 1995; Panno et al. 2006; Brown et al. 2009; Katz et al. 2011; Minnesota Department of Health 2011) and were used for that purpose in this study.

A total of three sampling rounds were conducted during 2010, 2011, and 2012 (Table 4.1). Temporal resolution was achieved by conducting time sequenced sampling. Sampling was conducted twice per month for several months during each sampling period in 2010 and 2012. Previous work had suggested that viruses may travel between the sewer and unit wells in a few weeks to months. The ability to

compare microbial and chemical wastewater indicators over several months at multiple locations was necessary to assess preferential flow pathways and determine how much time elapsed between virus genome detections at different points.

Table 4.1. Information on sampling rounds described in this study.

Year	Start Date	End Date	Frequency	Sampling Rounds	Total Samples	Locations Sampled
2010	13 May	21 Jul	2x/month	6	30	Sewer, MW-A, MW-B, UW-7, WWTP
2011	24 Feb	24 Feb	single event	1	3	MW-A, MW-B, UW-7
2012	4 Jan	16 May	2x/month	10	49	MW-A, MW-B, MW-C, UW-7, WWTP

During May 2012 the Madison Water Utility removed the pump from UW-7 to perform maintenance. While the well was open, it provided a rare opportunity to log the borehole with multiple tools including an optical borehole imager, acoustic borehole imager, gamma tool, fluid conductivity/temperature tool, mechanical caliper, and spinner flow meter. The log data provided additional information with which to characterize the nature of groundwater flow between the upper and lower aquifers.

2.2. Sampling methods

Decontamination of equipment was an important step in the sampling protocol due to the low expected concentrations of virus genomes. Dedicated tubing was used for sampling each monitoring well. The day prior to sampling, all submersible pumps and tubing, peristaltic pump tubing and prefilter housings were sterilized. A solution of 50 mg/L chlorine was pumped through all equipment and allowed at least 15 minutes of contact time. The exterior of the monitoring well sample tubing was also disinfected.

Sampling equipment was then dechlorinated using a solution of 1g sodium thiosulfate per liter of deionized water. Prepared pumps and tubing were then stored in clean plastic bags until they were inserted into the monitoring wells. On the day of sampling, at least three well volumes were pumped through the tubing before sampling began in order to flush any residual sodium thiosulfate from the system. Complete details of decontamination are presented in Appendix D.

Groundwater sampling from UW-7 was conducted by attaching a peristaltic pump to a sampling port on the well discharge line prior to chlorination. The peristaltic pump was connected in such a way as to only function while the unit well was pumping in order to prevent drawing in chlorinated water downstream of the sampling port. Monitoring well sampling required submersible pumps and Figure 4.1 illustrates the standard configuration used for each well. A 10 micron wound polypropylene prefilter was required in MW-A to prevent suspended solids from clogging the glass wool filter. The pH for groundwater samples collected at the site was never greater than 7.5; therefore the acid adjustment step was not required. Virus genome samples were collected by pumping 800 to 1,000 L of water through glass wool filters at rates of approximately 4 L/min. A totalizer was used to track the total volume sampled. Groundwater geochemistry grab samples were collected in conjunction with virus sampling, after several hundred liters had been pumped from the monitoring wells.

Virus and water chemistry samples from the sanitary sewer near UW-7 were collected as 24-hour composite samples. Collection of samples every 15 minutes for 24 hours was accomplished using an ISCO sampler packed with ice and placed in a

manhole. Samples from the Nine Springs WWTP in 2010 were 24-hour composite samples collected by WWTP plant personnel from the plant intake and refrigerated at the WWTP laboratory. Changes to WWTP operating procedures in 2012 required collection of 72-hour composite samples. Due to variability in groundwater virus genome detection over time, it was necessary to sample for several months consecutively in order to maximize the possibility of detecting virus genomes during at least one sampling round.

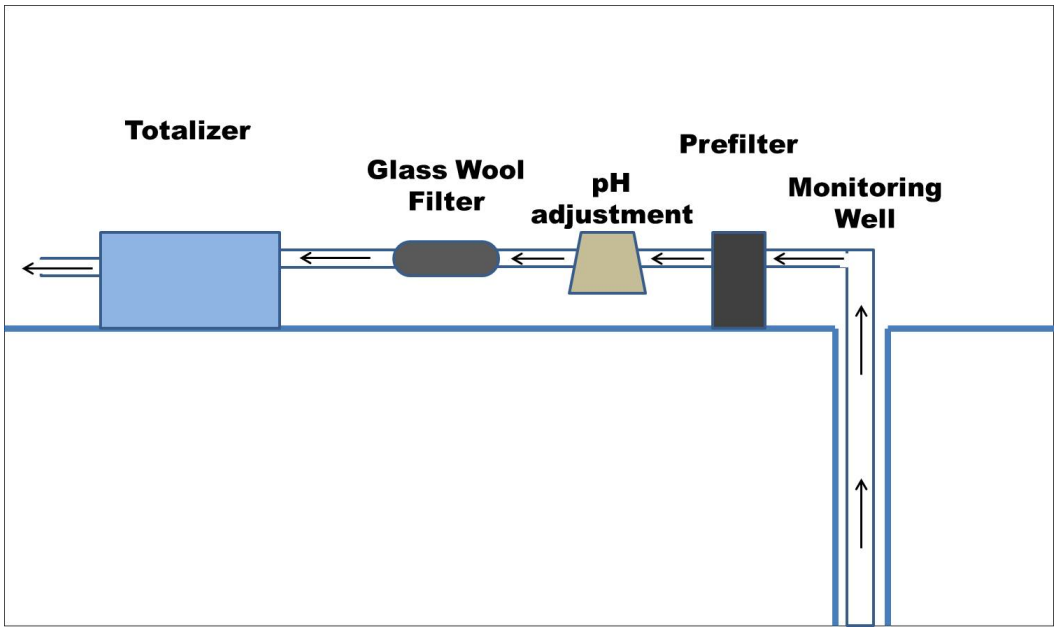

Figure 4.1. Schematic of standard monitoring well virus sampling using glass wool filtration. The prefilter was only required at MW-A due to high turbidity. The pH adjustment was not required for this study because groundwater pH was less than 7.5.

2.3. Initial 2010 and 2011 sampling

During the summer of 2010, six rounds of virus sampling were conducted at Unit Well 7, MW-A, MW-B, the sanitary sewer near UW-7, and the Nine Springs WWTP. The virus analysis procedure had been modified from previous studies in Madison (Borchardt et al. 2007; Bradbury et al. 2010) as part of the shift to a standardized, EPA

approved method. The analytical laboratory moved from the Marshfield Clinic Research Foundation to the U.S. Department of Agriculture (USDA)-Agricultural Research Station (ARS) in Marshfield, Wisconsin during the summer of 2010. This change in location also resulted in some alteration to the virus analysis procedures.

According to Dr. Mark Borchardt, USDA-ARS (personal communication) the following is a summary of the modified virus genome detection process. Viruses were eluted from the filters with a beef extract reagent and concentrated using organic flocculation. For molecular assays, the concentrated eluate was concentrated again by centrifugal ultrafiltration. The RNA was then extracted from the concentrate and tested for enterovirus and norovirus RNA using real time quantitative reverse transcription-polymerase chain reaction (qRT-PCR) using a Roche LightCycler 480. Virus concentrations for the molecular assay are calculated in terms of genomic copies of viral RNA per liter based upon a standard curve. The glass wool filter and prefilter elution steps were conducted in the UW-Madison hydrogeology laboratory; samples were then frozen at -20°C, and later transported to the USDA-ARS laboratory in Marshfield, WI for analysis. Samples were analyzed for the following virus groups, which had been detected in previous studies: enterovirus, rotavirus, adenovirus, hepatitis A virus, and norovirus genogroups I and II. The PCR results likely underestimate virus genome quantities because of losses during sample filtration, secondary concentration, and nucleic acid extraction steps (Borchardt et al. 2012).

Collection of sanitary sewer samples was accomplished by using an automated sampler that was hung in a manhole near UW-7 a few days before groundwater

sampling. The device was programmed to collect a sample every 15 minutes for a 24 hour period in order to obtain a composite sample. Frequently the flow in the sewer pipe was too low to collect a sample or the intake line would become clogged with debris. These problems resulted in samples that were not necessarily representative. For that reason, sampling from the sanitary sewer was not continued in later sampling rounds.

In order to evaluate the effects of snow melt recharge on virus transport, a one-time sampling event was conducted from MW-A, MW-B, and UW-7 on 24 February 2011 using the same methods as the 2010 virus sampling. The preceding week had been unusually warm with temperatures well above freezing. This resulted in much of the snow pack in Madison melting, potentially generating a large recharge event. Because this sampling iteration was conducted on short notice, only groundwater samples were collected.

Geochemical sampling was conducted concurrently with virus genome sampling during summer 2010. One liter grab samples of ground water and one liter composite samples of wastewater were collected in amber glass bottles and sent to the University of Minnesota Hydrogeochemistry Laboratory. Cations, anions, trace metals, alkalinity, and optical brighteners were analyzed. Field measurements of electrical conductivity and pH were taken during each sampling round from the sanitary sewer, monitoring wells, and municipal well.

2.4. 2012 sampling

In 2012, sampling locations changed slightly from previous iterations. Only the WWTP influent was sampled for wastewater due to the logistical concerns with the sanitary sewer location. The deepest monitoring well (MW-C) was constructed in December 2011 and was also included in this sampling round. The addition of MW-C allowed for greater spatial resolution in the upper aquifer.

Groundwater virus genome samples were collected in 2012 using the same glass wool filtration methods used in 2010 and validated by Lambertini et al. (2008). Unlike previous sampling rounds, the glass wool filters and prefilters were shipped at 4°C to the USDA-ARS lab the day after sampling. The elution of glass wool filters and prefilters was conducted at the lab using a beef extract solution with final pH adjustment to 7.0 using 1M HCl. The lab flocculated and concentrated the samples with polyethylene glycol, then analyzed by qRT-PCR for the same virus groups as the 2010 sampling.

Cations, anions, and alkalinity concentrations from the monitoring wells, UW-7, and the Nine Springs WWTP were measured for samples collected in 500 ml HDPE bottles. Because the 2010 sampling data indicated that optical brighteners were not a useful wastewater indicator at this site, no optical brightener samples were collected in 2012. Similarly, trace metal analyses were not made on these samples because no substantial temporal or spatial variations in these were detected in previous samples.

3. Results

3.1. Virus results

The results of 2010 and 2011 virus genome sampling are displayed in Table 4.2 along with data on cumulative and maximum daily precipitation over the preceding 14 day period. Virus genome detections are listed in the table as log concentrations. All of the wastewater samples contained between 160 ($10^{2.2}$) to 250,000 ($10^{5.4}$) gc/l of virus genomes but the positive groundwater sample concentrations ranged from as low as the method detection limit of 0.02 gc/l up to a maximum of 0.25 gc/l. For the 2010 data, only 25% of the monitoring well samples and none of the public supply well samples were virus genome positive. There was poor agreement between the WWTP and sanitary sewer samples due to the logistical problems mention in section 2.3 and the fact that the sampling location captured a very small fraction of the total flow measured at the WWTP intake. In some cases a virus group was detected in the sanitary sewer but not at the WWTP, likely due to dilution. The WWTP data were considered more representative of sewage that might exfiltrate from the sewers and contaminate the aquifer.

Because the 2010 sampling occurred over the relatively limited time of a three month period, a lack of virus genome positive samples in the municipal well is not surprising. In previous sampling at this location three month periods had elapsed without a virus detection (Borchardt et al. 2007; Bradbury et al. 2010). It is significant that virus genomes were detected in the upper aquifer because that was the portion of the pathway that had not been previously evaluated for viruses. Virus genomes were detected in both MW-A and MW-B during 2010, which indicates they were present at

Table 4.2. Results of 2010 and 2011 virus sampling reported as log concentration (gc/l). Precipitation data are for the total over the 14 days before sampling and the maximum daily value during that period.

Sampling Week		6-May-10	13-May-10	26-May-10	9-Jun-10	23-Jun-10	7-Jul-10	21-Jul-10	24-Feb-11
WWTP	Adenovirus A	No Sample	No Sample	No Sample	No Sample		2.4	2.6	No Sample
	Adenovirus C,D,F					3.6	3.8	3.8	
	Enterovirus					4.5	2.8	5.2	
	G1 Norovirus					5.4	3.8	5.4	
Sanitary Sewer	Adenovirus A	4.4	4.2		4.2	3.7			No Sample
	Adenovirus C,D,F			2.2	3.1				
	Enterovirus				3.9	3.9		3.7	
	G1 Norovirus					5.4	3.4	3.5	
MW-A	Adenovirus A	No Sample				-1.7	-1.7		
	Adenovirus C,D,F								
	Enterovirus								
	G1 Norovirus								
MW-B	Adenovirus A	No Sample							
	Adenovirus C,D,F								
	Enterovirus							-0.9	-0.7
	G1 Norovirus								
Unit Well	Adenovirus A	No Sample							
	Adenovirus C,D,F								
	Enterovirus								-0.6
	G1 Norovirus								
Precipitation (cm)	14 day total	3.6	7.7	4.2	7.5	9.3	6.8	5.4	33 cm Snow Melt
	Max daily	1.6	2.1	2.3	2.8	4.8	2.3	3.4	

the water table and also deeper in the upper aquifer. Adenovirus was detected in two consecutive MW-A samples with enterovirus detected in MW-B two weeks later. For the 2011 single sampling event, enterovirus was detected in both MW-B and UW-7 at approximately the same concentration. The data indicate an apparent 4 to 6 log reduction of virus genome concentration between the wastewater and upper aquifer.

The results of 2012 virus sampling are displayed in Table 4.3 along with data on cumulative and maximum daily precipitation over the preceding 14 day period. Virus genome detections are listed in the table as log concentrations. The first five daily maximum precipitation values in Table 4.3 are shaded blue to indicate that they quantify the reduction in snow pack depth due to melting rather than an amount of liquid water (or liquid water equivalent). The 14 day total precipitation values were recorded as either rainfall or water equivalent for snow.

The 2012 WWTP samples contained between 1300($10^{3.1}$) to 200,000($10^{5.3}$) gc/l concentration of virus genomes but the positive groundwater sample concentrations ranged from 0.03 to 6.3 gc/l. Virus genomes were detected in groundwater during 70% of the sampling rounds although no more than 2 of the 4 groundwater sampling locations were positive in any round. All monitoring wells and the unit well had at least one round with positive results. Three different virus groups were detected in samples from MW-A: enterovirus, G1 norovirus, and adenovirus groups C, D, F. Only G1 norovirus was detected in MW-B while MW-C samples contained enterovirus and adenovirus groups C, D, F. The samples from UW-7 contained G1 norovirus and adenovirus B, a group not detected in any monitoring well samples. An apparent 4 to 6

Table 4.3. Results of 2012 virus sampling reported as log concentration (gc/l). Precipitation data are for the total over the 14 days before sampling and the maximum daily value during that period. Blue shaded precipitation values are for snow melt.

Samping Week		4-Jan-12	25-Jan-12	8-Feb-12	22-Feb-12	7-Mar-12	21-Mar-12	4-Apr-12	18-Apr-12	2-May-12	16-May-12
WWTP	Adenovirus A	3.8	4.0	3.9	4.1	3.9	3.7	4.2	4.0	4.0	
	Adenovirus B	3.1									
	Adenovirus C,D,F	4.7	4.4	4.8	4.8	4.2	4.3	3.9	3.9	4.3	3.5
	Enterovirus	4.3	4.1	4.0	4.1	3.6	4.8	4.7		4.7	4.8
	G1 Norovirus	4.9	4.9	5.0	5.0	5.0	4.6	4.7	5.3	4.6	4.9
MW-A	Adenovirus A										
	Adenovirus B										
	Adenovirus C,D,F						-0.3				
	Enterovirus					0.01					
	G1 Norovirus		0.7			0.8					
MW-B	Adenovirus A										
	Adenovirus B										
	Adenovirus C,D,F										
	Enterovirus										
	G1 Norovirus							-0.4			
MW-C	Adenovirus A										
	Adenovirus B										
	Adenovirus C,D,F								-1.0		
	Enterovirus			-0.5	-0.2						
	G1 Norovirus										
Unit Well	Adenovirus A										No Sample
	Adenovirus B				-1.5						
	Adenovirus C,D,F										
	Enterovirus										
	G1 Norovirus			0.7							
Precipitation (cm)	14 day total	1.3	3.1	0.2	0.6	3.2	2.3	3.2	1.8	5.4	3.5
	Max daily	2.5	5.1	5.1	2.5	7.6	1.1	2.0	0.94	2.5	2.6

log reduction of virus genome concentration between the wastewater and upper aquifer can be inferred from these data, but the concentrations of virus genomes do not appear to change substantially with increasing depth in the aquifer system.

3.2. Water chemistry results

All data from water chemistry sampling rounds are included in Appendix E. The combination of field parameters and water chemistry data was used to further characterize the site. The average values of pH and conductivity collected in the field (Table 4.4) for 2010 differed substantially between MW-A and MW-B, with conductivity values in MW-B more than twice those in MW-A. Optical brightener data indicated that no brighteners, a typical wastewater indicator, were present in any of the samples. Cation and anion data from 2010 were plotted on a Piper diagram (Figure 4.2) and show a near linear trend between the sanitary sewer, monitoring wells, and unit well samples in terms of both cation and anion relative proportions. The sanitary sewer samples contained substantial proportions of sodium and chloride, the MW-B data plotted close to the sewer effluent, and the water table (MW-A) samples contained greater proportions of calcium, magnesium, and bicarbonate. The major ions in UW-7 samples consisted predominantly of calcium, magnesium, and bicarbonate, typical of Madison drinking water. Cation, anion, and trace metal data were analyzed in order to determine if there were spatial or temporal trends, with key wastewater indicators plotted in Figure 4.3.

The use of Cl/Br ratios may sometimes allow for detection of a wastewater signature in groundwater (Panno et al. 2006). The Cl/Br ratios were elevated in both

MW-A and MW-B, which meant that this ratio was not useful for distinguishing between those two monitoring wells. However, the Cl and Br concentrations were the greatest in the MW-B samples and the sanitary sewer, which suggests a connection between these sampling sites. The concentrations of two other wastewater indicators, Na^+ and NO_3-N (Rueedi et al. 2009), were also elevated in MW-B compared to MW-A.

Table 4.4. Average field parameter measurements at each location from 2010 sampling rounds.

	2010		2012	
Location	**pH**	**Conductivity (µS/cm)**	**pH**	**Conductivity (µS/cm)**
Sewer	6.8	1304		
WWTP			7.1	1471
MW-A	7.3	1072	7.2	1080
MW-B	7.0	2428	7.0	2296
MW-C			7.2	1240
UW-7	7.4	661	7.3	756

Cation and anion data from 2012 were plotted on a Piper diagram (Figure 4.4) and show similar relationships among the sanitary sewer, monitoring wells, and unit well samples as the 2010 samples in terms of both cation and anion relative proportions. One exception is the addition of the deepest monitoring well (MW-C). Both MW-A and MW-C plot in similar positions on the Piper diagram, which suggests that their ion composition is similar to UW-7, while MW-B, the well open to a depth intermediate to MW-A and MW-C, continues to exhibit an apparent wastewater influence. This indicates the linear trend in chemistry between wastewater and the deep confined aquifer is not simply a function of sampling depth.

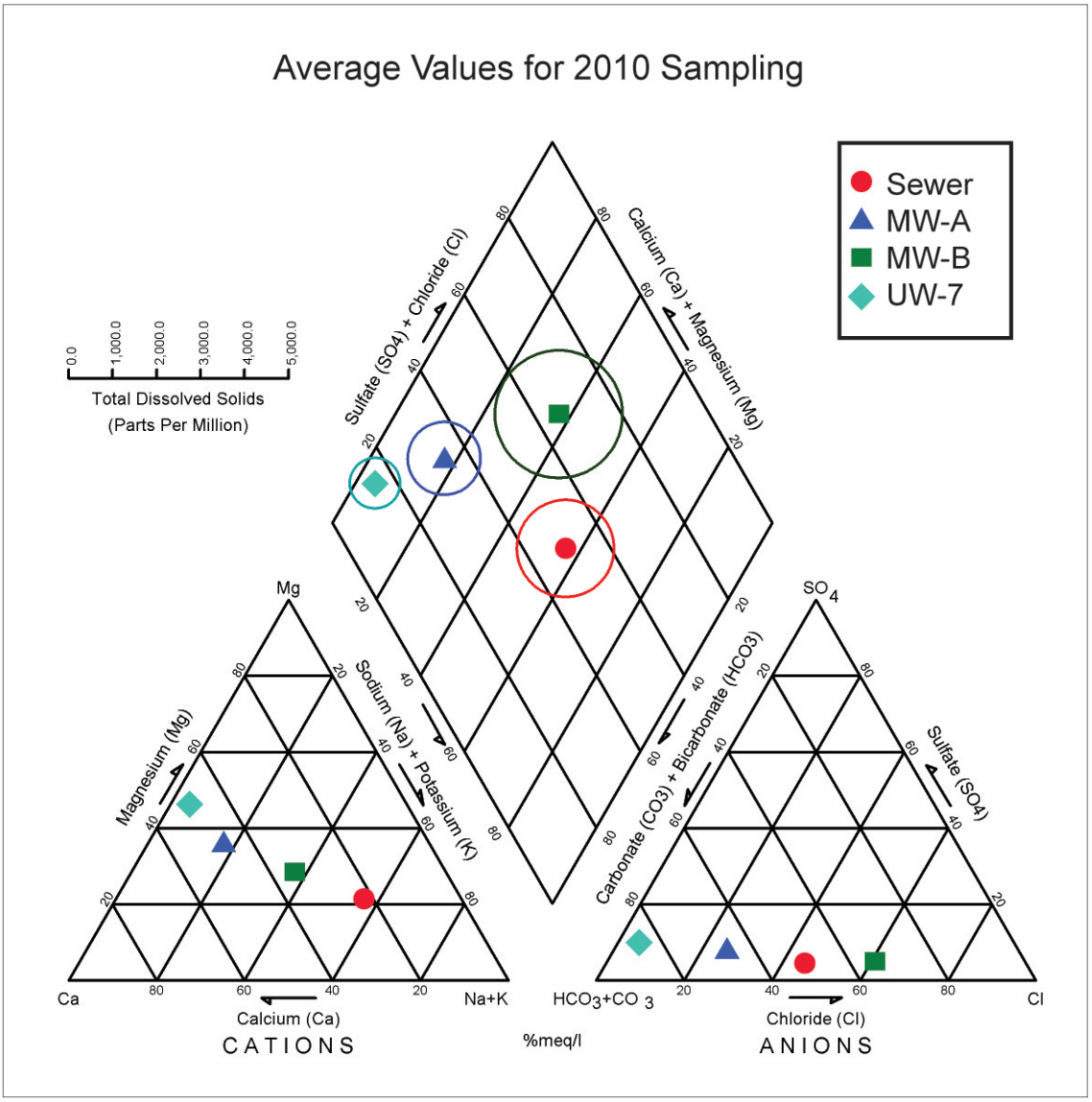

Figure 4.2. Piper diagram plot of average values from 2010 monitoring well, Unit Well 7, and sanitary sewer samples. The circles in the upper plot indicate total dissolved solids (ppm) based on the scale on the left side of the figure.

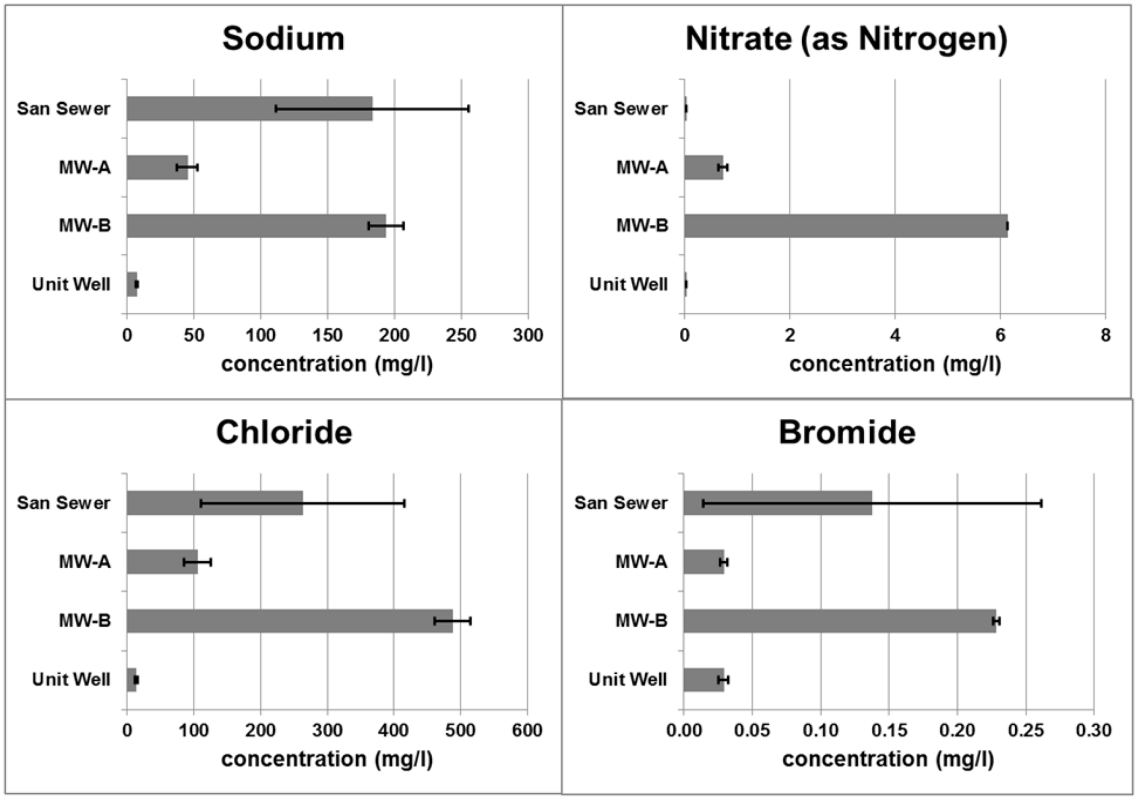

Figure 4.3. Average values for selected constituents from ten samples collected during 2010 with error bars indicating one standard deviation from the mean**.**

Field conductivity and pH measurements for 2012 averages are displayed on the right side of Table 4.4. Temporal and spatial variations in chemical constituents were examined to identify trends that could be related to potential preferential flow pathways. Selected wastewater indicators were plotted on Figure 4.5 and show a trend similar to that for the 2010 data (but with the addition of MW-C). The MW-C data indicate higher concentrations of wastewater indicators than MW-A, but concentrations in this well are still much lower than those from MW-B. Wastewater is typically reducing and ammonia is the predominant nitrogen species in that environment, in contrast to an oxidizing groundwater environment in which nitrate is the dominant nitrogen species. Therefore,

the nitrogen graph in Figure 4.5 uses NH_3-N values for wastewater and NO_3-N values for groundwater samples.

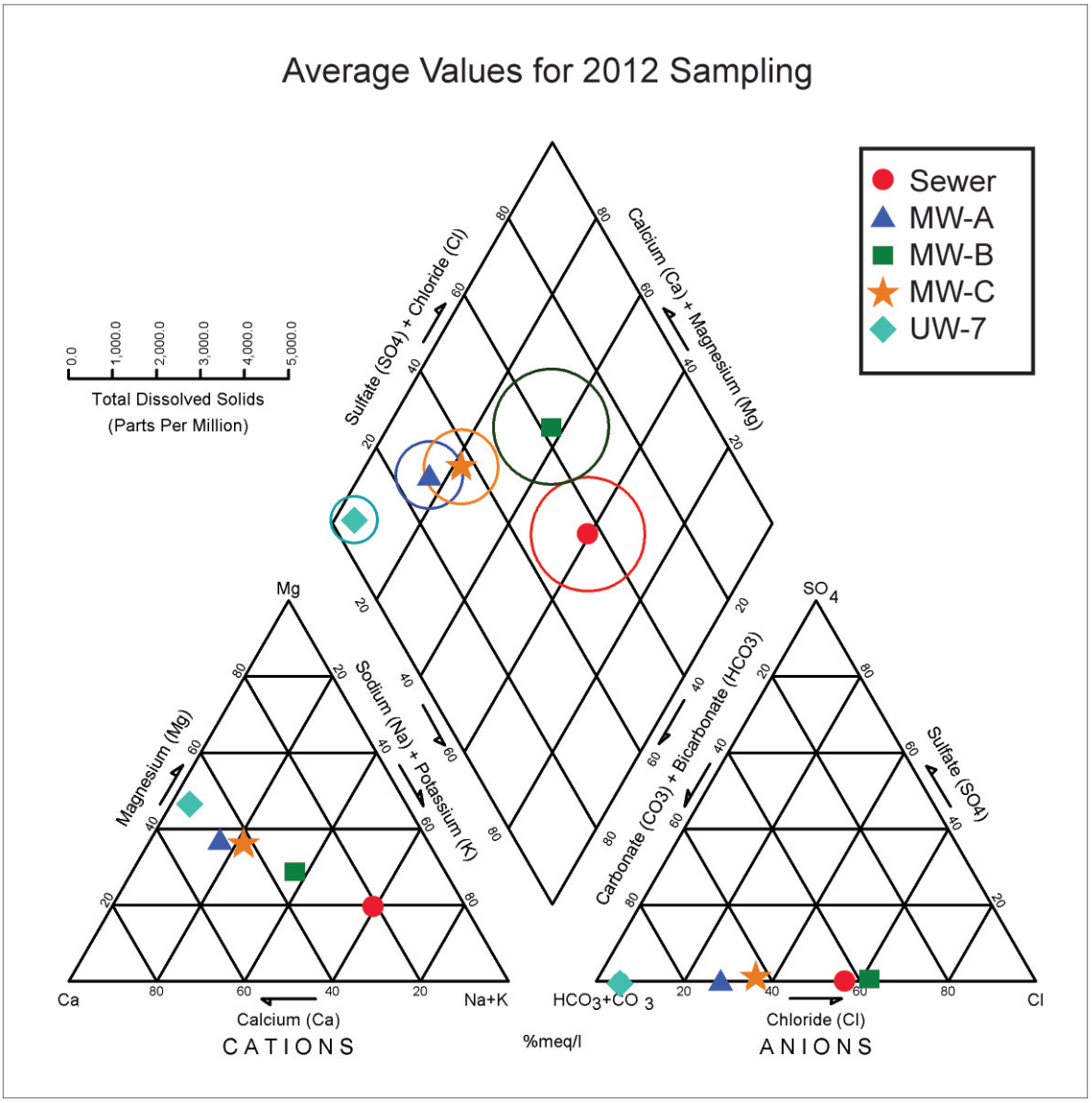

Figure 4.4. Piper diagram plot of average values from 2012 monitoring well, Unit Well 7, and sanitary sewer samples. The circles in the upper plot indicate total dissolved solids (ppm) based on the scale on the left side of the figure.

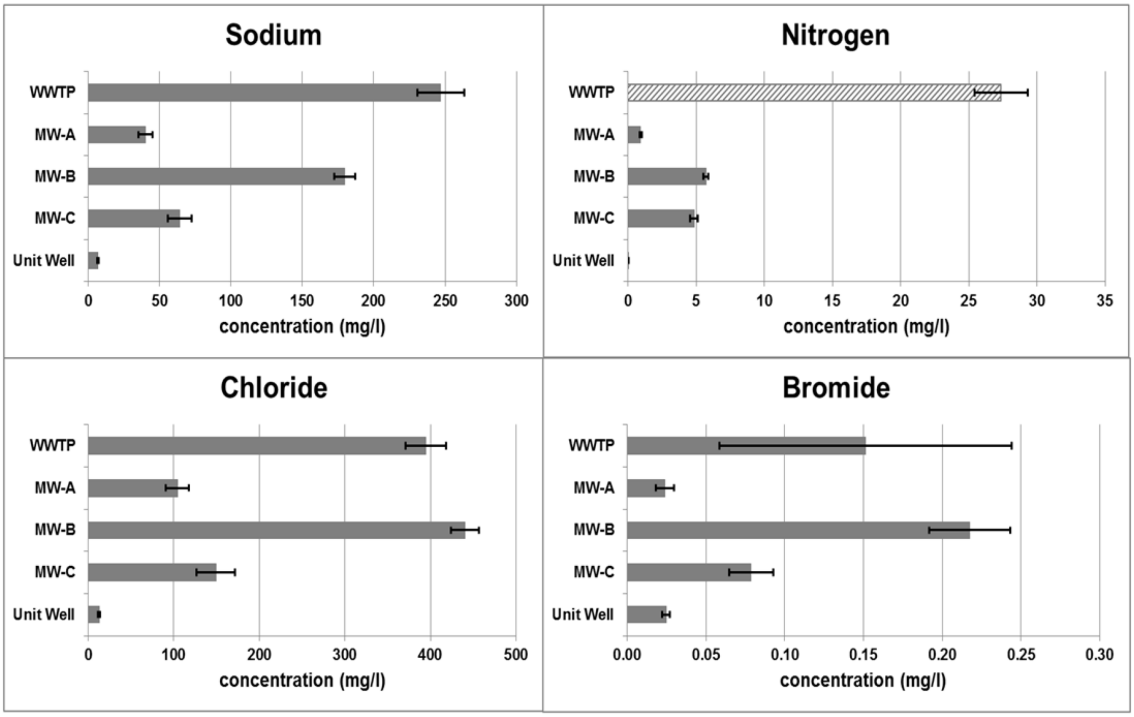

Figure 4.5. Average values for selected constituents from ten samples collected during 2012 with error bars indicating one standard deviation from the mean. Nitrogen values are reported as NH_3-N for wastewater treatment plant samples and NO_3-N for all others.

3.3. Coliform bacteria and E. coli results

Research on water quality in Minnesota discovered a link between detection of coliform bacteria and chemical wastewater indicators in PSWs (Minnesota Department of Health 2011). At UW-7 coliform bacteria and E. coli analyses were conducted on all groundwater samples collected during 2012. Collection of 100 ml samples in sterile bottles was followed by analysis by a most probable number (MPN) method to determine concentrations of bacteria as colony forming units (cfu) per 100 ml. Positive results for total coliforms were only found in two of the samples, both from MW-B. The January 4th, 2012 sample had 4.1 cfu/100ml and the January 25th sample had 1.0 cfu/100 ml.

4. Discussion

4.1. Precipitation, sewer flow, and virus detection

Sanitary sewers are the most likely source of human enteric viruses that have been detected in urban groundwater (Rueedi et al. 2009). Although Madison has separate storm and sanitary sewer systems, increased recharge in the form of precipitation or snow melt may increase sanitary sewer flow. As Bradbury et al. (2010) have demonstrated, increased precipitation in the Madison area during 2008 was linked to increased flow in the sanitary sewers. As the flow in the sewer pipes increases, more wastewater is able to leak from cracks and holes on the top and sides of the pipes. In some cases sewer pipes that normally drain by gravity may completely fill and become pressurized, further increasing leakage. Once the virus laden wastewater exfiltrates from the sewer it may reach the saturated zone and eventually migrate into the unit well. Weather data from the nearby Dane County Regional Airport were compared to virus results to determine if there is a correlation between recharge events and virus genome detections in groundwater.

4.2. 2010 data comparison

Sewer flow data were obtained for the WWTP intake and for MMSD Pumping Station #1, which collects sewage from the gravity drained sanitary sewers in the area surrounding UW-7 and pumps it into pressurized lines that lead to the WWTP. As seen in Figure 4.6, the flows measured during the spring and summer of 2010 at the WWTP and the pumping station both show the same trends over time. It is reasonable to assume that both sets of data reflect relative flow conditions in the sanitary sewers near UW-7 and both will be used in the following discussion based on data availability.

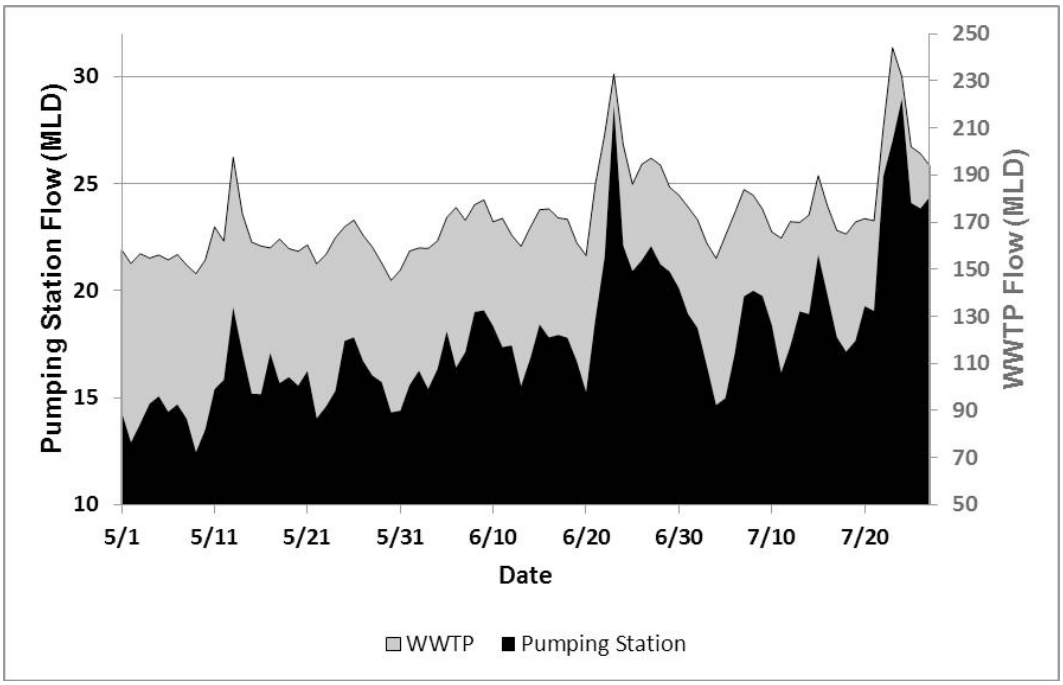

Figure 4.6. Daily flow data for both the Nine Springs Wastewater Treatment Plant (WWTP) and wastewater pumping station #1 from May 1st to July 27th, 2010.

The initial sampling from 2010 provides information about the link between precipitation, sewer flow, and virus genome detection. The bottom of Table 4.2 lists precipitation data for each sampling period. Figure 4.7 shows rainfall data during the 2010 sampling, pumping station flow, and virus sampling results. Early in the period there was less rainfall, but rain events increased in magnitude and frequency during late June and July. Viruses were detected in the monitoring wells during the last 3 sampling iterations, after a large rainfall event and a corresponding 75% surge in sewer flow. Comparison of precipitation data with virus genome detects in both Table 4.2 and Figure 4.7 reveals that the daily maximum rainfall appears to have more impact on virus transport than the cumulative rainfall over the preceding 14 days. Unfortunately the largest rainfall event of the period occurred the day after the final sampling iteration, so it was not possible to evaluate the impact of that event on virus transport.

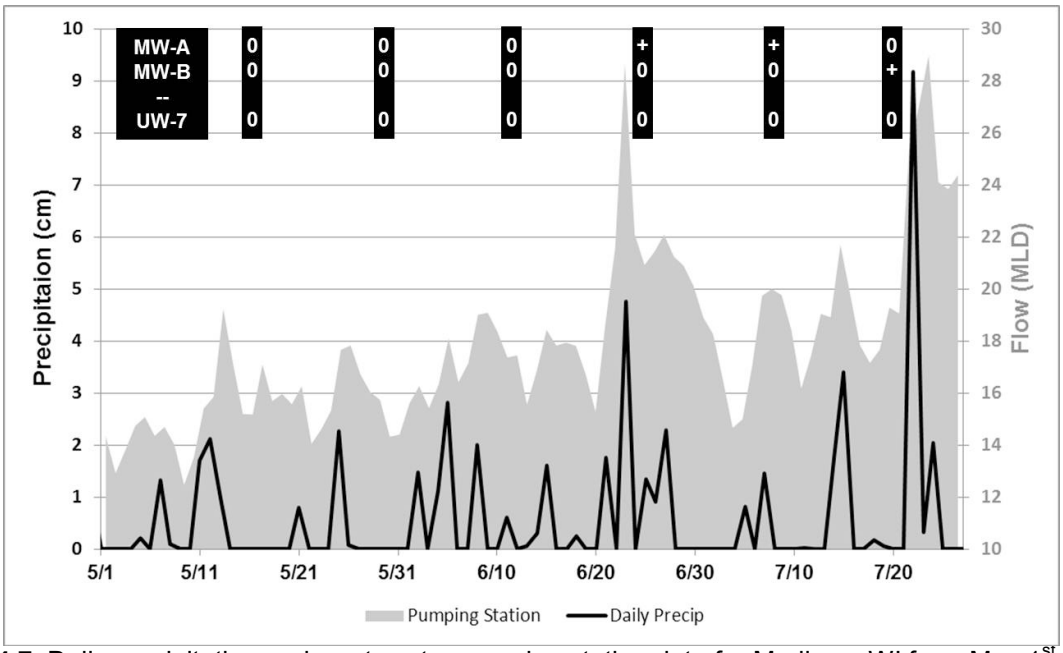

Figure 4.7. Daily precipitation and wastewater pumping station data for Madison, WI from May 1st to July 27th, 2010. The top of the figure indicates results of virus sampling for each well on that date. A "0" indicates no virus detection while a "+" indicates viruses were detected in that well.

4.3. 2011 snowmelt

In early February 2011 there was nearly 50 cm of snow on the ground in Madison (Figure 4.8) but several days of above freezing weather caused 33 cm of snow to melt. The flow in the sewers increased approximately 25% during this period. Groundwater virus samples collected one week later (Table 4.2) contained enterovirus in both MW-B and UW-7 and at approximately the same concentration. Although this was a one-time sampling event, it is important to note that after a substantial recharge event with a corresponding increase in sewer flow, enterovirus was detected in the upper aquifer and lower aquifer at the same time and at similar concentrations.

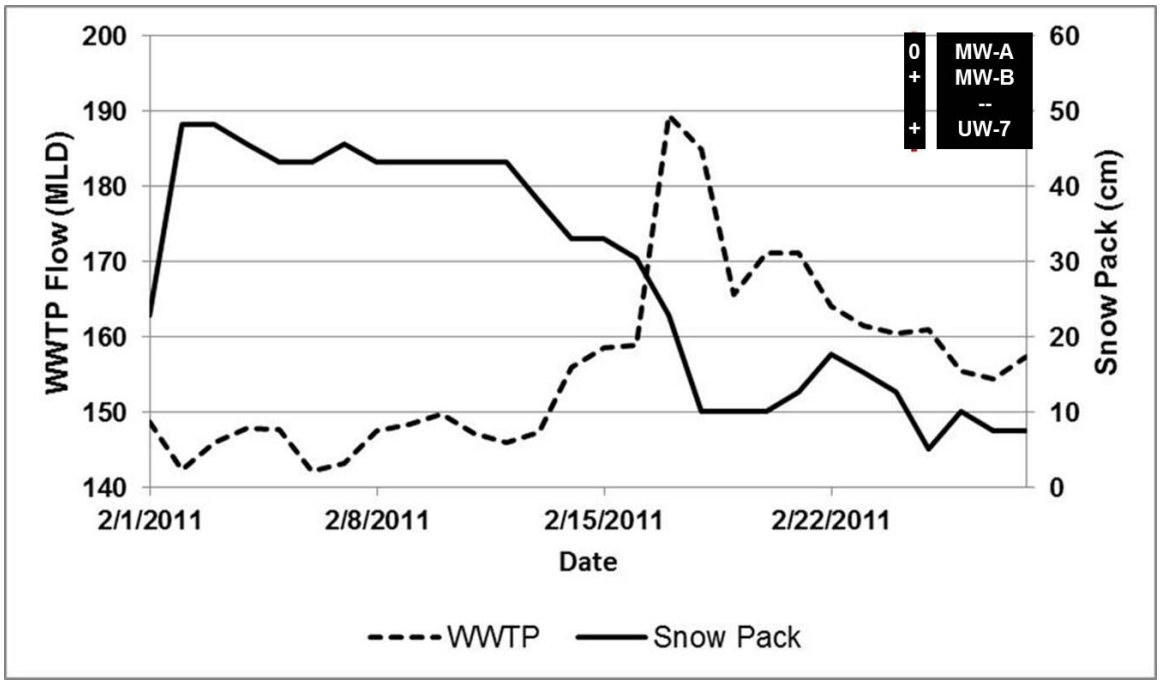

Figure 4.8. Comparison of flow into the Nine Springs Wastewater Treatment Plant (WWTP) with depth of snow on the ground in Madison, WI for February 2011. The top of the figure indicates results of virus sampling for each well on that date. A "0" indicates no virus detection while a "+" indicates viruses were detected in that well.

4.4. 2012 data comparison

The final iteration of sampling was conducted in the winter and spring of 2012. The expectation was that at least one substantial snow melt event would occur during that period followed by several large spring rain events. However, Madison experienced an usually warm and dry winter that led to less than 10 cm of snowpack at any time and most of January and February were without snow cover. By March temperatures rose to record levels over 80° F (27° C) and the snow cover had disappeared for the season by March 7th. The largest spring rainfall event of 2.6 cm did not noticeably affect flow in the sewers (Figure 4.9).

Virus data from this period (Table 4.3 and Figure 4.9) indicate that virus genomes were still present in the groundwater in the absence of substantial recharge or sewer

flow. Thus, it is apparent that recharge events are not required for virus genome detection in an aquifer, at least not within a period of several months. However, it is possible that the virus genomes detected were introduced into the aquifer during an earlier recharge event. Between January and May of 2012 the average sewer flow increased slightly but the two sampling rounds in May failed to detect any viruses in the groundwater samples. Adenovirus B was only detected in the wastewater during the January 4th sampling round but was detected six weeks later in UW-7 (Table 4.3). It can be inferred from these data that it took at least six weeks for the adenovirus B to travel from the sewer into the lower aquifer.

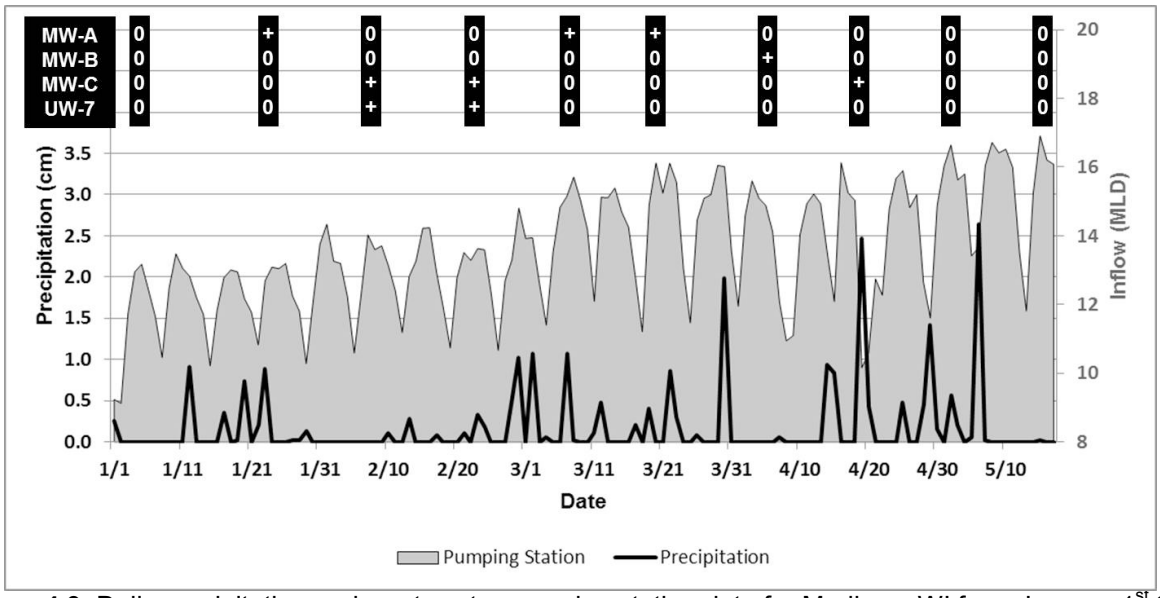

Figure 4.9. Daily precipitation and wastewater pumping station data for Madison, WI from January 1st to May 17th, 2012. The top of the figure indicates results of virus sampling for each well on that date. A "0" indicates no virus detection while a "+" indicates viruses were detected in that well.

4.5. Trends in virus detection (spatial and temporal)

Virus genomes were detected in all three monitoring wells at the UW-7 site. This is significant because the upper aquifer had not been previously sampled for viruses (Borchardt et al. 2007; Bradbury et al. 2010). The presence of virus genomes in the

monitoring wells indicates that viruses are present in the shallow aquifer at this site and could potentially move downward into MW-7. Spatial patterns of virus genome detection in the three monitoring wells can be used to test the working hypotheses related to preferential flow pathways between the sewer and unit well. Detection of virus genomes at all three depths would refute the hypothesis that the municipal well annulus is the primary pathway because viruses would not be expected to be present away from the annulus at depth if municipal well pumping is causing the downward migration of viruses from the water table along the casing. The detection of virus genomes in sequential sampling rounds, first in MW-A, then in MW-B, and finally in MW-C could reflect a plume of wastewater traveling downward by porous media flow. Sewer exfiltration is assumed to be a distributed source that may form a large plume at the water table initially before migrating downward. Detection of a virus group in the unit well that was only present in one of the monitoring wells would support the hypothesis that flow is primarily along fractures, since the absence of virus genome detections in the other monitoring wells would be inconsistent with downward migration of a uniform plume from the water table. Depending on the connectivity of a fracture network, viruses might be detected in multiple monitoring wells simultaneously. Fracture flow might be enhanced by recharge events and result in virus genome detection at multiple depths.

Currently there are no robust statistical methods developed for evaluating data from time sequenced groundwater virus sampling (Mark Borchardt, personal communication). This limits the ability to correlate virus genome detection data from

this project with potential mechanisms that might cause rapid transport of wastewater into the subsurface. Variables including recharge, sewer flow, well depth, and unit well pumping rate must be taken into consideration for such analysis. Efforts are planned by the WGNHS to involve a statistician to develop these statistical methods using data from this and other projects.

During the 2012 sampling (Table 4.3) many of the positive samples were found in MW-A. The one norovirus positive sample on January 25th in MW-A had the same concentration as that found in UW-7 two weeks later, but none of the other three MW-A detects in 2012 or the two detects in 2010 had a corresponding detect in UW-7. These data, combined with the fact that the analysis of water level responses (Chapter 3) revealed that MW-A water levels did not respond to unit well pumping, refutes the hypothesis that the unit well annulus is the preferential flow pathway that allows viruses to reach the unit well.

The positive virus samples in MW-B from July 2010 and February 2011 both followed substantial recharge events. The UW-7 sample from February 2011 also was positive for enterovirus at approximately the same concentration as that found in MW-B. More data would be required to develop a convincing causal link between recharge and viruses in MW-B, but it is possible that during high recharge events the virus laden wastewater travelled along fractures to reach both MW-B and UW-7 at approximately the same time and with little dilution or decay. This is in agreement with fracture connectivity conclusions from Chapter 2 and pumping impacts on MW-B discussed in Chapter 3.

4.6. Water chemistry trends

Many homes in Madison have water softening devices that utilize salt and discharge brine to the sanitary sewer during back flushing. This water softening salt is the most likely source of Na^+ and Cl^- in the sewer and MW-B, but there may be other sources of Na^+ and Cl^- in the groundwater such as road salt (Wenta and Sorsa 2011). If road salt were the source of Na^+ and Cl^- in the groundwater, a seasonal variation in these ions in the upper aquifer would be expected (Kelly et al. 2012). In addition to the conductivity measurements and ion measurements for the sampling periods mentioned above, conductivity values have been measured in the upper aquifer during other seasons and compared with conductivities at known chloride concentration (Table 4.3). As noted by Panno et al. (2006), in groundwater with high concentrations of chloride there is a strong correlation between chloride and conductivity measurements in groundwater with greater than 750 µS/cm conductivity.

Public Health Madison – Dane County submits an annual report to the City of Madison to discuss road salt application and levels of sodium and chloride in the city's public supply wells. These reports provide additional information on sources of sodium and chloride in the aquifer. The most recent of these reports (Wenta and Sorsa 2011) stated that during the past 50 years the chloride levels have increased in the Madison area lakes but generally remain below 100 mg/l. These levels indicate that the lakes are impacted by road salt, but the concentrations are too low for the lakes alone to be the source of elevated levels of chloride in the upper aquifer. Peak conductivity values were greater than 1,000 µS/cm for small urban streams and greater than 5,800 µS/cm

for street runoff during February 2011 but these values were only detected for a short period of time. The report also indicates that sodium and chloride levels are steadily increasing in the PSWs and suggests a link with road salt usage. The water utility only sampled the PSWs once per year for sodium and chloride so it is not possible to use the data from the road salt study to determine a seasonal pattern for the confined aquifer. However, the data obtained from this research indicate that throughout the year consistent levels of sodium, chloride, and conductivity are present in the upper aquifer monitoring wells near Unit Well 7 and in the unit well itself. This lack of a seasonal trend suggests that road salt is not the primary source of sodium and chloride in the upper aquifer or UW-7.

It is possible that in addition to loading the groundwater with viruses, leaking sanitary sewers may be the primary source contributing sodium and chloride to the Madison aquifers. Assuming that 10% of effluent in the sewers is lost through exfiltration, the value estimated by Rueedi et al. (2009) on the basis of a study in Doncaster, United Kingdom, 12 million liters of wastewater would be entering the upper aquifer in Madison each day. Using the average WWTP concentrations of 250 mg/l for sodium and 400 mg/l for chloride (Figure 4.5) a total of 1 million kg/yr of sodium and 3 million kg/yr of chloride might be loading the upper aquifer. The City of Madison used approximately 10 million kg of road salt each year from 2000-2009 (Wenta and Sorsa 2011) but only a portion of this mass is expected to directly impact the upper aquifer. It is possible that the annual loading from sewers could contribute substantially more sodium and chloride to the aquifer than the seasonal application of road salt.

Chloride/bromide ratios above 1,000 are typical for all of the monitoring well samples, with the MW-B samples exceeding 4,000 (Appendix E). Chloride values above 100 mg/l combined with Cl/Br ratios above 600 have been attributed to wastewater sources (Panno et al. 2006; Kelly et al. 2010). Using those criteria, it appears that all monitoring well samples are likely impacted by some degree of wastewater contamination. The nitrate data collected from both the monitoring wells and the straddle packer samples (Figure 2.9) indicate elevated nitrate, another wastewater indicator, throughout the upper aquifer with the exception of the water table. Most of the upper aquifer may be impacted by wastewater but MW-B appears to have the greatest concentration of chemical wastewater indicators.

Comparisons of chloride concentrations in MW-B and the wastewater samples (Figures 4.2, 4.3, 4.4. and 4.5) indicate that groundwater samples from MW-B may have higher chloride concentrations than expected for the wastewater source. This disparity might be explained by wastewater with higher levels of chloride in leaky sections of sewer pipe loading groundwater but later being diluted with lower chloride wastewater in downstream sections of the sewer before sewer sample collection.

4.7. Link between water chemistry and virus detection

Unlike viruses, chemical constituents are more consistently detected over time at any one location. If sewer effluent travelled from the water table down the well annulus then we would expect the highest levels of wastewater indicators near the water table and there would be less similarity between the constituents found in the sewer and the two deeper monitoring wells. Instead, the highest levels of wastewater indicators are

found in the middle of the upper aquifer (MW-B) while the top of the aquifer (MW-A) and base of the aquifer (MW-C) have lower values of these indicators. As discussed in Chapter 2, there are also fractures at a depth between MW-A and MW-B that contain high levels of wastewater indicators. This suggests that wastewater is preferentially flowing along individual fractures and not along the well annulus or uniformly downward due to porous media flow.

MW-B has the highest concentrations of wastewater indicators and the only total coliform detections, but the fewest virus genome detects. If MW-B was the most impacted by wastewater, both the chemical and microbiological indicators should reflect that impact. The chloride concentration in MW-B is substantially higher than in the other two monitoring wells. In a study involving virus inactivation in fresh surface water, Hurst (1988) determined that elevated chloride concentrations are correlated with increased virus inactivation. The elevated chloride concentrations in the groundwater may act to similarly decrease virus genome concentrations in MW-B and reduce detections. For that reason, slightly elevated levels of wastewater indicators may be associated with the presence of enteric viruses, but excessive amounts of those same indicators in groundwater may not necessarily lead to detection of those same viruses.

4.8. Geochemical evidence for connection between aquifers

In addition to the geochemical and microbial evidence of preferential flow paths obtained through the sampling campaign described above, a rare opportunity to directly log UW-7 became available near the end of the research project due to a need to replace the submersible pump. Fluid electrical conductivity data obtained from

geophysical logging of UW-7 provided supplemental information about possible fracture connectivity and responses to pumping in the system. The mechanical caliper log revealed that the diameter of the borehole below the well casing increased from the reported diameter of 41 cm to more than 1.0 m (the maximum diameter of the mechanical caliper) from 79 m to 110 m bgs (Figure 4.10). This interval, in which the pump was seated, was most impacted by the effects of the well pumping. Two days after the pump was removed from UW-7 the first round of geophysical logging occurred. Fluid conductivity readings (Figure 4.10) in this enlarged interval were approximately 1500 μS/cm near the top and gradually declined to 1200 μS/cm at 110 m bgs. Below this depth, the borehole returned to a 41 cm diameter and the electrical conductivity rapidly dropped to 1050 μS/cm. Although several other intervals in the borehole also had larger diameters due to blasting of the borehole, the fluid conductivity remained at 1050 μS/cm from 110 m bgs to the bottom of the well at 202 m bgs. Vertical flow logging with the spinner tool was unable to detect vertical flow in the borehole under ambient conditions. Six days later, with the pump still out of the borehole, UW-7 was logged again. At this time, conductivity readings were approximately 1100 μS/cm throughout the entire enlarged interval. After another five days UW-7 was logged for a final time and had a similar uniform 1100 μS/cm conductivity profile. The water temperature logs in Figure 4.10 also reflect a decrease in temperature between the first and second logging iterations.

The straddle packer chemistry sampling described in Chapter 2 indicated that fractures in the upper aquifer contain water with electrical conductivities between 2200

and 2900 μS/cm. During previous sampling of UW-7 during pumping, the conductivities in the unit well were approximately 700 μS/cm. The head difference between the upper and lower aquifers is approximately 3 m when UW-7 is inactive but can increase to more than 30 m during pumping. A likely explanation for the observed conductivity readings from the enlarged interval of UW-7 is that, during pumping, large head differences between the aquifers allow higher conductivity water from the upper aquifer to be pulled into the enlarged interval through a high angle fracture. During pumping this water is diluted with the lower conductivity water from the Mount Simon Formation, which provides the majority of the water to the well. After the pump was removed, residual high conductivity water remained in the enlarged interval but, without pumping, dilution with low conductivity water was reduced. The enlarged interval, therefore, acted like a borehole dilution chamber in which high conductivity water was present at the cessation of pumping. With minimal vertical flow in the borehole, the conductivity values declined in the interval largely due to horizontal flow from lower conductivity Mount Simon groundwater. This suggests a fracture flow connection between the upper and lower aquifers that is active primarily during pumping of UW-7. Similar high angle fractures have been identified in the Eau Claire Formation at other locations in the Madison area in WGNHS well logs.

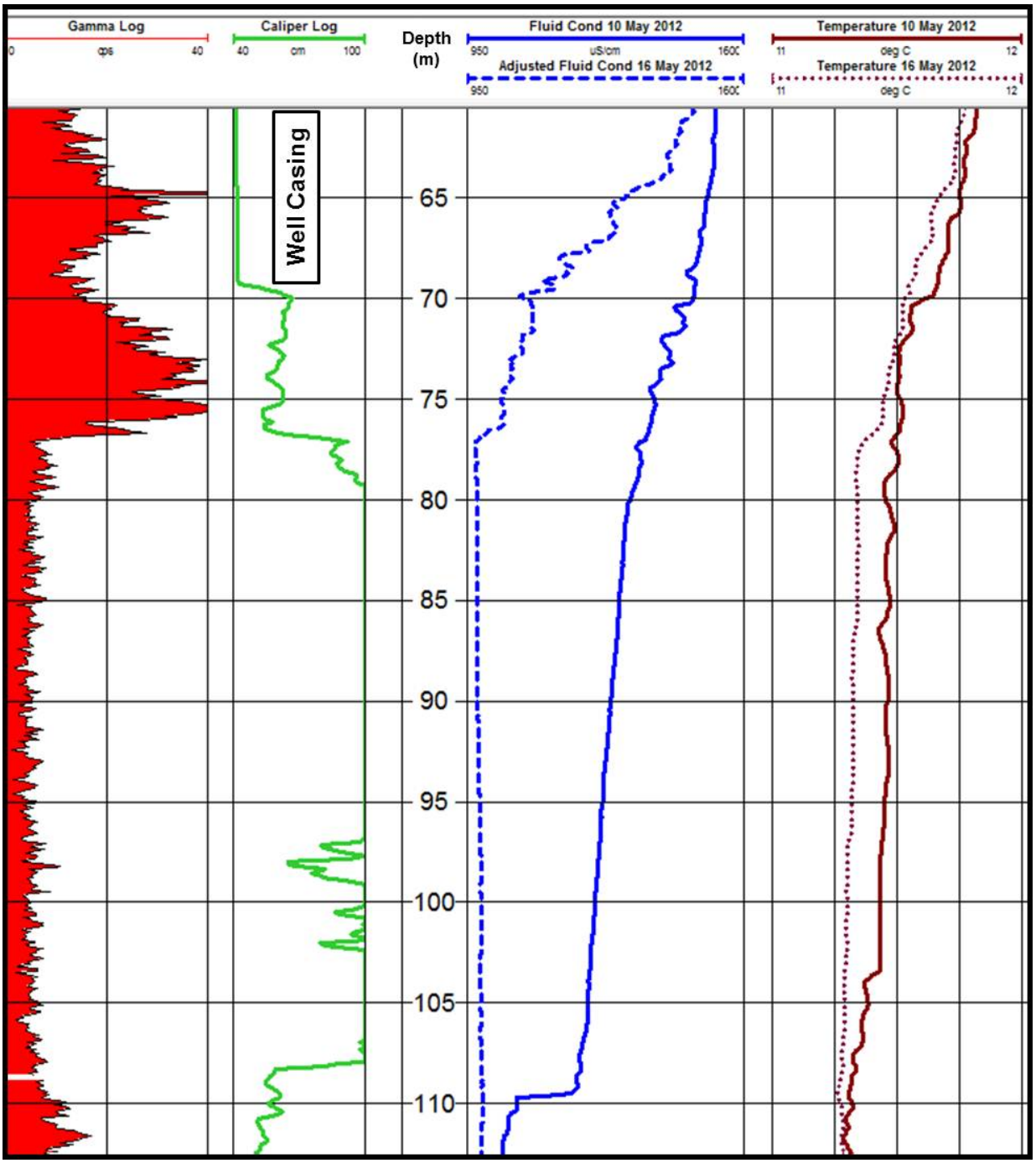

Figure 4.10. Geophysical logs from Unit Well 7 for enlarged interval in which the pump was seated. Both fluid conductivity and temperature decreased between 10 and 16 May as the well was open during pump replacement. Depth is in meters below top of casing, which is located in the well house basement, approximately 3 m below ground surface.

4.9. Conceptual model

A conceptual model was created to evaluate preferential flow pathways in terms of chemical and microbial wastewater indicators (Figure 4.11). This model is based on the fracture flow conceptual model described in Chapter 2 but modified to include electrical conductivity and virus data. As described earlier, conductivity can be used as a proxy for chloride and other wastewater indicators and at this site conductivity correlates with sodium and chloride concentrations and chloride/bromide ratios. The upper aquifer conductivity values on the figure were determined from the MW-C borehole using the straddle packer described in Chapter 2 and Appendix B. Most conductivity values listed in the upper aquifer are associated with a specific fracture except that the shallowest value of 1288 μS/cm is from an unfractured interval above Fracture 2. The value of 1546 μS/cm depicted at approximately 55 m bgs is from the high angle Fracture 9. The lower aquifer value of 1100 μS/cm was obtained from the UW-7 geophysical logging described in section 4.5.

Based on the conductivity values in the conceptual model, the conductivity values at the water table are relatively low, increase rapidly at 20 m bgs, decrease rapidly for a few meters downward, and decrease more slowly with depth to the bottom of the upper aquifer. If fractures only account for increased horizontal flow, the expected results for monitoring well samples should have a similar pattern as described above with low values at MW-A, higher values at MW-B, and slightly lower values at MW-C. As seen in the lower right corner of Figure 4.11, during 2012 the water table (MW-A) had lower conductivity than the shallowest packer value of 1288 μS/cm. This is

to be expected since no high transmissive fractures are located near the water table and lower conductivity rain water might infiltrate and mix with groundwater at the water table. At MW-B the conductivity should have a value of approximately 1733 µS/cm, corresponding to the value measured for Fracture 6, but the measured value was 2296 µS/cm, much higher than expected. In contrast, the values from MW-C were lower than expected based on values measured for Fracture 12, which intersects the well screen. The values of water pumped from UW-7 were lower than would be expected based on measurements made during the logging of the open well.

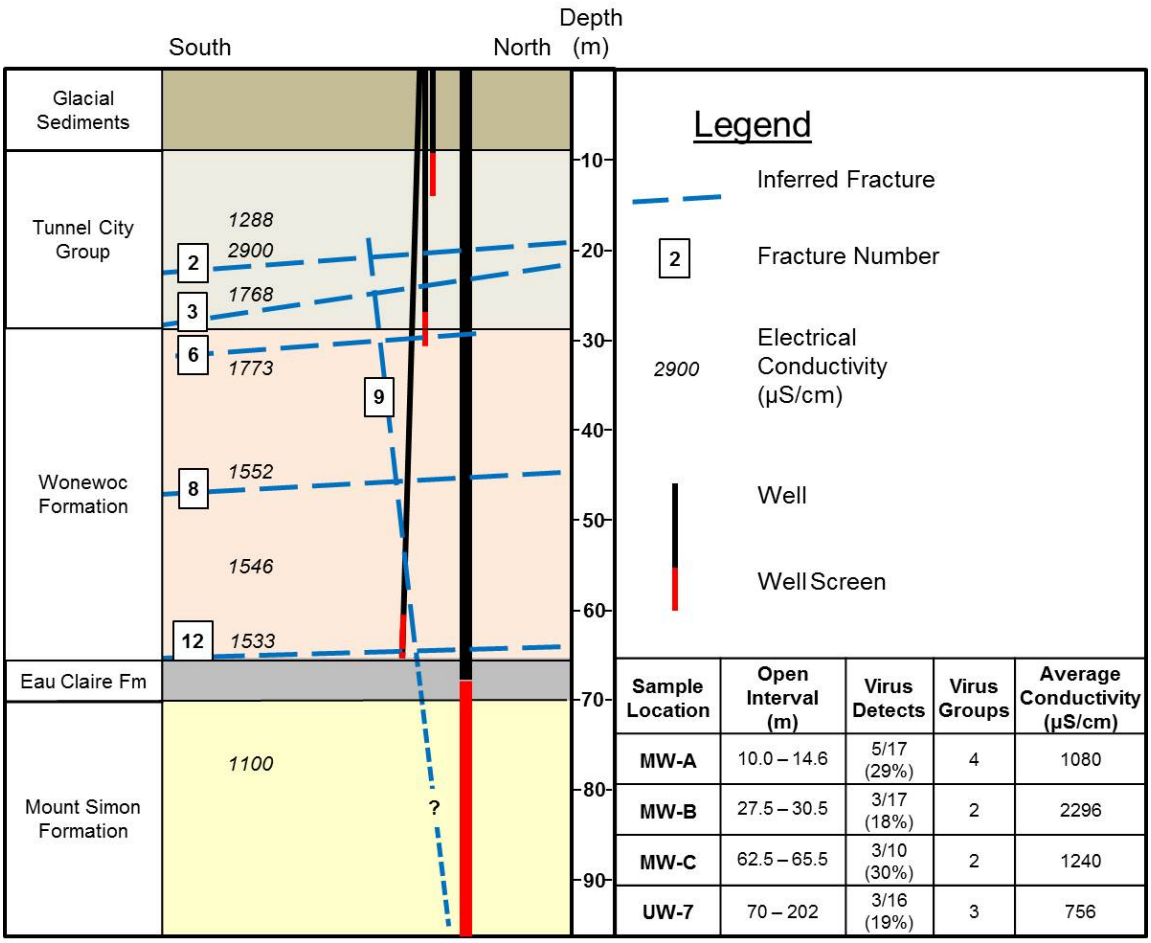

Sample Location	Open Interval (m)	Virus Detects	Virus Groups	Average Conductivity (µS/cm)
MW-A	10.0 – 14.6	5/17 (29%)	4	1080
MW-B	27.5 – 30.5	3/17 (18%)	2	2296
MW-C	62.5 – 65.5	3/10 (30%)	2	1240
UW-7	70 – 202	3/16 (19%)	3	756

Figure 4.11. Conceptual model of Unit Well 7 based on Figure 2.7. The lower 100+ m of the Mount Simon Formation and Unit Well 7 are not shown.

If vertical fracture flow is assumed in the model, the monitoring well values are more consistent with expected results. As noted above, the values in MW-B were much higher than those measured in Fracture 6. Mixing of groundwater from Fractures 2 and 6 in almost equal proportions would explain the observed values in MW-B. This is possible if Fracture 2 groundwater migrates downward along Fracture 9 during the pumping of MW-B. The values in MW-C can be explained by mixing one part Fracture 12 groundwater with two parts Mount Simon groundwater as measured at the top of the UW-7 borehole during logging. Since these conductivity values were measured while pumping a total volume of 1,000 L over several hours, this mixing would only be possible if a vertical fracture near MW-C allowed substantial amounts of water from the lower aquifer to flow through the Eau Claire aquitard. Insufficient data were collected on potential fracture flow pathways in the UW-7 borehole to explain the lower conductivity values measured while UW-7 was being pumped.

Microbial data collected during this study were not sufficient to clearly identify preferential flow pathways, but did provide some support for the conceptual model of horizontal and vertical fracture flow. The only total coliform detects were from MW-B. This wastewater indicator was not detected at the water table and suggests horizontal and vertical fracture flow between the source and MW-B. As seen in the in Figure 4.11, virus genomes were most often found in MW-A during low recharge sampling in 2012. However, during the highest recharge event in February 2011 MW-B and UW-7 both had enterovirus positive samples. This suggests that high recharge events are required for migration of viruses deep into the aquifer system. The model would predict virus

genome concentrations to be several orders of magnitude lower in UW-7 compared with the upper aquifer. Virus sampling in the monitoring wells was conducted at a pumping rate of 4 l/min while UW-7 was being pumped at thousands of l/min, drawing most of its water from the lower aquifer. The high volume of water produced from the Mount Simon aquifer would lead to dilution of any wastewater that flowed from the upper aquifer into UW-7, reducing the virus genome concentration substantially. The ranges of virus genome concentrations detected in both the upper aquifer and UW-7 are similar. One explanation for this similarity is that the pathway from the surface does not pass directly through any of the monitoring wells but, instead, travels through fractures to a location close to the UW-7 pump. In that scenario viruses would be subject to dilution before entering a monitoring well as they mixed with uncontaminated groundwater from the pore water or other fractures.

5. Conclusions

Time sequenced sampling for human enteric viruses and geochemical parameters is a useful tool for characterizing transport within an aquifer system. The microbiological and chemical data from wastewater and groundwater samples at the UW-7 site improved the understanding of how near surface wastewater may travel into a deep confined aquifer and reach a public supply well. There is an apparent connection between recharge events and increased flow in the sanitary sewer and, based on limited data, these increased wastewater flows appear linked with virus genome detection in groundwater at short times after these events. During lower recharge periods, viruses are more likely to be detected at the water table. In contrast,

during periods of higher recharge virus genomes are found in MW-B, which intersects a network of fractures that contains high levels of wastewater indicators. The lack of substantial recharge events during the 2012 sampling precluded a more extensive evaluation of the impact of recharge on transport.

The combination of virus genome and water chemistry data is useful for evaluating whether the UW-7 annulus is the preferential flow pathway. As discussed in Chapter 3, the lack of a pronounced water level response at the water table (MW-A) during unit well pumping suggests the well annulus is not leaking. Only one of the six virus genome detections in MW-A over a 2 year period had a corresponding detection in UW-7. Water chemistry data also indicate that the deeper MW-B has a more enhanced wastewater signature than MW-A. These virus and chemical data further support the conclusion that no direct connection exists along the UW-7 annulus between the water table and unit well pump. The results of the UW-7 borehole logging support the likelihood of a fracture connection between the upper and lower aquifers that allows high conductivity water to migrate downward. In summary, the combination of geochemical and virus sampling builds support for a conclusion that fractures create the preferential flow pathways at this site that allow wastewater contaminants to reach the lower aquifer.

The results of the geochemical and virus sampling at Madison UW-7 have implications for other urban areas in similar hydrogeologic settings. Madison has separate storm and sanitary sewer systems but still experiences increased sanitary sewer flows during recharge events. Combined sewer systems would be expected to

pose an even greater risk of groundwater contamination. In the U.S. more than 40 million people in 700 communities, mostly in the Northeast and Great Lakes regions, are served by combined sewer systems. These combined sewer systems are known to negatively impact surface water through combined sewer overflows during large rain events. It is likely that combined sewers may also impact local aquifers due to high levels of exfiltration during rain events. Consideration must also be given to the contribution of sewers to increased sodium and chloride levels in groundwater that may currently be attributed to road salt application. This is more likely in areas with home water softeners that use salt. Other urban areas that attempt to assess PSW vulnerability due to virus contamination in groundwater must be prepared to conduct sampling that includes both temporal and spatial factors to ensure representative samples are collected. Fractures in these hydrostratigraphic units have been described in the Minneapolis region, another Upper Midwestern urban area that relies on these units for drinking water. These types of fractures may also be present in other siliciclastic aquifer systems but their contribution to groundwater flow and transport may not be appreciated. The location of vertical and horizontal fractures must be considered so that sampling can include potential preferential flow pathways.

Chapter 5. Conclusions

1. Conclusions

The overall goals of this research were to better understand the primary mechanisms that control the transport of human enteric viruses and other wastewater contaminants in bedrock multi-aquifer systems and to develop effective methods for assessing the vulnerability of public water supply wells (PSWs) in such settings. The results of this research are summarized below to address the hypotheses and questions posed in Chapter 1.

1. Preferential flow pathways associated with either fracture flow or defective well casings promote rapid downward transport of wastewater contaminants into the subsurface. What are the dominant transport pathways and how might one distinguish among these? What is the contribution of fracture flow in a siliciclastic aquifer?

The most effective methods for distinguishing between fracture flow and defective well construction pathways included (1) evaluating the relationship between water level responses at various depths in the aquifer, particularly propagation of reverse water-level fluctuations (RWFs), and unit well pumping; (2) comparing patterns of spatial and temporal virus genome detection between locations in the upper aquifer and those detected in unit well; and (3) comparison of the relative concentrations of chemical wastewater indicators by depth in the aquifer system. Rapid propagation of

RWFs may provide the most diagnostic evidence of a connected fracture network. A borehole in which a flexible liner was installed appeared to act as a proxy for a leaky well annulus. While the liner was installed, the water levels experienced substantial reverse water-level fluctuations (RWFs) when the unit well was in operation. When the liner was removed and the borehole grouted, those RWFs at the water table were no longer detected.

Flow through fractures in the upper aquifer was identified as the most likely mechanism for rapid transport of wastewater contaminants. Multiple borehole methods described in Chapter 2 detected several fractures with transmissivities that were substantially higher than the transmissivity of the surrounding aquifer matrix. Straddle packer slug tests, pumping test, and vertical flow assessment suggest that highly transmissive fractures could account for between 60% and 80% of the horizontal flow in the upper aquifer. Most fractures were near-horizontal but at least one high angle fracture was detected. Based on hydraulic head data this fracture appears connected with multiple near-horizontal fractures. Straddle packer water chemistry data from Chapter 2 show that one fracture (Fracture 2) contained wastewater indicators at much higher concentrations than in other fractures and this fracture is likely the source of these contaminants detected in MW-B. The rapid propagation of RWFs through the upper aquifer was attributed to a connected fracture network.

2. The cycling frequency and discharge of a high capacity public supply wells affects the rate of transport for sewer effluent in a multi-aquifer system. What is the mechanism responsible for reverse water-level fluctuations that are observed in the upper aquifer during pumping of the lower aquifer? How do RWFs rapidly propagate through the upper aquifer and what might these indicate about connectivity of fractures or other preferential flow paths?

Based on the limited virus data collected during this study, it was not possible to directly correlate PSW cycling frequency and discharge with wastewater transport rates. The method tested in this research to quantify rates of subsurface transport of effluent from leaking sewers was to conduct time sequenced sampling and to evaluate patterns of virus genome detections throughout the aquifer system combined with data on PSW operation. Unfortunately, it appears that a longer time sequence, and more favorable weather conditions to generate large recharge events, would be necessary to fully test the assumption that this is an effective method.

The key discovery from this research that is related to PSW pumping was the use of RWFs as a diagnostic indicator of fracture network connectivity. In a multi-aquifer system the likely mechanism for the generation of RWFs in an aquifer is a poroelastic effect in the adjacent aquitard. Pumping from a lower aquifer rapidly decreases the head surrounding the PSW and generates a Noordbergum effect (initial increase in water level at the start of pumping) in the overlying aquitard. When the unit well ceases pumping it generates a Rhade effect (initial decrease in water level when

pumping ceases) in the aquitard. These poroelastic effects are generated close to the pumping well and calculations based on matrix hydraulic diffusivity would not account for rapid propagation through an overlying aquifer. Shortly after the start or cessation of pumping, the RWFs were observed in private wells located hundreds of meters radially from the pumping well and tens of meters vertically above the aquitard, with a fracture network the most likely pathway for rapid propagation of these pressure changes. The ability to trace RWF propagation through an aquifer has the potential to provide information about the extent and connectivity of the fracture network.

Unlike previously described RWFs in observations wells, many RWFs in this study were preceded by an initial, brief drawdown or recovery that was quickly obscured by the larger RWF. These phenomena may be the result of fractures transmitting the drawdown/recovery pulse before the poroelastic response can generate a RWF and transmit it through the upper aquifer. Wells that are open to fractured intervals were most likely to experience RWFs. The rate of PSW pumping and the frequency at which the well cycles are factors that control the magnitude and duration of the RWFs.

3. Because they are detectable even after significant dilution and decay, human enteric viruses are a useful spatial and temporal tracer of sewage contaminant transport in the subsurface. Can virus data provide constraints on preferential pathways and processes that contribute to rapid contaminant migration? Is there a correlation between large recharge events, high rates of sewer flow, and detection of virus genomes at various depths in the subsurface?

Human enteric virus genomes were detected at all groundwater sampling locations at some time during the two year period of the project. Virus data provided insight on the question of flow pathways but results were limited due to a lack of clear patterns in the data. During periods of low recharge the most common location for virus genome detection was at the water table, but only one of those detections appears to correlate with the presence of the same virus group in the PSW. If a defective unit well casing or annular grout were the preferential flow pathway, then virus groups at the water table should appear in the PSW more often. During two recharge events (July 2010 and February 2011) virus genomes were detected in the intermediate monitoring well. A lack of consistent detection of specific virus groups in multiple groundwater locations, combined with little variation in virus groups detected in the wastewater, complicated efforts to define a travel time. The lack of substantial decreases in virus concentration with depth in the aquifer system suggests fractures are the preferential flow pathway.

There was a correlation between recharge events and flow in the sanitary sewer system. Data suggest that virus detection was linked with recharge events. However, viruses were also detected at multiple depths during the period in 2012 when no substantial recharge events occurred. Time sequenced sampling during additional periods with several large recharge events is required to collect data to further evaluate this question.

4. Because the cost and effort of virus genome sampling may not be practical for routine monitoring, other chemical and physical parameters may be more useful for identifying preferential flow pathways in a multi-aquifer system subject to wastewater contamination. Which chemical constituents are the most appropriate indicators of wastewater effluent in these settings? Which chemical or physical parameters correlate with virus genome detection in groundwater?

The elevated concentrations of sodium, chloride, and bromide in the upper aquifer are likely related to the widespread use of home water softeners in Madison. The absence of a seasonal trend in sodium and chloride levels suggests that road salt is not the source of these constituents. In other urban areas without widespread home water softening sodium and chloride have also been used as wastewater indicators (Eiswirth et al. 1995; Panno et al. 2006; Brown et al. 2009). Nitrate is likely related to the high levels of ammonia detected in the reducing environment of the sewer pipes. In these settings sodium, chloride, bromide, and nitrate are the most appropriate indicators of wastewater. Although all three monitoring wells displayed signs of wastewater

contamination, the intermediate monitoring well had the largest concentration of these indicators. Based on relative concentrations of the constituents above, shallow and deep wells have similar water compositions to the PSW while water quality in the intermediate well is more closely related to sewer effluent.

During the periods sampled, there did not appear to be a correlation between the wastewater indicators and virus detection. During the 2012 sampling the intermediate well contained the highest concentrations of wastewater indicators but the fewest virus detections. It is possible the high levels of chloride have an effect on virus decay. Alternatively, viruses may be more common in that well only during high recharge events that can move wastewater rapidly through deeper fractures. Since no large recharge events occurred during the five months of sampling in 2012 it is difficult to determine the cause of this relationship.

2. Significance

This research project was focused on one public supply well, Unit Well 7, in Madison, Wisconsin but has relevance to a much larger area. Specifically, the geological units from this project in Madison can also be found across a wide swath of the upper Midwest from Illinois to the Upper Peninsula of Michigan and from Minnesota to Iowa (Olcott 1992). In many of these locations the Mount Simon Formation is utilized as an aquifer and is overlain by the Eau Claire aquitard, Wonewoc Formation, and Tunnel City Group (or their equivalents). Many of the lessons learned in this dissertation may apply directly to these areas. More generally, other urban areas in the United States and across the world obtain drinking water from similar siliciclastic aquifer

systems consisting of several sandstone aquifers separated by one or more fine grained aquitards.

Traditional thinking has held that porous media flow is the primary method of transport in sandstone aquifers. The results of this project indicate that more than half of the flow in a sandstone aquifer may be attributed to flow through fractures. This finding implies that predictive analysis of such aquifers (for instance numerical modeling, designation of wellhead protection areas, and estimates of contaminant transport) need to consider rapid flow paths and flow through fractures. The identification and characterization of fractures and fracture related flow in sandstone aquifers is more important than previously thought.

The the observed responses to PSW pumping at this site further alters the perception of how sandstone aquifers behave. Pumping of an aquifer has long been known to create poroelastically generated RWFs in overlying aquitards. However, this research has demonstrated that RWFs can propagate through aquifers much farther and faster than predicted by diffusivity through porous media alone. The presence of high transmissivity fractures might allow these RWFs to propagate hundreds of meters in a few minutes and change hydraulic heads on the order of 10 cm or more. These rapid head changes within highly transmissive fractures might allow for rapid transport of contaminants and this phenomenon is deserving of additional study. The spatial and temporal patterns associated with aquifer RWF propagation might also be useful for characterizing fracture flow networks in other locations.

The detection of human enteric viruses in the shallow aquifer suggests that viruses detected in the PSW do not originate from within the well house and travel along a defective casing or grouting. Instead, a hydrogeological pathway through the upper aquifer must be responsible for transport of near surface wastewater contaminants reaching deep confined aquifers. Such pathways may be common elsewhere in these formations as well as in other siliciclastic aquifers.

As other areas are investigated it is becoming evident that it is important to continue expanding time sequenced groundwater sampling for enteric virus genomes to include more locations that have the potential to be subjected to wastewater contamination. The connection between recharge events, sewer flow, and virus detection is also significant. Many urban areas in the U.S. are served by combined sewers that rapidly overflow during heavy rainfall. In addition to the negative effects on surface water bodies from these combined sewer overflows, there may be an even greater long term impact on groundwater attributed to leakage from these combined sewers. Even areas with separate storm and sanitary sewers face a potential increased risk of virus contaminated groundwater after large recharge events.

Although flexible borehole liners are normally installed to prevent the vertical flow of groundwater, they may have utility as a proxy for a defective PSW annulus. By comparing the changes in water levels with depth in an aquifer during either a pumping test or normal PSW operation it might be possible to gain a better understanding of natural or man-made vertical conduits of flow. In an area where the hydrostratigraphy and details of PSW integrity are well known it might be possible to use similar data to

directly evaluate the ability of a borehole liner to prevent either flow or propagation of a pressure change. This may result in improved guidelines for determining the optimal head difference between the aquifer and inside the liner.

Hydrogeologists and water utility employees should consider the results of this research when siting, installing, and operating PSWs in siliclastic aquifer systems. Additional focus should be given to fracture identification and the contribution of fractures to flow in hydrostratigraphic settings that are similar to Madison. During pumping tests it is important to monitor water levels in the aquitards and other aquifers in the system on a time interval that will allow for the identification and quantification of any RWFs that are present. The use of RWFs as described in this research has the potential to characterize fracture network connectivity and the potential for near surface contaminants to rapidly reach PSWs. When operating PSWs in these settings it is important to consider pumping rates and frequency. High pumping rates and rapid cycling of PSWs might lead to substantial head changes and predominantly fracture flow in an aquifer. Low discharge, long duration pumping is more likely to allow the aquifer to transition from fracture dominated to matrix dominated flow and act as a dual porosity system, minimizing rapid head changes due to RWFs. The use of variable frequency drives that allow for adjustment of pumping rate will reduce the impact of high discharge, short duration pumping. The identification and utilization of RWFs might be an important, but overlooked, tool in the evaluation of PSW vulnerability to near surface contamination.

3. Future Research Needs

This project accomplished several goals and provided new insight into the problem of public supply well vulnerability. Some questions were not answered and new questions arose during the course of the research. The following related questions should be addressed in future projects.

3.1. Unsaturated zone transport

The unsaturated zone between the sanitary sewer and water table was not specifically studied in this project. For a full understanding of wastewater transport it is important to determine the mechanism and pathway for wastewater to travel from sanitary sewers to the water table through the unsaturated zone. Investigating this portion of the pathway is also the best option for obtaining a definitive answer to the question of whether the sanitary sewers are the actual source of enteric viruses in urban groundwater. Gravel utility trenches may also serve as horizontal preferential flow pathways that ultimately are connected to anthropogenic or natural vertical conduits. Estimates of sewer leakage under various flow rates and the distributed nature of the loading of groundwater with wastewater would improve understanding of the source. The use of dye tracing in sewers may be useful for confirming suspected flow pathways to the water table.

3.2. Evaluation of RWF duration

Analysis of RWFs during pumping allows for estimation of how much these phenomena could impact pumping test data. In some cases pumping test data are not evaluated until after the RWF has been overtaken by drawdown. The Noordbergum

response and the pumping drawdown have been considered two distinct phases, but they should be treated as two superimposed phenomena that interfere with each other. Both are present at the initiation of pumping but the Noordbergum response is initially much larger and causes water levels to rise. As the Noordbergum response diminishes and the effect of pumping drawdown increases, the water level will begin to fall. The evaluation of drawdown data from monitoring wells and public supply wells at multiple sites may be used in order to determine the relative influence of reverse water-level fluctuations compared with pumping and drawdown. Correction of drawdown data to remove the influence of the Noordbergum response may allow for more accurate estimates of aquifer parameters during pumping test analysis.

3.3. Numerical fracture flow modeling

An attempt was made to create a finite element hydromechanical model of the Unit Well 7 site in order to replicate the observed RWFs and develop a predictive model. However, as the importance of fracture flow in the upper aquifer was realized, it became apparent that existing hydromechanical modeling packages are not able to replicate the behavior of a fracture flow dominated aquifer that has observed RWFs. For future work it would be useful to create numerical models of pumping impacts on fractured aquifers using a software package to model discrete fracture networks. The fracture model might provide useful information by itself or be coupled with a hydromechanical model that may be able to better simulate fractures.

3.4. Long term virus sampling

Virus data from this project revealed that sampling of one site over several months was not adequate to characterize virus transport in these settings. Previous studies of multiple sites did not investigate the upper aquifer but did sample multiple PSWs. In order to properly characterize virus transport, it is important to conduct long term, time sequenced virus genome sampling at multiple sites to assess the impact of well pumping, recharge, and other factors on virus transport to public supply wells. At each site the upper aquifer should be sampled at multiple depths with wells positioned to intersect any highly transmissive fractures.

Wastewater samples are required for virus source characterization but obtaining a representative sample can be problematic. The wastewater treatment plant receives sewage from the entire metropolitan area. As a result, virus groups that are only present in local areas of the sewer system, such as near the PSW, might be diluted in the WWTP samples. Conversely, WWTP samples might contain virus groups that are present in other areas but not in the immediate vicinity of the PSW. The sanitary sewer near the PSW serves only a small portion of the neighborhood and did not typically have enough flow to allow collection of representative samples during a 24 hour period. A better location for collection of wastewater samples might be at the sewer pumping station that captures sewage from the entire neighborhood surrounding the PSW.

References

Abbaszadegan, M., M.S. Huber, C.P. Gerba, and I.L. Pepper. 1993. Detection of enteroviruses in groundwater with the polymerase chain reaction. *Appl. Environ. Microbiol.* 59 no. 5: 1318-1324.

Abbaszadegan, M., M. Lechevallier, and C. Gerba. 2003. Occurrence of viruses in US groundwaters. *Journal American Water Works Association* 95 no. 9: 107-120.

Abbaszadegan, M., P. Stewart, and M. LeChevallier. 1999. A Strategy for Detection of Viruses in Groundwater by PCR. *Appl. Environ. Microbiol.* 65 no. 2: 444-449.

Advanced Logic Technologies Inc. 2009. *WellCAD version 4.3 User's Manual*. Luxembourg: Advanced Logic Technologies, Inc.

Albinana-Gimenez, N., P. Clemente-Casares, B. Calgua, J.M. Huguet, S. Courtois, and R. Girones. 2009. Comparison of methods for concentrating human adenoviruses, polyomavirus JC and noroviruses in source waters and drinking water using quantitative PCR. *Journal of Virological Methods* 158 no. 1-2: 104-109.

Anderson, K.M. 2002. Hydrogeologic Controls on Flow to Frederick Springs in the Pheasant Branch Watershed, Middleton, WI, Department of Geology and Geophysics, University of Wisconsin-Madison, Madison, WI.

Andreasen, G.E., and J.W. Brookhart. 1963. Reverse water-level fluctuation. In *Methods of Collecting and Interpreting Ground-Water Data*, ed. R. Bentall. U.S. Geological Survey Water-Supply Paper 1544-H. pp. 30-35.

Aswasereelert, W., J.A. Simo, and D.L. LePain. 2008. Deposition of the Cambrian Eau Claire Formation, Wisconsin: hydrostratigraphic implications of fine-grained cratonic sandstones. *Geoscience Wisconsin* 19 no. 1: 1-21.

Blackwood, D.J., J.B. Ellis, D.M. Revitt, and D.J. Gilmour. 2005. Factors influencing exfiltration processes in sewers. *Water Science and Technology* 51 no. Compendex: 147-154.

Borchardt, M.A., K.R. Bradbury, E.C. Alexander, R.J. Kolberg, S.C. Alexander, J.R. Archer, L.A. Braatz, B.M. Forest, J.A. Green, and S.K. Spencer. 2010. Norovirus Outbreak Caused by a New Septic System in a Dolomite Aquifer. *Ground Water* 49 no. 1: 85-97.

Borchardt, M.A., K.R. Bradbury, M.B. Gotkowitz, J.A. Cherry, and B.L. Parker. 2007. Human enteric viruses in groundwater from a confined bedrock aquifer. *Environmental Science & Technology* 41 no. 18: 6606-6612.

Borchardt, M.A., N.L. Haas, and R.J. Hunt. 2004. Vulnerability of drinking-water wells in La Crosse, Wisconsin, to enteric-virus contamination from surface water contributions. *Applied and Environmental Microbiology* 70 no. 10: 5937-5946.

Borchardt, M.A., S.K. Spencer, B.J.A. Kieke, E. Lambertini, and F.J. Loge. 2012. Viruses in Non-Disinfected Drinking Water from Municipal Wells and Community Incidence of Acute Gastrointestinal Illness. *Environ Health Perspect*.

Bosch, A. 1998. Human enteric viruses in the water environment: a minireview. *International Microbiology* 1 no. 3: 191-196.

Bosch, A., S. Guix, D. Sano, and R.M. Pinto. 2008. New tools for the study and direct surveillance of viral pathogens in water. *Current Opinion in Biotechnology* 19 no. 3: 295-301.

Boutt, D.F. 2010. Poroelastic Loading of an Aquifer Due to Upstream Dam Releases. *Ground Water* 48 no. 4: 580-592.

Bradbury, K.R., M.A. Borchardt, M.B. Gotkowitz, and R.J. Hunt. 2008. Assessment of Virus Presence and Potential Virus Pathways In Deep Municipal Wells. Wisconsin Geological and Natural History Survey Wisconsin Geological and Natural History Survey Open-File Report 2008-08, 48.

Bradbury, K.R., M.A. Borchardt, M.B. Gotkowitz, and S.K. Spencer. 2010. Human viruses as tracers of wastewater pathways into deep municipal wells. Wisconsin Geological and Natural History Survey Wisconsin Geological and Natural History Survey Open-File Report 2010-04A, 47.

Bradbury, K.R., and M.A. Muldoon. 1994. Effects of fracture density and anisotropy on delineation of wellhead-protection areas in fractured-rock aquifers. *Applied Hydrogeology* 2 no. 3: 17-23.

Bradbury, K.R., S.K. Swanson, J.T. Krohelski, and A.K. Fritz. 1999. Hydrogeology of Dane County, Wisconsin. Wisconsin Geological and Natural History Survey, Open-File Report 1999-04, 66.

Brahana, J.V., J. Thrailkill, T. Freeman, and W.C. Ward. 1988. Carbonate rocks. In *Hydrogeology*, ed. W. Back, J. S. Rosenshein and P. R. Seaber. Boulder, Colorado: Geological Society of America. pp. 333–352.

Brown, C.J., J.J. Starn, K.G. Stollenwerk, R.A. Mondazzi, and T.J. Trombley. 2009. Aquifer chemistry and transport processes in the zone of contribution to a public-supply well in Woodbury, Connecticut, 2002-06. *Scientific Investigations Report, Report: SIR* 158.

Burlingame, M.J. 2008. Determination of Aquifer and Aquitard Properties by Inverse Hydromechanical Modeling In *Continuum and Distinct Element Numerical Modeling in Geo-Engineering (Proceedings, 1st International FLAC/DEM Symposium, Minneapolis, August 2008)*, ed. R. Hart, C. Detournay and P. Cundall. Minneapolis, MN: Itasca Consulting Group, Inc.

Butler, J.J., Jr. 1998. *The Design, Performance, and Analysis of Slug Tests*: Lewis Publishers.

Carslaw, H.S., and J.C. Jaeger. 1959. *Conduction of Heat in Solids, 2nd ed.*: Oxford University Press.

Charles, K.J., J. Shore, J. Sellwood, M. Laverick, A. Hart, and S. Pedley. 2009. Assessment of the stability of human viruses and coliphage in groundwater by PCR and infectivity methods. *Journal of Applied Microbiology* 106 no. 6: 1827-1837.

Chisala, B.N., and D.N. Lerner. 2008. Distribution of sewer exfiltration to urban groundwater. *Proceedings of the Institution of Civil Engineers: Water Management* 161 no. Compendex: 333-341.

Cline, D.R. 1965. Geology and ground-water resources of Dane County, Wisconsin. United States Government Printing Office U.S. Geological Survey Water Supply Paper 1779-U, 64.

Cronin, A.A., R.G. Taylor, K.L. Powell, M.H. Barrett, S.A. Trowsdale, and D.N. Lerner. 2003. Temporal variations in the depth-specific hydrochemistry and sewage-related microbiology of an urban sandstone aquifer, Nottingham, United Kingdom *Hydrogeology Journal* 11 no. 2: 205-216.

Day-Lewis, F.D., C.D. Johnson, F.L. Paillet, and K.J. Halford. 2011. A Computer Program for Flow-Log Analysis of Single Holes (FLASH). *Ground Water* 49 no. 6: 926-931.

DeBorde, D.C., W.W. Woessner, Q.T. Kiley, and P. Ball. 1999. Rapid transport of viruses in a floodplain aquifer. *Water Research* 33 no. 10: 2229-2238.

DeBorde, D.C., W.W. Woessner, B. Lauerman, and P.N. Ball. 1998. Virus Occurrence and Transport in a School Septic System and Unconfined Aquifer. *Ground Water* 36 no. 5: 825-834.

Dongdem, J.T., S. Ireneous, and A. Ocloo. 2009. Public health significance of viral contamination of drinking water. *African Journal of Microbiology Research* 3 no. 12: 856-861.

Eberts, S.M., M.L. Erwin, and P.A. Hamilton. 2005. Assessing the vulnerability of public-supply wells to contamination from urban, agricultural, and natural sources. USGS Fact Sheet 2005-3022, 4 p.

Eiswirth, M., H. Hoetzl, and C. Schonfeldt. 1995. Ground water contamination by leaking sewerage systems. In *Groundwater Quality: Remediation and Protection. IAHS Publication no. 225*, 337-346.

Golder Associates Inc. 2010. *FracMan User's Manual Release 7.3*. Redmond, Washington: Golder Associates Inc.

Gordon, C., and S. Toze. 2003. Influence of groundwater characteristics on the survival of enteric viruses. *Journal of Applied Microbiology* 95 no. 3: 536-544.

Hsieh, P.A. 1996. Deformation-Induced Changes in Hydraulic Head During Ground-Water Withdrawal. *Ground Water* 34 no. 6: 1082-1089.

Hunt, R.J., M.A. Borchardt, K.D. Richards, and S.K. Spencer. 2010. Assessment of Sewer Source Contamination of Drinking Water Wells Using Tracers and Human Enteric Viruses. *Environmental Science & Technology* 44 no. 20: 7956-7963.

Hurst, C.J. 1988. Effect of environmetnal variables on enteric virus survival in surface fresh-waters. *Water Science and Technology* 20 no. 11-12: 473-476.

Jacob, C.E. 1939. Fluctuations in artesian pressure produced by passing railroad-trains as shown in a well on Long Island, New York. *Transactions - American Geophysical Union* 20: 666-674.

Jaeger, J.C., N.G.W. Cook, and R.W. Zimmerman. 2007. *Fundamentals of Rock Mechanics*. 4th ed. Malden, MA: Wiley-Blackwell.

John, D.E., and J.B. Rose. 2005. Review of Factors Affecting Microbial Survival in Groundwater. *Environmental Science & Technology* 39 no. 19: 7345-7356.

Katz, B., S. Eberts, and L.J. Kauffman. 2011. Using Cl/Br ratios and other indicators to assess potential impacts on groundwater quality from septic systems: A review and examples from principal aquifers in the United States. *Journal of Hydrology* 397: 151–166.

Keller, C. 2012. Hydrogeologic Spatial Resolution using Flexible Liners. *The Professional Geologist* 49 no. 3: 45-51.

Kelly, W.R., S.V. Panno, and K.C. Hackley. 2012. Impacts of Road Salt Runoff on Water Quality of the Chicago, Illinois, Region. *Environmental & Engineering Geoscience* 18 no. 1: 65-81.

Kelly, W.R., S.V. Panno, K.C. Hackley, H.-H. Hwang, A.T. Martinsek, and M. Markus. 2010. Using chloride and other ions to trace sewage and road salt in the Illinois Waterway. *Applied Geochemistry* 25 no. 5: 661-673.

Keswick, B., and C. Gerba. 1980. Viruses in groundwater. *Environmental Science & Technology* 14 no. 11: 1290-1297.

Kim, J.M., and R.R. Parizek. 1997. Numerical simulation of the Noordbergum effect resulting from groundwater pumping in a layered aquifer system. *Journal of Hydrology* 202 no. 1-4: 231-243.

———. 2005. Numerical simulation of the Rhade effect in layered aquifer systems due to groundwater pumping shutoff. *Advances in Water Resources* 28 no. 6: 627-642.

Krohleski, J.T., K.R. Bradbury, R.J. Hunt, and S.K. Swanson. 2000. Numerical model of groundwater flow in Dane County, Wisconsin. Wisconsin Geological and Natural History Survey Bulletin 98, 31.

Lacombe, S., E.A. Sudicky, S.K. Frape, and A.J.A. Unger. 1995. Influence of leaky boreholes on cross-formational groundwater-flow and contaminant transport. *Water Resources Research* 31 no. 8: 1871-1882.

Lambertini, E., S.K. Spencer, P.D. Bertz, F.J. Loge, B.A. Kieke, and M.A. Borchardt. 2008. Concentration of enteroviruses, adenoviruses, and noroviruses from drinking water by use of glass wool filters. *Applied and Environmental Microbiology* 74 no. 10: 2990-2996.

Landon, M., B. Jurgens, B. Katz, S. Eberts, K. Burow, and C. Crandall. 2010. Depth-dependent sampling to identify short-circuit pathways to public-supply wells in multiple aquifer settings in the United States. *Hydrogeology Journal* 18 no. 3: 577-593.

Langguth, H.R., and C. Treskatis. 1989. Reverse water level fluctuations in semiconfined aquifer systems -- "rhade effect". *Journal of Hydrology* 109 no. 1-2: 79-93.

Leaf, A.T., D.J. Hart, and J.M. Bahr. 2012. Active Thermal Tracer Tests for Improved Hydrostratigraphic Characterization. *Ground Water*.

Madison Water Utility. 2011. Well 7 Water Quality Report, 3p.

Mattison, K., and S. Bidawid. 2009. Analytical Methods for Food and Environmental Viruses. *Food and Environmental Virology* 1 no. 3: 107-122.

Maxey, G.B. 1964. Hydrostratigraphic units. *Journal of Hydrology* 2 no. 2: 124-129.

Meyer, J., B. Parker, and J. Cherry. 2008. Detailed hydraulic head profiles as essential data for defining hydrogeologic units in layered fractured sedimentary rock. *Environmental Geology* 56 no. 1: 27-44.

Minnesota Department of Health. 2011. Assessment Monitoring Pilot Study. 58p.

Moench, A.F. 1984. Double-Porosity Models for a Fissured Groundwater Reservoir With Fracture Skin. *Water Resources Research* 20 no. 7: 831-846.

Muldoon, M.A., J.A. Simo, and K.R. Bradbury. 2001. Correlation of hydraulic conductivity with stratigraphy in a fractured-dolomite aquifer, northeastern Wisconsin, USA. *Hydrogeology Journal* 9 no. 6: 570-583.

Nilson, R.H., E.W. Peterson, K.H. Lie, N.R. Burkhard, and J.R. Hearst. 1991. Atmospheric Pumping: A Mechanism Causing Vertical Transport of Contaminated Gases Through Fractured Permeable Media. *J. Geophys. Res.* 96 no. B13: 21933-21948.

Olcott, P.G. 1992. Groundwater Atlast of the United States, Segment 9. USGS Hydrologic Investigations Atlas 730-J.

Paillet, F.L. 1998. Flow modeling and permeability estimation using borehole flow logs in heterogeneous fractured formations. *Water Resources Research* 34 no. 5: 997-1010.

Paillet, F.L. 2000. A Field Technique for Estimating Aquifer Parameters Using Flow Log Data. *Ground Water* 38 no. 4: 510-521.

Panno, S.V., K.C. Hackley, H.H. Hwang, S.E. Greenberg, I.G. Krapac, S. Landsberger, and D.J. O'Kelly. 2006. Characterization and Identification of Na-Cl Sources in Ground Water. *Ground Water* 44 no. 2: 176-187.

Powell, K.L., R.G. Taylor, A.A. Cronin, M.H. Barrett, S. Pedley, J. Sellwood, S.A. Trowsdale, and D.N. Lerner. 2003. Microbial contamination of two urban sandstone aquifers in the UK. *Water Research* 37 no. 2: 339-352.

Rayne, T.W., K.R. Bradbury, and M.A. Muldoon. 2001. Delineation of capture zones for municipal wells in fractured dolomite, Sturgeon Bay, Wisconsin, USA. *Hydrogeology Journal* 9 no. 5: 432-450.

Rueedi, J., A.A. Cronin, and B.L. Morris. 2009. Estimation of sewer leakage to urban groundwater using depth-specific hydrochemistry. *Water and Environment Journal* 23 no. 2: 134-144.

Runkel, A.C., R.G. Tipping, E.C. Alexander Jr, and S.C. Alexander. 2006. Hydrostratigraphic characterization of intergranular and secondary porosity in part of the Cambrian sandstone aquifer system of the cratonic interior of North America: Improving predictability of hydrogeologic properties. *Sedimentary Geology* 184 no. 3-4: 281-304.

Rutqvist, J., J. Noorishad, C.-F. Tsang, and O. Stephansson. 1998. Determination of fracture storativity in hard rocks using high-pressure injection testing. *Water Resources Research* 34 no. 10: 2551-2560.

Schweisinger, T., E. Svenson, and L. Murdoch. 2011. Hydromechanical behavior during constant-rate pumping tests in fractured gneiss. *Hydrogeology Journal* 19 no. 5: 963-980.

Seaber, P.R. 1988. Hydrostratigraphic units. In *The geology of North America volume O-2*, vol. 2, ed. W. Back, J. S. Rosenshein and P. R. Seaber. Boulder, CO: The Geological Society of America. pp. 9-14.

Swanson, S.K. 2001. Hydrogeologic controls on spring flow near Madison, Wisconsin, Department of Geology and Geophysics, University of Wisconsin -- Madison, Madison, WI.

Swanson, S.K. 2007. Lithostratigraphic controls on bedding-plane fractures and the potential for discrete groundwater flow through a siliciclastic sandstone aquifer, southern Wisconsin. *Sedimentary Geology* 197 no. 1-2: 65-78.

Swanson, S.K., J.M. Bahr, K.R. Bradbury, and K.M. Anderson. 2006. Evidence for preferential flow through sandstone aquifers in Southern Wisconsin. *Sedimentary Geology* 184 no. 3-4: 331-342.

Taylor, R., A. Cronin, S. Pedley, J. Barker, and T. Atkinson. 2004. The implications of groundwater velocity variations on microbial transport and wellhead protection – review of field evidence. *FEMS Microbiology Ecology* 49 no. 1: 17-26.

U.S. Environmental Protection Agency. 1999. A review of contaminant occurrence in public water systems. 78p.

———. 2006. National Primary Drinking Water Regulations: Ground Water Rule, vol. 71, 65574-65660. Washington, DC: Federal Register.

———. 2009. Drinking Water Contaminant Candidate List 3 -- Final, vol. 74, 51850-51862. Federal Register.

Underwood, C.A., M.L. Cooke, J.A. Simo, and M.A. Muldoon. 2003. Stratigraphic controls on vertical fracture patterns in Silurian dolomite, northeastern Wisconsin. *AAPG Bulletin* 87 no. 1: 121-142.

Verruijt, A. 1969. Elastic storage of aquifers. In *Flow through porous media*, ed. R. J. M. de Weist. New York: Academic Press. pp. 331-376.

Wang, H.F. 2000. *Theory of linear poroelasticity with applications to geomechanics and hydrogeology*. Princeton, New Jersey: Princeton University Press.

Wenta, R., and K. Sorsa. 2011. Road Salt Report – 2011, ed. P. H. M.-.-D. County, 26. Madison, WI.

Williams, J.H., and R.W. Conger. 1990. Preliminary Delineation of Contaminated Water-Bearing Fractures Intersected by Open-Hole Bedrock Wells. *Ground Water Monitoring & Remediation* 10 no. 4: 118-126.

Yates, M.V. 2007. Classical Indicators in the 21st Century -- Far and Beyond the Coliform. *Water Environment Research* 79 no. 3: 279-86.

Yates, M.V., C.P. Gerba, and L.M. Kelley. 1985. Virus persistence in groundwater. *Appl. Environ. Microbiol.* 49 no. 4: 778-781.

Yates, M.V., S.R. Yates, J. Wagner, and C.P. Gerba. 1987. Modeling virus survival and transport in the subsurface. *Journal of Contaminant Hydrology* 1 no. 3: 329-345.

Yeh, H.-Y., M.V. Yates, W. Chen, and A. Mulchandani. 2009. Real-time molecular methods to detect infectious viruses. *Seminars in Cell & Developmental Biology* 20 no. 1: 49-54.

Appendix A: Well drilling logs

1. MW-B log

Wisconsin Geological & Natural History Survey
3817 W. Mineral Point Road, Madison, Wi 53705

WG&NHS Log No: DN -6017

Title: Geologic Log

Site Name: UW-Madison Monitoring Well 7-MW-1

County: DANE
Completed:
Field Check:

Owner: UW-Madison Geoscience Department
Address:

Driller(s):
Engineer:

Elevation: 889 ±3'
Well Use: monitoring
Static Level: 40'

Location: **SW, NW, NW, Sec. 31, T8N, R10E**

Topo Name: Madison East
Sample Nos.: AP14
Perm No.:
WI-Unique ID#:

Pump Test:
Pumped at GPM for hrs. with ft. of drawdown.
On 4/2010

Drill Hole Dimensions		
Diameter	From	To

Drilling Method		
Method	From	To

Grout		
Kind	From	To

Samples Rec'd:
4/15/2010 0' to 100'

Studied By:
Roger M. Peters 5' to 100'

Open Interval Characteristics			
Diameter	From	To	Opening Type

Casing & Liner Information				
Diameter	From	To	Casing	Weight

Types of records available for this site (* indicates indexing term):

Detailed location map, Geologic log, *subsurface boring (non-core) site, Drill cuttings available

Formations:

Horicon Member, Mazomanie Formation, Wonewoc Formation

Log Comments:

Driller reported very friable bedrock at 30 feet. No geophysical logs run.

This geologic log has undergone basic review. Some information may need to be added or further reviewed. If essential information is missing or incorrect, please contact WG&NHS at rpeters@wisc.edu or (608)-263-7387.

Version tracking:
6/23/2010 Initial digital version
4/25/2011 Updated digital version

Wisconsin Geological & Natural History Survey

WG&NHS Log No: DN -6017

3817 W. Mineral Point Road, Madison, Wi 53705

Site Name: UW-Madison Monitoring Well 7-MW-1

Title: Geologic Log

	Depths	Graphic	RockType	Color	Mode	Range	Miscellaneous Characteristics
	0-5		NO SAMPLE				--
	at 5		clay	brown	--	--	Very silty. Trace organic material, sand up to coarse-grained. One 7.5mm piece of gravel.
	at 10		clay	brown	--	--	Much silt, sand up through fonr grained. Trace M/VC sand, granules.
	at 15		clay & sand	brown	Vfn/Fn	Vfn/VC	Much silt. Trace gravel up to large pebble.
Horicon Member	at 18		clay & sand	pale brown	M	Vfn/VC	Pale brown very fine clay. All sand and gravel is coated with pale brown clay. Little gravel up to medium pebble, silt. Clay is very coating - it reminds me of a taconite pellet operation.
	at 25		sand	pale brown	M	Vfn/VC	Radical change. Clay free. Trace silt, gravel up to large pebble.
	at 30		sand	pale brown	Fn	Vfn/VC	Little/much very fine coating clay. Little silt. Trace granules.
	at 35		sand	pale brown	Fn	Vfn/VC	Little/much very fine coating clay. Little silt. Trace granules/small pebbles.
	at 40		sandstone	pale yellow brown	Fn	Vfn/C	Radical change. Well sorted. Little dolomite cement. Trace silt.
	at 45		sandstone	pale yellow brown	Fn	Vfn/M	Slightly coarser. Well sorted. Little dolomite cement, Vfn pale brown clay coating on cemented sanstone pieces. Trace silt.
	at 50		sandstone	pale yellow brown	Fn	Vfn/M	Well sorted. Little dolomite cement, Vfn pale brown clay coating on cemented sanstone pieces. Trace silt.
	at 55		sandstone	pale yellow brown	Fn	Vfn/M	Well sorted. Little dolomite cement (less than above), silt. Trace silt-sized glauconite.
	at 60		sandstone	pale yellow brown	Fn	Vfn/C	Well sorted. Much dolomite cement. Little silt. Trace silt-sized glauconite. Coarse grains are rare.
Mazomanie Formation	at 65		sandstone	pale yellow brown	Vfn/Fn	Vfn/C	Little dolomite cement, silt. Trace silt/fine grain-sized glauconite. Coarse grains are rare.
	at 70		sandstone	pale yellow brown	Fn	Vfn/M	Much dolomite cement. Little light gray to pale gray green shale, silt. Trace silt/VC grain-sized glauconite. One 30mm pebble of red brown/purple shale with some flaoting Fn/M quartz sand - probably caved.
	at 75		sandstone	pale yellow brown	Fn	Vfn/C	Little dolomite cement, silt. Trace silt/Vfn grain-sized glauconite, caved light gray shale.
	at 80		sandstone	pale yellow brown	Fn	Vfn/VC	Somewhat coarser. Little caved drift gravel (chert, trap, M-grained dolomite). Trace silt/medium grain-sized glauconite, dolomite cement, silt.
	at 85		sandstone	pale yellow brown	Fn/M	Vfn/VC	Somewhat darker. Little dolomite cement. Trace silt, caved drift sand & gravel, silt/medium grain-sized glauconite. VC grains are rare.
	at 90		sandstone	pale yellow brown	Fn	Vfn/C	Light in color again. Trace dolomite cement, silt, silt/medium grain-sized glauconite, caved sand & gravel.
Wonewoc Formation	at 95		sandstone	pale yellow brown	M	Vfn/VC	Little caved sand & gravel. Trace silt, silt/medium grain-sized glauconite. No apparent cementation.
	at 100		sandstone	pale yellow brown	M/C	Vfn/VC	Little caved sand & gravel (dolomite, trap). Trace silt. No apparent cementation, glauconite.

2. MW-C log

Wisconsin Geological & Natural History Survey
3817 Mineral Point Road, Madison, WI 53705

WG&NHS Log No: DN -6039

Title: Geologic Log

Site Name: Monitoring Well 7-MW-3 (Madison City Well #7)

County: DANE
Completed: 4/20/2011
Field Check:

Owner: UW-Madison Geoscience Department
Address: 1215 W. Dayton St.
Madison, WI 53706
Driller(s): Ground Source, Inc.
Engineer: Chris Gellasch

Elevation: 889 ±5'
Well Use: monitoring
Static Level: 39.4'

Location: **SW, NW, NW, Sec. 31, T8N, R10E**
Topo Name: Madison East
Sample Nos.: AQ10
Perm No.:
WI-Unique ID#: VX597

Pump Test:
Pumped at GPM for hrs. with ft. of drawdown.
On 4/21/2011

Samples Rec'd:
4/20/2011 30' to 220'

Studied By:
Roger M. Peters 30' to 220'

Drill Hole Dimensions		
Diameter	From	To
6"	0'	218'

Drilling Method		
Method	From	To
rotary wash	0'	30'
air rotary	30'	218'

Grout		
Kind	From	To

Open Interval Characteristics			
Diameter	From	To	Opening Type

Casing & Liner Information				
Diameter	From	To	Casing	Weight
6"	0'	30'	steel	

Types of records available for this site (* indicates indexing term):

*geophysical log(s) exist, Geologic log, *subsurface boring (non-core) site, Drill cuttings available

Formations:

Horicon Member, Tunnel City Group, Wonewoc Formation, trans Eau Claire / Wonewoc, Eau Claire Formation

Log Comments:

This geologic log has undergone basic review. Some information may need to be added or further reviewed. If essential information is missing or incorrect, please contact WG&NHS at rpeters@wisc.edu or (608)-263-7387.

Version tracking:

9/19/2011 Initial digital version
9/29/2011 Revised/updated log

Wisconsin Geological & Natural History Survey
3817 Mineral Point Road, Madison, WI 53705

WG&NHS Log No: DN -6039

Site Name: Monitoring Well 7-MW-3 (Madison City Well #7)

Title: Geologic Log

	Depths	Graphic	RockType	Color	Mode	Range	Miscellaneous Characteristics
Horicon Member	0-30		NO SAMPLE				--
Tunnel City Group	30-35		sandstone	brown yellow	Fn	Vfn/VC	Little dolomite cement. Trace silt/fine glauconite.
	35-40		sandstone	brown yellow	Fn/M	Vfn/VC	Well sorted. Trace to little dolomite cement. No glauconite.
	40-45		sandstone	pale brown	Vfn	Vfn/C	Trace silt/Vfn glauconite, dolomite cement. C grains are rare.
	45-50		sandstone	pale yellow brown	Vfn/Fn	Vfn/M	Minor trace glauconite.
	50-55		sandstone	pale yellow brown	Vfn/Fn	Vfn/M	Trace silt. No glauconite.
	55-60		sandstone	gray yellow brown	Fn	Vfn/C	Little dolomite cement. Trace glauconite, silt.
	60-65		sandstone	gray yellow brown	Fn	Vfn/M	Much dolomite cement. Little silt. Trace glauconite.
	65-70		sandstone	weak yellow brown	Vfn/Fn	Vfn/M	Much silt. Little dolomite cement. Minor trace glauconite.
	70-75		sandstone	weak yellow brown	Vfn/Fn	Vfn/M	Little dolomite cement, silt. Trace silt/M glauconite.
	75-80		sandstone	weak yellow brown	Fn	Vfn/VC	Little dolomite cement. Trace silt/M glauconite, pink sand grains, silt.
	80-85		sandstone	very pale brown	Fn	Vfn/C	Trace dolomite cement, silt/M glauconite, silt.
Wonewoc Formation	85-90		sandstone	very pale brown	M	Vfn/VC	Trace Vfn/Fn glauconite, silt.
	90-95		sandstone	very pale brown	Fn & C	Vfn/VC	Trace silt/M glauconite, silt. Poorly sorted.
	95-100		sandstone	very pale brown	M	Vfn/VC	Browner looking. Trace Vfn/M glauconite, quartz granules. Poorly sorted.
	100-105		sandstone	very pale brown	M	Vfn/VC	Trace Vfn/M glauconite. Poorly sorted.
	105-110		sandstone	very pale brown	M	Vfn/VC	Trace Fn/M glauconite. Poorly sorted.
	110-115		sandstone	very pale brown	Fn	Vfn/VC	Trace Fn/C glauconite.
	115-120		sandstone	very pale brown	M	Vfn/VC	Paler looking. Trace silt/M glauconite rusty drill bit fragments.
	120-125		sandstone	very pale brown	M	Vfn/VC	Minor trace glauconite.
	125-130		sandstone	very pale brown	M	Vfn/VC	Minor trace glauconite.
	130-135		sandstone	very pale brown	M	Vfn/VC	Trace very poor limonite cement, gray green shale, silt.
	135-140		sandstone	very pale brown	M	Vfn/VC	Trace silt.

Wisconsin Geological & Natural History Survey
3817 Mineral Point Road, Madison, WI 53705

WG&NHS Log No: DN -6039

Site Name: Monitoring Well 7-MW-3 (Madison City Well #7)

Title: Geologic Log

	Depths	Graphic	RockType	Color	Mode	Range	Miscellaneous Characteristics
Wonewoc Formation	140-145		sandstone	very pale brown	M	Vfn/VC	Trace silt, gray green shale.
	145-150		sandstone	very pale brown & or bn	M	Vfn/VC	50% orange brown, 50% very pale brown. Orange brown is an iron oxide coating. Trace limonite cement.
	150-155		sandstone	pale orange brown	M/C	Vfn/VC	20% iron oxide coated. One 7.5mm chunk of caved dolomite-cemented glauconitic Tunnel City. Trace caved glauconite.
	155-160		sandstone	orange brown	C	Vfn/VC	90% iron oxide coated.
	160-165		sandstone	yellow brown	M/C	Vfn/VC	90% iron oxide coated.
	165-170		sandstone	orange brown	C	Vfn/VC	90% iron oxide coated.
	170-175		sandstone	yellow brown	M/C	Vfn/VC	90% iron oxide coated. Trace excellent calcite cement.
	175-180		sandstone	yellow brown	M/C	Vfn/VC	90% iron oxide coated. Trace excellent calcite cement. One HCl test.
	180-185		sandstone	orange brown	M/C	Vfn/VC	60% iron oxide coated. Little excellent calcite cement. Trace limonite cement, caved glauconite, caved dolomite-cemented glaucic Tunnel City.
	185-190		sandstone	orange brown	M	Vfn/VC	60% iron oxide coated. Trace to little excellent calcite cement. Minor trace caved glauconite.
trans Eau Claire / Wonewoc	190-195		sandstone	v pale yellow brown	Fn	Vfn/C	Abrupt change. Trace silt.
	195-200		sandstone	very pale brown	Vfn/Fn	Vfn/C	Trace silt, rusty drill bit fragments.
	200-205		sandstone	pale brown	Fn	Vfn/VC	Little silt/C glauconite. Trace dolomite cement.
	205-210		sandstone	very pale brown	Fn	Vfn/VC	Little silt/M glauconite, silt.
	210-215		sandstone	very pale brown	Fn	Vfn/VC	Trace silt/M glauconite, gray green shale, silt, rusty drill bit fragments,
Eau Claire Formation	215-220		sandstone	very pale yellow brown	Fn	Vfn/VC	Little yellow brown grading to gray green shale with little pyrolusite. Trace silt/C glauconite, very poor dolomite cement, silt. One caved 30mm piece of dolomite-cemented glaucicTunnel City. HCl test.

Appendix B: Standard operating procedure for the light weight straddle packer

Construction: The system was built in August 2011 by Pete Chase (WGNHS) and Chris Gellasch (UW-Madison) using Lansas Flow-Thru™ packers (www.lansas.com) and a one foot long steel, 2-inch diameter well screen. The top packer was custom built with connectors and air ports on both ends and the bottom packer is a standard part number 092-48 packer. The bottom of the assembly is sealed with an expanding well plug. Both packers are connected in series to an airline and inflate at the same time. The top of the assembly is a 2 inch diameter schedule 80 PVC connector with NPT threads on the bottom. Two inch diameter schedule 80 PVC pipe is used as a riser to the surface. For measurement purposes, the top of the assembly is the seam between the PVC connector and the riser pipe.

Important Measurements (see figure):

A. Total length of packer assembly: 4.33 feet

B. Length from center of well screen to top of assembly: 2.44 feet

C. Length of open interval during packer inflation: 2.31 feet

Technical Data:

- Minimum well diameter: 3.8 inches
- Maximum well diameter: 6.25 inches
- Packer inflation pressure: 30 PSI (at surface)*
- Maximum head difference across packer: 15 PSI or ~35 feet
- Bypass diameter: 2 inches Note: upper packer bypass contains an inflation line and may not allow pumps to pass.

*If inflating packer below water level the following calculation must be used

[Depth of packer below water (ft) x 0.43 PSI/ft] + 30 PSI

Ex. At 100 feet below water, the packer must be inflated to (100 ft x 0.43 PSI/ft) + 30 PSI = 73 PSI

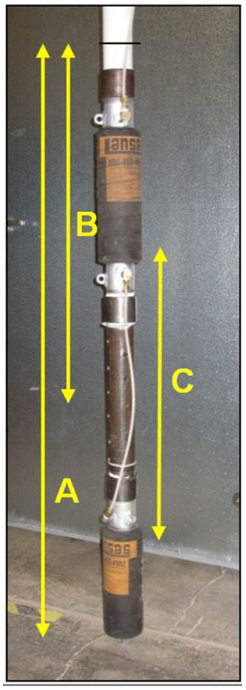

Before deployment in borehole:

1. Secure a safety line to the eyelet on the top packer.

2. Connect the air line from a compressed nitrogen tank to the packer air port.

3. Connect the assembly to a 10 foot PVC riser pipe followed by a lifting cap with eyelet. Connect the chain from the lowering winch to the lifting cap.

4. Use electrical tape to attach a measuring tape to the PVC riser pipe with 2.44 feet aligned with the seam between the bottom of the riser and the top of the PVC to NPT connector. This will allow for accurate depth determination for the center of the screen. Fold up the first 2+ feet of the tape and secure it to the riser.

Packer deployment:

1. Lower the packer assemble to the desired depth in borehole. When adding additional riser sections, use a well pipe clamp to secure the assembly. Also ensure the safety line is taut before disconnecting the lifting cap. Use electrical tape to secure the measuring tape and a zip tie to secure the air line and measuring tape to the top of each section of riser.

2. Once at the proper depth, use the clamp and safety line to secure the assembly before removing the lifting cap. Use an electric tape to measure the water level inside the riser. Subtract the height of the PVC riser above the reference point (i.e. top of steel casing) to have a consistent water level measurement.

3. Calculate required pressure for inflation of the packers (see above) using the difference between the depth to water from top of casing and the packer depth. Multiply this depth by 0.43 PSI/ft and then add 30 PSI.

4. Insert a levelogger connected to real time cable into the riser until it is approx. 10 feet below water level. Use electrical tape to secure the cable to the riser to prevent movement. Record this depth and also log the data on the laptop using the real time data feature and/or internal logger data collection. It is recommended to record data at one second intervals.

5. Inflate the packer assembly with compressed nitrogen. Ensure the pressure does not exceed the calculated value to avoid damaging the packers. Use the levelogger real time data display to determine when the head in the packed interval has reached equilibrium. Use the electric tape to record the water level.

6. Conduct slug testing once the head reaches equilibrium. Ensure the slug is fully submerged and be aware that riser height above the datum will vary at different depths, which will require new calculations and measurements for rope length. Save slug testing data to a file.

7. Conduct well sampling. If using the Grundfos pump, the levelogger will have to be removed because the pump is too large to accommodate the real time data cable. The pump can be lowered to the top of the packer assembly but the air lines that run inside the packer bypass prevent the pump from being lowered to the level of the well screen.

8. Deflate the packer by closing off the regulator and opening the bleed valve. Ensure the line pressure is at zero PSI.

9. Attach the lifting cap, remove the clamp, double check that the packer is deflated, and move the assembly to the next depth.

Appendix C: Pumping test data

The MW-C borehole was pumped for approximately 20 hours at 95 liters per minute from 26-27 May 2011 to assess aquifer properties at the Unit Well 7 site. The borehole was open over the entire saturated thickness of the upper aquifer. The shallow and intermediate monitoring wells (MW-A and MW-B respectively) were used as observation wells. It is important to note that water from the pumping was discharged into a nearby ditch; some ponding occurred and likely resulted in recharge to the aquifer. This is evident in the data as drawdown values either remained constant or decreased at late times. The observation wells were only a few meters from the pumping well, with the shallow well screened in the low permeability Tunnel City Group and the intermediate well screened into a higher permeability and fractured interval at the Tunnel City/Wonewoc contact.

All data were evaluated with AQTESOLV using the Moench (1984) fractured aquifer solution with slab blocks (Accompanying material CD). The system also did not begin at steady state due to the influence of the public supply well pumping. For these reasons, the late data were either not included or not matched closely during the analyses. While the hydraulic conductivity values for fractures (K) and matrix (K') are useful based on this analysis, the specific storage values for fractures (Ss) and matrix (Ss') are not as reliable. The well skin factor (Sw) and fracture skin (Sf) are also provided as part of the analysis.

1. MW-A Observation Data

Pumping Well: MW-C	Aquifer Model: Fractured
Observation Well: MW-A	Solution: Moench with slab blocks
Parameters	
K = 5.2 x 10^{-3} cm/sec	K' = 4.1 x 10^{-5} cm/sec
Ss = 2.9 x 10^{-4} cm^{-1}	Ss' = 1.0 x 10^{-9} cm^{-1}
Sw = .005	Sf = 0.0046
Saturated thickness: 54.25 m	Slab block thickness: 10.67 m

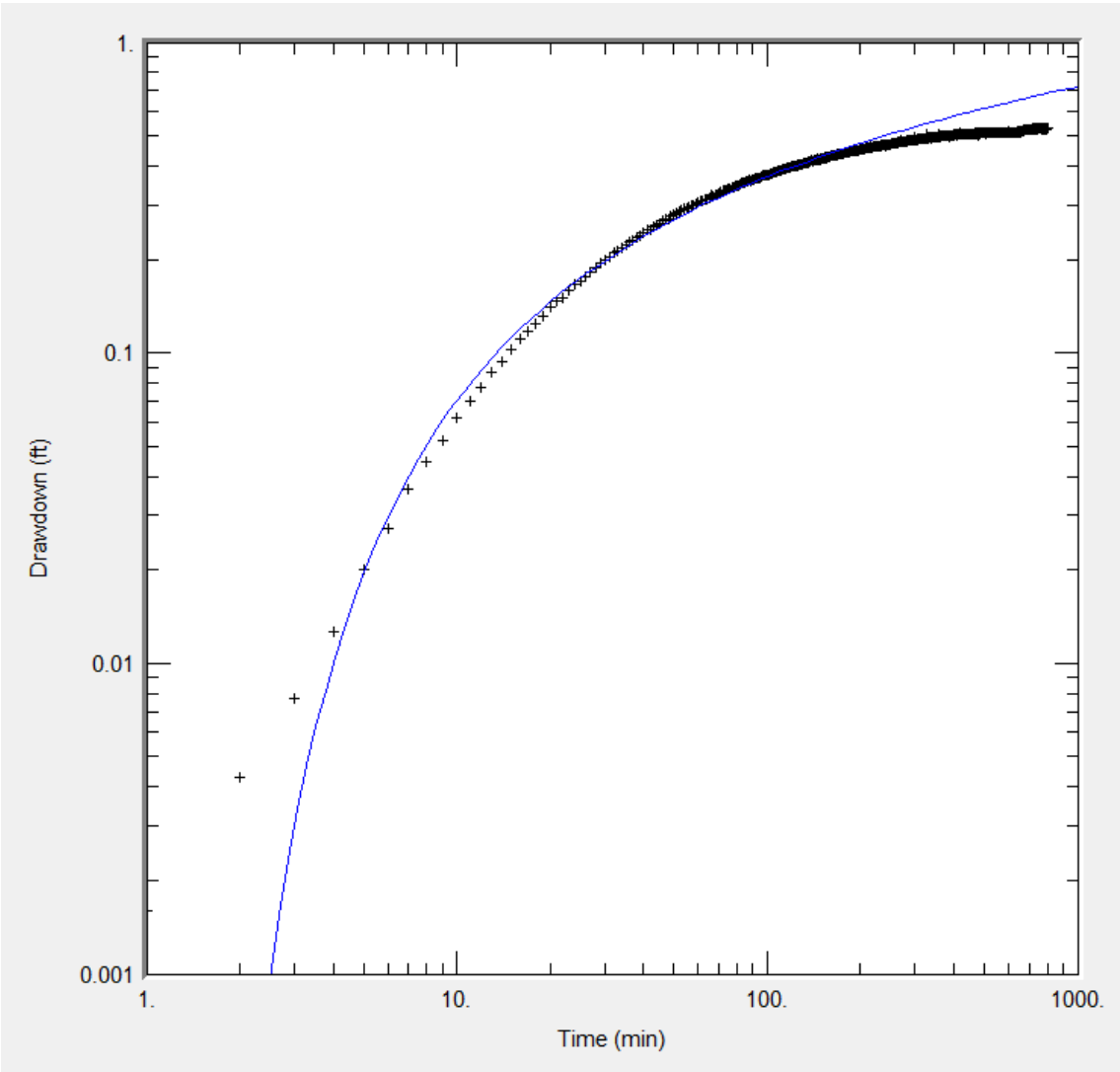

Figure C-1. Curve matching of MW-A pumping test data using AQTESOLV.

MW-A Pumping Test Summary of Observations, 26-27 May 2011

Elasped Time (min)	Drawdown (ft)		Elasped Time (min)	Drawdown (ft)		Elasped Time (min)	Drawdown (ft)		Elasped Time (min)	Drawdown (ft)
1	0.002		20	0.141		48	0.271		200	0.452
2	0.004		21	0.147		50	0.278		220	0.460
3	0.008		22	0.151		55	0.292		240	0.468
4	0.013		23	0.159		60	0.305		260	0.475
5	0.020		24	0.166		65	0.316		280	0.480
6	0.027		25	0.170		70	0.326		300	0.496
7	0.036		26	0.176		75	0.337		320	0.490
8	0.045		27	0.182		80	0.346		340	0.494
9	0.052		28	0.188		85	0.354		360	0.496
10	0.062		29	0.195		90	0.361		380	0.500
11	0.070		30	0.198		95	0.367		400	0.504
12	0.078		32	0.210		100	0.375		450	0.508
13	0.087		34	0.218		110	0.388		500	0.510
14	0.094		36	0.229		120	0.398		550	0.512
15	0.102		38	0.236		130	0.406		600	0.515
16	0.111		40	0.244		140	0.415		650	0.514
17	0.117		42	0.250		150	0.424		700	0.525
18	0.124		44	0.257		160	0.430		800	0.527
19	0.132		46	0.267		180	0.443			

Note: complete data set of observations available on CD included with dissertation.

2. MW-B Observation Data

Pumping Well: MW-C	Aquifer Model: Fractured
Observation Well: MW-B	Solution: Moench with slab blocks
Parameters	
K = 3.6 x 10^{-3} cm/sec	K' = 6.0 x 10^{-5} cm/sec
Ss = 1.1 x 10^{-8} cm^{-1}	Ss' = 3.3 x 10^{-12} cm^{-1}
Sw = 0.05	Sf = 0.05
Saturated thickness: 54.25 m	Slab block thickness: 10.67 m

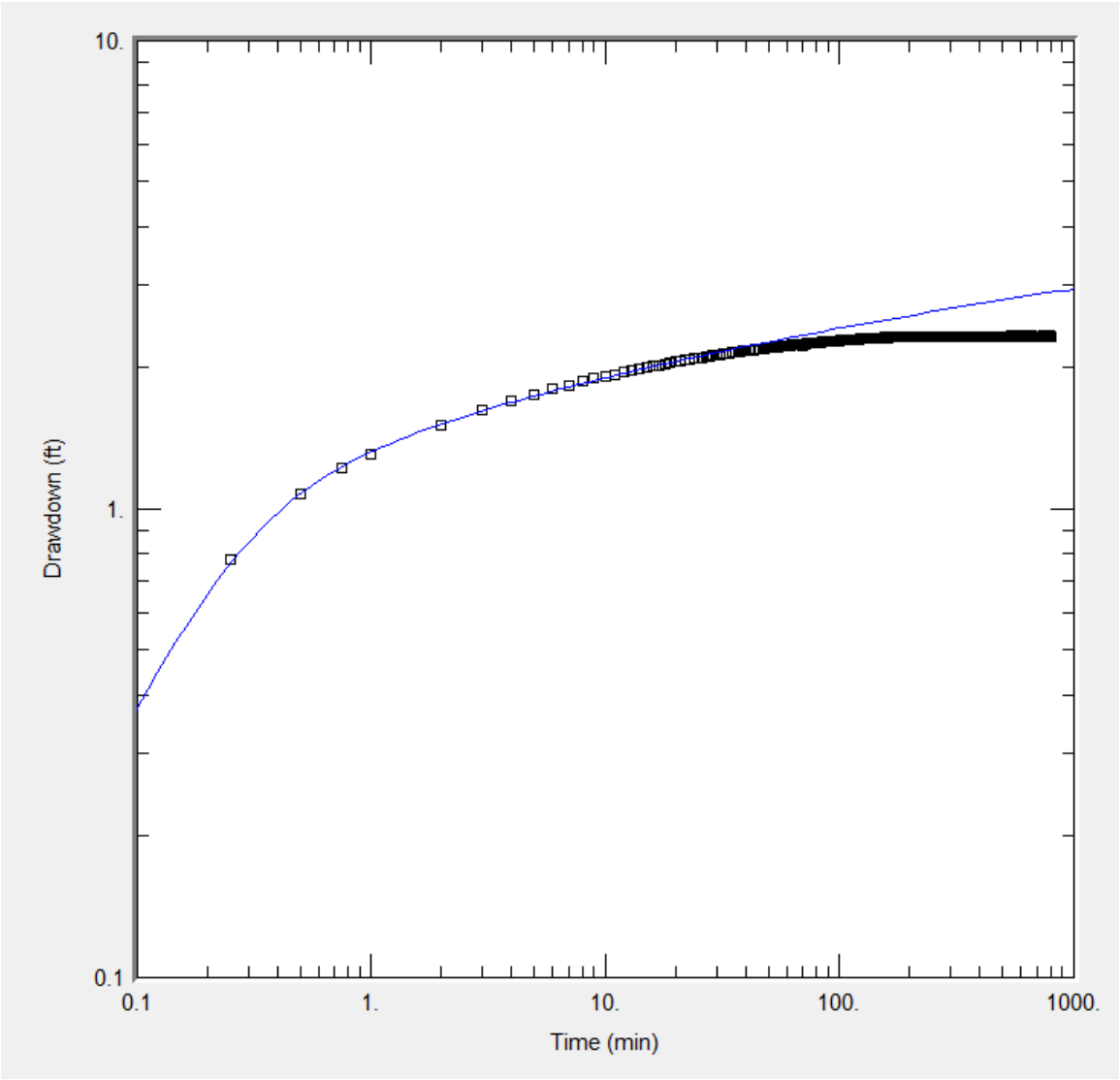

Figure C-2. Curve matching of MW-B pumping test data using AQTESOLV.

MW-B Pumping Test Summary of Observations, 26-27 May 2011

Elasped Time (min)	Drawdown (ft)		Elasped Time (min)	Drawdown (ft)		Elasped Time (min)	Drawdown (ft)		Elasped Time (min)	Drawdown (ft)
0.25	0.78		11	1.93		40	2.17		140	2.31
0.5	1.07		12	1.95		45	2.19		160	2.32
0.75	1.22		13	1.97		50	2.20		180	2.32
1	1.30		14	1.99		55	2.21		200	2.32
2	1.51		15	2.00		60	2.23		220	2.33
3	1.62		16	2.01		65	2.24		250	2.33
4	1.70		17	2.02		70	2.23		300	2.32
5	1.75		18	2.03		75	2.25		350	2.32
6	1.80		19	2.04		80	2.26		400	2.32
7	1.84		20	2.06		90	2.27		450	2.32
8	1.87		25	2.09		100	2.28		500	2.33
9	1.89		30	2.13		110	2.29		600	2.33
10	1.91		35	2.15		120	2.30		700	2.33
						130	2.31		800	2.33

Note: complete data set of observations available on CD included with dissertation.

3. MW-C Observation Data

Pumping Well: MW-C	Aquifer Model: Fractured
Observation Well: MW-C	Solution: Moench with slab blocks
Parameters	
K = 2.9 x 10^{-3} cm/sec	K' = 5.9 x 10^{-4} cm/sec
Ss = 2.2 x 10^{-5} cm^{-1}	Ss' = 3.9 x 10^{-5} cm^{-1}
Sw = 0	Sf = 0.1466
Saturated thickness: 54.25 m	Slab block thickness: 10.67 m

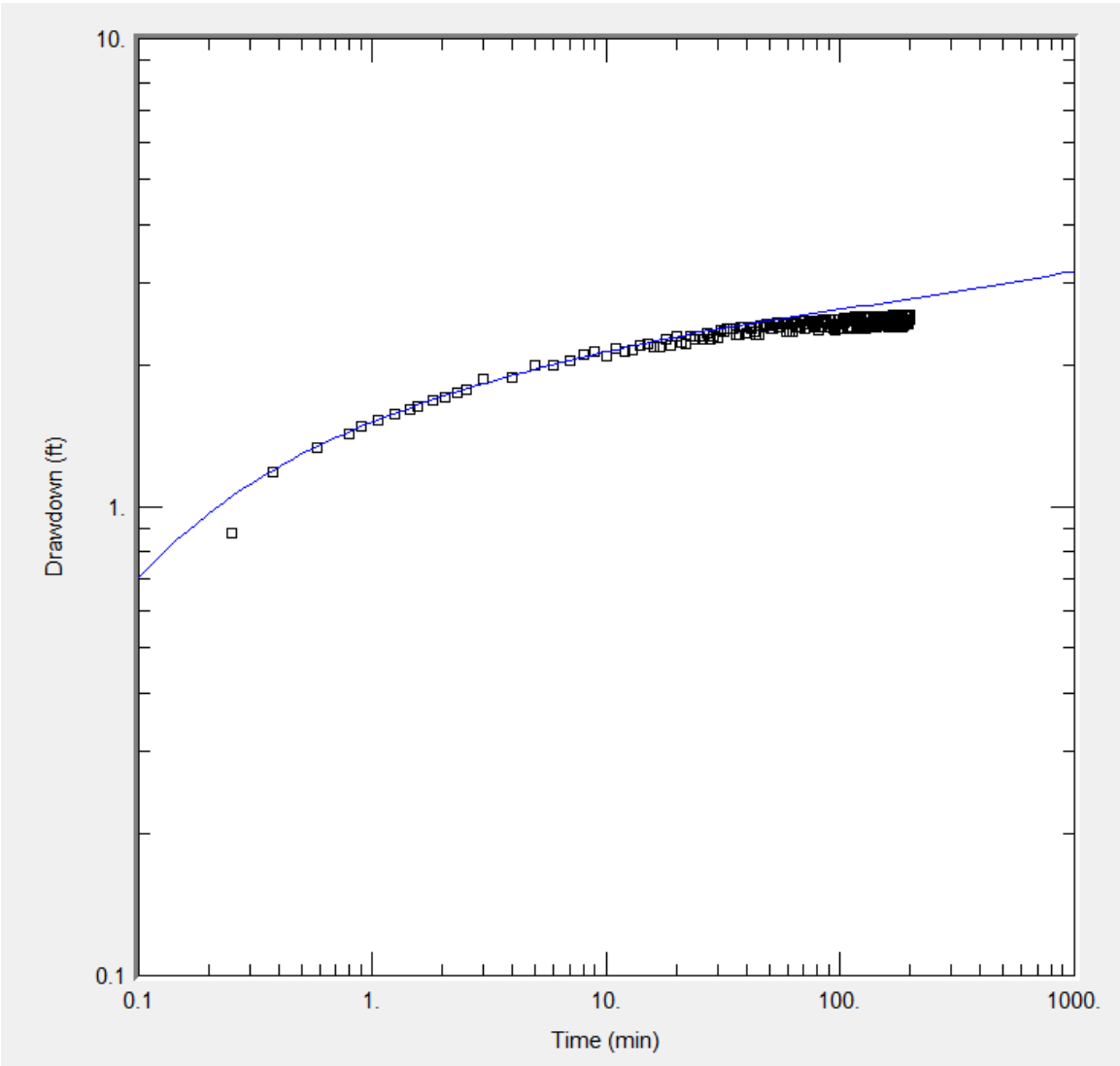

Figure C-3. Curve matching of MW-C pumping test data using AQTESOLV.

MW-C Pumping Test Summary of Observations, 26-27 May 2011

Elapsed Time (min)	Drawdown (ft)		Elapsed Time (min)	Drawdown (ft)		Elapsed Time (min)	Drawdown (ft)		Elapsed Time (min)	Drawdown (ft)
0.25	0.88		3	1.87		16	2.19		90	2.42
0.38	1.18		4	1.88		17	2.20		100	2.39
0.58	1.33		5	2.00		18	2.28		110	2.50
0.8	1.43		6	2.00		19	2.21		120	2.50
0.9	1.48		7	2.05		20	2.30		130	2.42
1.067	1.53		8	2.11		25	2.32		140	2.41
1.25	1.58		9	2.14		30	2.29		150	2.51
1.45	1.61		10	2.10		35	2.39		160	2.42
1.567	1.63		11	2.18		40	2.35		170	2.56
1.83	1.68		12	2.14		50	2.42		180	2.50
2.067	1.71		13	2.16		60	2.47		190	2.51
2.317	1.75		14	2.21		70	2.49		200	2.54
2.55	1.78		15	2.22		80	2.48			

Note: complete data set of observations available on CD included with dissertation.

Appendix D: Groundwater sampling standard operating procedures

There was some variation between the procedures utilized during the 2010/2011 and the 2012 sampling events. Two different types of submersible pumps (Keck and Grundfos) were used in 2010/2011 for monitoring well sampling but during 2012 three Grundfos pumps were used.

Preparation and Decontamination

The day prior to sampling it is important to prepare all equipment and decontaminate the pumps, tubing, and prefilter housings.

1. Use a 50 mg/l chlorine solution for decontamination by filling a clean 20 gallon trash can with tap water and then adding 200 ml of 3% NaOCl household bleach. Use chlorine test strips with a high range to ensure solution is at least 50 mg/l. Place the submersible pumps in the solution and pump until the solution is in contact with all of the pump tubing. The chlorine solution can be recirculated back into the trash can. Submerge any pre-filter housings into the solution. The product of the chlorine concentration (mg/l) and contact time (min) is known as the CT value (mg-min/l). Allow the 50 mg/l chlorine solution to remain in contact with the equipment for at least 10 minutes or until a CT value that will result in 6.0 log inactivation of viruses is achieved. The CT value is reduced by low water temperature or high pH. Example: For a solution with a pH of 7, temperature of 10 deg C, and 50 mg/l free available chlorine a contact time of 8.1 minutes is required to achieved a CT value for 6.0 log reduction of viruses.

2. In order to remove the residual chlorine from equipment, prepare a sodium thiosulfate solution by adding 1 gram of sodium thiosulfate to each liter of deionized (DI)

water. This solution will neutralize up to a 200 mg/l chlorine solution. Fill a tall, narrow container with at least 20 liters of sodium thiosulfate solution. Thoroughly rinse any equipment in this solution and place submersible pumps into a container of the solution and pump it through all of the tubing. More solution may need to be added to the container if the tubing exceeds 100ft in length. Equipment should be rinsed with DI water.

3. If using a Keck pump, charge the deep cycle marine battery overnight so it will have a maximum charge. Bring the battery charger to the field and use it to trickle charge the battery during pumping to prolong the amount of time the pump will operate.

4. Ensure all items from the groundwater sampling packing list are loaded into the vehicle.

5. Call the water utility operator to inform them sampling will take place the following day and to ensure that the deep well will be pumping.

Monitoring Well Sampling

1. Arrive on site and call Water Utility Operator to gain access to well house. Ensure the deep well is pumping. Arrive before 8:30am in order to complete all sampling by 5pm.

2. Open flush mounts for each well, take water level measurements, and remove leveloggers. After virus sampling has started, each levelogger can be downloaded onto a laptop using the optical reader.

3. Prepare a small container of 50 mg/l chlorine solution and another container with 1g/l sodium thiosulfate solution. Decontaminate the outside of the submersible pumps, wiring, and tubing by having one person wipe everything with a rag saturated with chlorine solution. A second person will them wipe everything with a rag saturated with the sodium thiosulfate solution while a third person lowers the pump into the monitoring well.

4. Install a new 10 micron Culligan wound polypropylene sediment cartridge prefilter (from Dorn Hardware) into the housing and remove a glass wool filter from the cooler. Record the serial number and “born on” date from the glass wool filter. Attach a small white sticker label on the glass wool filter with the sample number. Sample numbers include the unit well number, monitoring well name, and sample iteration (for example 7-MW2-04).

5. Set the pump 1 foot above the bottom of the well or 10 feet below water level – whichever is shallower. Run the pump for at least 5-10 minutes (depending on tube length) at 2+ GPM to ensure all sodium thiosulfate solution from the previous day’s decon is flushed out. Take a field measurement of temperature, pH, and conductivity from the discharge hose. Record the number from the AMCO 5/8” totalizer onto the data sheet and calculate the reading required to obtain a 1,000 l (264 gallon) sample. If using the Keck Model SP-81A pump, attach it to the deep cycle marine battery and battery charger. The Grundfos RediFlo-2 pump control box can be plugged into an extension cord running to the well house.

6. Connect the prefilter housing, glass wool filter, and totalizer and ensure that the pumping rate is approximately 1 gallon per minute. If the pH is greater than 7.5, connect an acid pump before the glass wool filter. Use the totalizer and stopwatch to calculate discharge. Take periodic water level measurements in the well to ensure that the water does not drop below the pump or the well does not go dry.

7. When the totalizer indicates 264 gallons has been pumped through the filter (approx. 5 hours for Grundfos and 8 hours for Keck), disconnect the tubing from the prefilter. Use a permanent marker to label sample numbers on separate Ziploc bags for the prefilter and glass wool filter, place the filters in each bag, and keep on ice in a cooler. Fill out the virus sampling sheet with relevant information and note any deviations from the standard procedures.

8. Use the discharge hose to collect a grab sample for University of Minnesota water chemistry analysis. A 1 liter amber glass jar is required if optical brighteners, major ions, metals, and alkalinity are to be analyzed but only a 500 ml HDPE bottle is require for major ions and alkalinity. Take field measurements of temperature, pH, and conductivity from the discharge hose. Attach a sample label to the bottle and complete the Univ. of Minnesota chain of custody form and sample sheet. For any well that is not finished sampling by noon, temporarily disconnect the discharge hose from the filters and collect the water chemistry grab sample.

9. Pack up all of the water chemistry samples in a small cooler. Include ample bubble wrap for padding and double Ziploc bags of ice to keep samples cold. Tape a Ziploc bag containing copies of the sample and chain of custody forms to the inside top of the

cooler. Tape the cooler closed. Coordinate sampling to avoid Friday shipments since the Minnesota lab will not be able to receive samples on the weekend.

10. Once all wells have been sampled, insert the leveloggers and close the flush mounts.

11. Glass wool filters and prefilters must be eluted within 48 hours. The following day either elute filters using the Marshfield lab elution SOP or ship filters to Marshfield via the veterinarian courier service.

Appendix E: Geochemistry data

1. 2010 Geochemistry Data

Name	MW-A	MW-B	UW-7	Sewer
Date	05/13/10	05/13/10	05/13/10	05/11/10
pH	7.37	7.10	7.37	7.00
Conductivity (µS/cm @ 25°C)	1170	2220	664	N/A
Cations (in ppm)				
Ca	104	153	76.2	45.9
Mg	50.4	76.4	43.0	29.4
Na	41.6	175	8.16	96.7
K	0.98	2.68	1.39	16.1
Li	0.0044	0.0074	0.0033	0.0071
Al	<0.005	<0.005	<0.005	0.018
Fe	<0.005	<0.005	<0.005	0.193
Mn	0.054	0.008	0.028	0.020
Sr	0.124	0.215	0.142	0.086
Ba	0.0907	0.102	0.0402	0.0408
Si	14.0	12.5	6.40	6.18
Anions (in ppm)				
Alk. (as $CaCO_3$)	385	392	331	438
Cl	99.0	447	15.2	60.8
Br	0.029	0.209	0.033	0.384
NO_3-N	0.734	6.23	0.027	0.033
NO_2-N	0.003	0.002	0.003	0.016
SO_4	39.3	56.2	40.0	35.5
S_2O_3	<0.006	<0.006	<0.006	<0.006
PO_4-P	0.110	0.185	0.091	5.66
Total P	0.095	0.179	0.064	5.97
F	0.179	0.078	0.094	1.19
Cl/Br (wt)	3,414	2,139	461	158
Charge Balance				
Cations (meq/kg)	11.18	21.61	7.74	9.33
Anions (meq/kg)	11.37	22.06	7.89	11.28
% difference	-0.85	-1.04	-0.96	-9.45

Name	MW-A	MW-B	UW-7	Sewer
Date	05/26/10	05/26/10	05/26/10	05/25/10
pH	7.21	6.91	7.15	6.50
Conductivity (µS/cm @ 25°C)	968	2230	680	1450
Cations (in ppm)				
Ca	103	157	75.6	77.5
Mg	48.9	77.8	42.4	45.6
Na	31.7	180	6.84	250
K	0.95	2.79	1.51	13.8
Li	0.0076	<0.0010	0.0041	0.0123
Al	0.013	<0.005	<0.005	0.016
Fe	<0.005	<0.005	<0.005	0.209
Mn	0.035	0.004	0.028	0.030
Sr	0.164	0.157	0.107	0.115
Ba	0.102	0.121	0.0603	0.0579
Si	14.3	12.7	6.03	6.50
Anions (in ppm)				
Alk. (as $CaCO_3$)	386	390	330	220
Cl	72.2	466	12.4	398
Br	0.025	0.206	0.028	0.061
NO_3-N	0.573	6.26	0.026	0.012
NO_2-N	<0.003	<0.003	<0.003	<0.003
SO_4	40.2	55.6	37.2	41.6
S_2O_3	<0.006	<0.006	<0.006	<0.006
PO_4-P	0.064	0.052	0.018	2.45
Total P	0.080	0.054	0.019	3.41
F	0.201	0.080	0.097	1.09
Cl/Br (wt)	2,888	2,262	3,500	6,525
Charge Balance				
Cations (meq/kg)	10.57	22.14	7.60	18.85
Anions (meq/kg)	10.64	22.55	7.73	16.55
% difference	-0.32	-0.91	-0.83	6.51

Name	MW-A	MW-B	UW-7	Sewer
Date	06/09/10	06/09/10	06/09/10	06/08/10
pH	7.34	7.06	7.48	7.00
Conductivity (µS/cm @ 25°C)	1042	2490	571	1300
Cations (in ppm)				
Ca	108	158	75.4	63.6
Mg	51.5	79.3	42.2	38.5
Na	43.8	198	6.67	227
K	0.83	2.74	1.46	14.9
Li	0.0049	0.0035	<0.0010	0.0070
Al	<0.005	<0.005	0.003	0.014
Fe	0.005	0.011	0.011	0.363
Mn	0.033	0.004	0.029	0.025
Sr	0.093	0.134	0.110	0.129
Ba	0.0923	0.117	0.0598	0.0506
Si	14.5	12.8	6.04	6.10
Anions (in ppm)				
Alk. (as $CaCO_3$)	380	383	319	433
Cl	105	492	12.1	348
Br	0.028	0.222	0.026	0.063
NO_3-N	0.692	6.06	0.023	0.009
NO_2-N	<0.002	<0.002	<0.002	<0.003
SO_4	45.2	54.6	35.4	24.8
S_2O_3	<0.004	<0.004	<0.004	<0.004
PO_4-P	0.043	0.038	0.007	3.32
Total P	0.090	0.045	0.016	4.11
F	0.182	0.082	0.117	1.12
Cl/Br (wt)	3750	2216	2216	5524
Charge Balance				
Cations (meq/kg)	11.56	23.10	7.57	16.60
Anions (meq/kg)	11.56	23.11	7.46	19.05
% difference	0.01	-0.02	0.70	-6.86

Name	MW-A	MW-B	UW-7	Sewer
Date	06/23/10	06/23/10	06/23/10	06/22/10
pH	7.21	6.99	7.38	6.50
Conductivity (µS/cm @ 25°C)	1051	2470	687	1050
Cations (in ppm)				
Ca	111	161	76.3	54.3
Mg	52.5	80.5	42.6	34.0
Na	47.4	201	6.67	144
K	0.82	2.75	1.43	13.5
Li	0.0033	0.0016	<0.0010	0.0051
Al	0.026	0.009	0.015	0.033
Fe	0.017	0.007	0.008	0.184
Mn	0.026	0.003	0.028	0.022
Sr	0.099	0.125	0.108	0.096
Ba	0.0842	0.112	0.0523	0.0790
Si	14.7	12.9	6.05	6.11
Anions (in ppm)				
Alk. (as $CaCO_3$)	386	387	320	416
Cl	105	502	12.2	173
Br	0.030	0.239	0.029	0.054
NO_3-N	0.722	6.11	0.020	<0.002
NO_2-N	<0.002	<0.002	<0.002	0.013
SO_4	52.5	54.9	35.9	30.6
S_2O_3	<0.004	<0.004	<0.004	<0.004
PO_4-P	0.133	0.098	0.089	2.58
Total P	0.107	0.049	0.014	3.73
F	0.193	0.079	0.105	1.10
Cl/Br (wt)	3,500	2,100	421	3,204
Charge Balance				
Cations (meq/kg)	11.95	23.48	7.64	12.12
Anions (meq/kg)	11.83	23.48	7.50	13.89
% difference	0.48	-0.01	0.97	-6.80

Name	MW-A	MW-B	UW-7	Sewer
Date	07/07/10	07/07/10	07/07/10	07/07/10
pH	7.21	6.99	7.38	6.50
Conductivity (µS/cm @ 25°C)	1099	2630	694	1490
Cations (in ppm)				
Ca	112	158	77.8	74.5
Mg	53.8	80.7	44.0	45.0
Na	50.1	204	8.08	182
K	0.83	2.82	1.39	13.0
Li	0.0029	0.0049	<0.0010	0.0112
Al	0.004	0.011	0.015	0.014
Fe	0.002	0.011	0.004	0.164
Mn	0.026	0.002	0.027	0.025
Sr	0.091	0.125	0.094	0.112
Ba	0.0916	0.126	0.0620	0.104
Si	14.6	12.8	6.53	6.51
Alk. (as $CaCO_3$)	386	390	327	431
Cl	119	502	15.7	283
Br	0.032	0.240	0.033	0.084
NO_3-N	0.793	6.11	0.032	0.029
NO_2-N	0.005	<0.002	<0.002	<0.002
SO_4	51.5	54.2	40.1	40.5
S_2O_3	<0.004	<0.004	<0.004	<0.004
PO_4-P	<0.002	<0.002	<0.002	2.18
Total P	0.081	0.053	0.011	3.06
F	0.183	0.083	0.128	1.15
Cl/Br (wt)	3,719	2,092	476	3,369
Charge Balance				
Cations (meq/kg)	12.22	23.48	7.89	15.68
Anions (meq/kg)	12.21	23.53	7.82	17.50
% difference	0.04	-0.10	0.45	-5.51

Name	MW-A	MW-B	UW-7	Sewer
Date	07/21/10	07/21/10	07/21/10	07/21/10
pH	7.36	7.19	7.54	7.00
Conductivity (µS/cm @ 25°C)	1099	2530	672	1230
Cations (in ppm)				
Ca	115	162	76.3	62.7
Mg	55.4	81.1	42.8	38.5
Na	54.6	204	6.95	104
K	0.90	3.02	1.50	14.4
Li	0.0066	0.0064	0.0027	0.0089
Al	0.006	0.004	0.004	0.016
Fe	0.009	0.004	0.008	0.254
Mn	0.023	0.002	0.028	0.025
Sr	0.108	0.152	0.104	0.100
Ba	0.0874	0.119	0.0571	0.0561
Si	14.7	12.9	6.02	6.50
Anions (in ppm)				
Alk. (as $CaCO_3$)	385	389	320	439
Cl	130	518	13.2	111
Br	0.032	0.253	0.024	0.092
NO_3-N	0.806	6.04	0.028	0.028
NO_2-N	<0.003	<0.003	<0.003	<0.003
SO_4	52.7	54.0	36.1	46.5
S_2O_3	<0.006	<0.006	<0.006	<0.006
PO_4-P	0.088	0.065	0.076	0.068
Total P	0.096	0.071	0.009	6.17
F	0.184	0.086	0.112	1.11
Cl/Br (wt)	4,063	2,047	550	1,207
Charge Balance				
Cations (meq/kg)	12.70	23.71	7.67	11.19
Anions (meq/kg)	12.53	23.95	7.53	12.93
% difference	0.69	-0.49	0.95	-7.21

2. 2012 Geochemistry Data

Name	MW-A	MW-B	MW-C	UW-7	WWTP
Date	4-Jan-12	4-Jan-12	4-Jan-12	4-Jan-12	5-Jan-12
pH	7.23	7.12	7.15	7.47	7.00
Conductivity (µS/cm @ 25°C)	1037	2410	1369	693	1850
Cations (in ppm)					
Ca	106	152	114	76.5	78.6
Mg	49.7	77.0	59.3	43.4	43.6
Na	31.4	198	78.5	7.56	236
K	0.99	2.96	3.34	1.29	12.76
Al	0.03	0.013	0.007	0.005	0.012
Fe	0.009	nd	nd	0.313	0.174
Mn	0.008	nd	nd	0.026	0.058
Sr	0.102	0.1177	0.0921	0.0901	0.0951
Ba	0.246	0.099	0.099	0.036	0.231
Si	13.9	13.5	10.7	6.29	7.40
Anions (in ppm)					
Alk. (as $CaCO_3$)	384	387.0	378	322	433
Cl	78.5	480.6	186.0	14.7	376.9
Br	0.015	0.262	0.105	0.029	0.158
NO_3-N	0.880	5.76	5.216	0.048	0.004
NO_2-N	<0.002	<0.002	<0.002	<0.002	<0.002
SO_4	30.1	47.9	41.7	36.0	34.5
PO_4-P	0.020	0.030	0.009	<0.005	1.854
Total P	0.217	0.044	0.015	0.014	2.02
F	0.257	0.078	0.095	0.092	0.775
Acetate	<0.01	<0.01	<0.01	<0.01	0.126
Formate	<0.01	<0.01	<0.01	<0.01	0.034
Oxalate	<0.01	<0.01	<0.01	<0.01	0.124
Charge Balance					
Cations (meq/kg)	10.76	22.59	14.08	7.76	18.12
Anions (meq/kg)	10.58	22.70	14.05	7.61	19.99
% difference	0.82	-0.24	0.12	0.99	-4.92
Cl/Br (wt)	5233	1834	1771	507	2385

Name	MW-A	MW-B	MW-C	UW-7	WWTP
Date	25-Jan-12	25-Jan-12	25-Jan-12	25-Jan-13	26-Jan-12
pH	7.21	7.04	7.19	7.38	7
Conductivity (µS/cm @ 25°C)	1053	2330	1330	684	1610
Cations (in ppm)					
Ca	107	146.4	114	75.1	77.3
Mg	51.0	75.4	58.3	43.2	43.7
Na	37.4	185	76	6.81	285
K	1.12	2.91	3.30	1.41	13.2
Al	0.023	0.025	0.015	0.010	0.014
Fe	0.043	0.012	0.006	0.30	0.22
Mn	0.002	0.001	0.002	0.027	0.049
Sr	0.1028	0.1154	0.0919	0.0920	0.1012
Ba	0.0656	0.0946	0.0986	0.0367	0.1237
Si	13.8	13.5	10.7	6.1	7.4
Anions (in ppm)					
Alk. (as $CaCO_3$)	382	390	379	329	439
Cl	102.1	447	180.0	12.9	449
Br	0.019	0.264	0.099	0.027	0.160
NO_3-N	0.952	5.988	5.252	0.028	0.010
NO_2-N	<0.002	<0.002	<0.002	<0.002	<0.002
SO_4	31.5	47.6	42.3	35.1	36.3
PO_4-P	0.058	0.034	0.010	<0.005	2.27
Total P	0.071	0.04	0.012	0.004	2.39
F	0.287	0.083	0.101	0.093	0.763
Acetate	<0.01	<0.01	<0.01	<0.01	12.900
Formate	<0.01	<0.01	<0.01	<0.01	<0.01
Oxalate	<0.01	<0.01	<0.01	<0.01	0.192
Charge Balance					
Cations (meq/kg)	11.22	21.64	13.88	7.64	20.19
Anions (meq/kg)	11.24	21.84	13.91	7.67	22.18
% difference	-0.08	-0.47	-0.11	-0.23	-4.72
Cl/Br (wt)	5,373	1,694	1,818	478	2,804

Name	MW-A	MW-B	MW-C	UW-7	WWTP
Date	8-Feb-12	8-Feb-12	8-Feb-12	8-Feb-12	9-Feb-12
pH	7.24	7.03	7.20	7.37	7.0
Conductivity (µS/cm @ 25°C)	1047	2340	1284	694	1400
Cations (in ppm)					
Ca	105	147.0	112	75.1	75.1
Mg	51.0	75.9	58.3	43.3	42.3
Na	34.5	181	70.3	6.94	243.2
K	1.61	2.91	3.01	1.36	12.4
Al	0.19	0.14	0.011	0.008	0.016
Fe	0.16	0.036	nd	0.03	0.20
Mn	0.007	nd	0.001	0.027	0.054
Sr	0.1059	0.1159	0.0905	0.0923	0.0950
Ba	0.0668	0.0946	0.0989	0.0361	0.0952
Si	14.4	13.6	10.6	6.08	7.24
Anions (in ppm)					
Alk. (as $CaCO_3$)	364	372	381	324	429
Cl	89.9	450.1	167.7	12.6	383
Br	0.018	0.225	0.087	0.025	0.136
NO_3-N	0.826	5.989	5.172	0.020	0.017
NO_2-N	<0.002	<0.004	<0.002	<0.002	<0.004
SO_4	31.5	48.6	42.2	35.5	35.0
PO_4-P	0.064	0.099	0.020	0.006	2.41
Total P	0.099	0.04	0.004	0.002	2.45
F	0.275	0.085	0.094	0.085	0.772
Acetate	<0.01	0.047	<0.01	<0.01	18.5
Formate	<0.01	<0.02	<0.01	<0.01	<0.02
Oxalate	<0.01	<0.02	<0.01	<0.01	0.045
Charge Balance					
Cations (meq/kg)	10.96	21.52	13.50	7.65	18.12
Anions (meq/kg)	10.54	21.58	13.60	7.56	20.10
% difference	1.96	-0.13	-0.35	0.57	-5.17
Cl/Br (wt)	4,992	2,000	1,928	505	2,816

Name	MW-A	MW-B	MW-C	UW-7	WWTP
Date	22-Feb-12	22-Feb-12	22-Feb-12	22-Feb-12	23-Feb-12
pH	7.31	7.08	7.18	7.38	7.3
Conductivity (µS/cm @ 25°C)	1076	2300	1264	685	1400
Cations (in ppm)					
Ca	107.6	147.9	110.5	75.5	78.9
Mg	51.2	75.5	57.5	43.3	44.5
Na	36.75	179.4	66.17	7.00	251
K	2.13	3.39	3.00	1.30	1.35
Al	0.27	0.021	0.021	0.016	0.029
Fe	0.236	nd	nd	0.283	0.218
Mn	0.009	nd	0.002	0.027	0.095
Sr	0.1058	0.1148	0.0898	0.0920	0.0969
Ba	0.0693	0.0932	0.0966	0.0378	0.0812
Si	14.85	13.23	10.50	6.17	7.51
Anions (in ppm)					
Alk. (as $CaCO_3$)	380	383	373	320	438
Cl	91.2	441.7	156.8	12.9	399
Br	0.020	0.212	0.078	0.025	0.156
NO_3-N	0.919	5.892	4.975	0.030	0.030
NO_2-N	<0.002	0.009	<0.002	<0.002	<0.004
SO_4	32.86	48.91	42.10	35.46	37.96
PO_4-P	0.052	0.027	<0.005	<0.005	2.19
Total P	0.100	0.041	0.027	0.006	2.35
F	0.264	0.072	0.084	0.083	0.814
Acetate	<0.01	<0.02	<0.01	<0.01	10
Formate	<0.01	<0.02	<0.01	<0.01	<0.02
Oxalate	<0.01	<0.02	<0.01	<0.01	0.282
Charge Balance					
Cations (meq/kg)	11.24	21.49	13.20	7.67	18.57
Anions (meq/kg)	10.93	21.56	13.11	7.51	20.81
% difference	1.40	-0.15	0.36	1.04	-5.68
Cl/Br (wt)	4,559	2,084	2,011	518	2,559

Name	MW-A	MW-B	MW-C	UW-7	WWTP
Date	7-Mar-12	7-Mar-12	7-Mar-12	7-Mar-12	8-Mar-12
pH	7.18	7.00	7.15	7.29	7.25
Conductivity (µS/cm @ 25°C)	1102	2290	1244	682	1390
Cations (in ppm)					
Ca	110.5	145.0	110.2	74.4	77.0
Mg	52.5	74.7	57.1	43.2	43.4
Na	41.97	178.3	63.75	6.81	262
K	2.17	3.97	3.02	1.40	13.11
Al	0.013	0.006	0.005	0.003	0.010
Fe	nd	nd	nd	0.289	0.190
Mn	nd	nd	0.003	0.027	0.109
Sr	0.1082	0.1132	0.0883	0.9180	0.9940
Ba	0.1225	0.0897	0.0931	0.0359	0.2556
Si	13.48	12.95	10.31	6.06	7.16
Anions (in ppm)					
Alk. (as $CaCO_3$)	375	379	368	321	420
Cl	109.4	437.5	146.7	12.2	420
Br	0.024	0.209	0.075	0.023	0.114
NO_3-N	1.008	5.734	4.782	0.019	0.061
NO_2-N	<0.002	<0.004	<0.002	<0.002	<0.004
SO_4	34.39	48.10	40.47	33.79	37.60
PO_4-P	0.067	0.037	0.009	0.006	2.30
Total P					
F	0.300	0.082	0.092	0.085	0.854
Acetate	0.10	<0.020	<0.011	<0.011	<0.02
Formate	0.03	<0.020	<0.011	<0.011	<0.020
Oxalate	<0.01	<0.020	<0.011	<0.011	0.293
Charge Balance					
Cations (meq/kg)	11.72	21.25	13.05	7.62	19.19
Anions (meq/kg)	11.37	21.32	12.69	7.46	21.02
% difference	1.51	-0.18	1.40	1.03	-4.56
Cl/Br (wt)	4,557	2,093	1,956	531	3,686

Name	MW-A	MW-B	MW-C	UW-7	WWTP
Date	21-Mar-12	21-Mar-12	21-Mar-12	21-Mar-12	22-Mar-12
pH	7.12	7.04	7.12	7.33	7.25
Conductivity (µS/cm @ 25°C)	1114	2290	1224	699	1450
Cations (in ppm)					
Ca	109.9	144.3	110.1	75.3	79.1
Mg	52.9	74.0	56.8	43.5	44.1
Na	43.02	177.9	61.60	6.66	237
K	2.32	4.07	2.95	1.35	13.07
Al	0.023	0.005	0.024	0.011	0.020
Fe	0.018	0.001	nd	0.270	0.233
Mn	0.001	0.001	0.003	0.027	0.119
Sr	0.1128	0.1126	0.0877	0.0915	0.1003
Ba	0.0755	0.0894	0.0927	0.0357	0.1503
Si	13.32	12.81	10.17	5.97	7.27
Anions (in ppm)					
Alk. (as $CaCO_3$)	361	369	367	314	413
Cl	113.3	431.6	140.8	12.5	381
Br	0.031	0.206	0.074	0.025	0.383
NO_3-N	1.024	5.636	4.725	0.012	0.050
NO_2-N	<0.002	<0.004	<0.002	<0.002	<0.004
SO_4	35.36	49.00	40.62	34.97	39.79
PO_4-P	0.057	0.034	0.011	<0.006	2.05
Total P	0.059	0.033	0.004	0.003	2.11
F	0.294	0.079	0.088	0.083	0.874
Acetate	<0.011	<0.020	<0.011	<0.011	<0.02
Formate	<0.011	<0.020	<0.011	<0.011	0.174
Oxalate	<0.011	<0.020	<0.011	<0.011	0.112
Charge Balance					
Cations (meq/kg)	11.77	21.13	12.93	7.66	18.22
Anions (meq/kg)	11.23	20.97	12.49	7.36	19.85
% difference	2.37	0.38	1.73	1.99	-4.27
Cl/Br (wt)	3,656	2,095	1,903	500	995

Name	MW-A	MW-B	MW-C	UW-7	WWTP
Date	4-Apr-12	4-Apr-12	4-Apr-12	4-Apr-12	5-Apr-12
pH	7.18	7.00	7.15	7.28	7.25
Conductivity (µS/cm @ 25°C)	1077	2250	1194	673	1400
Cations (in ppm)					
Ca	108.7	143.8	108.7	74.7	80.0
Mg	52.3	74.0	56.0	43.0	43.9
Na	42.92	176.4	59.38	6.37	253
K	2.90	4.02	2.78	1.34	13.01
Al	0.008	0.010	0.003	0.001	0.011
Fe	nd	nd	nd	0.284	0.231
Mn	nd	nd	0.003	0.026	0.124
Sr	0.112	0.116	0.090	0.096	0.105
Ba	0.0745	0.0902	0.0920	0.0372	0.2141
Si	13.40	12.94	10.21	6.05	7.49
Anions (in ppm)					
Alk. (as $CaCO_3$)	363	365	362	309	406
Cl	110.5	428.0	134.7	12.0	401.6
Br	0.029	0.206	0.071	0.024	0.101
NO_3-N	0.951	5.611	4.620	0.019	0.055
NO_2-N	<0.002	<0.004	<0.002	<0.002	<0.004
SO_4	34.68	47.46	40.51	34.01	38.55
PO_4-P	0.055	0.029	<0.006	<0.006	1.95
Total P	0.069	0.041	0.009	0.007	2.35
F	0.273	0.078	0.087	0.082	0.823
Acetate	<0.011	<0.020	<0.011	<0.011	<0.020
Formate	<0.011	<0.020	<0.011	<0.011	<0.020
Oxalate	<0.011	<0.020	<0.011	<0.011	0.228
Charge Balance					
Cations (meq/kg)	11.67	21.04	12.70	7.58	18.92
Anions (meq/kg)	11.17	20.75	12.20	7.22	20.26
% difference	2.20	0.69	2.00	2.46	-3.40
Cl/Br (wt)	3,812	2,078	1,897	502	3,976

Name	MW-A	MW-B	MW-C	UW-7	WWTP
Date	18-Apr-12	18-Apr-12	18-Apr-12	18-Apr-12	19-Apr-12
pH	7.22	7.07	7.18	7.35	7.0
Conductivity (µS/cm @ 25°C)	1080	2270	1169	674	1475
Cations (in ppm)					
Ca	111.1	144.9	109.7	75.1	78.7
Mg	53.1	73.3	55.8	42.7	43.3
Na	44.14	175.7	57.68	6.42	235
K	3.00	3.97	2.87	1.44	13.79
Al	0.015	0.013	0.016	0.014	0.029
Fe	0.010	0.005	0.006	0.204	0.287
Mn	0.001	0.001	0.005	0.028	0.110
Sr	0.112	0.114	0.086	0.093	0.099
Ba	0.0747	0.0886	0.0886	0.0345	0.3302
Si	13.40	13.01	10.21	6.04	7.48
Anions (in ppm)					
Alk. (as $CaCO_3$)	374	380	372	317	428
Cl	116.2	430.0	131.1	11.7	379.6
Br	0.030	0.205	0.070	0.021	0.154
NO_3-N	1.013	5.582	4.610	0.014	0.057
NO_2-N	<0.002	<0.004	<0.002	<0.002	<0.004
SO_4	35.34	47.53	40.14	33.44	38.74
PO_4-P	0.053	0.033	0.013	0.009	2.50
Total P	0.060	0.035	0.007	<0.001	2.65
F	0.276	0.057	0.075	0.070	0.798
Acetate	<0.011	<0.020	<0.011	<0.011	14.8
Formate	<0.011	<0.020	<0.011	<0.011	0.239
Oxalate	<0.011	<0.020	<0.011	<0.011	0.094
Charge Balance					
Cations (meq/kg)	11.91	21.02	12.65	7.58	18.06
Anions (meq/kg)	11.56	21.11	12.29	7.37	20.07
% difference	1.51	-0.22	1.45	1.39	-5.26
Cl/Br (wt)	3,874	2,098	1,873	559	2,465

Name	MW-A	MW-B	MW-C	UW-7	WWTP
Date	2-May-12	2-May-12	2-May-12	2-May-12	3-May-12
pH	7.15	7.02	7.13	7.31	7.0
Conductivity (µS/cm @ 25°C)	1090	2260	1198	702	1325
Cations (in ppm)					
Ca	110.0	144.9	108.1	75.2	77.7
Mg	52.3	74.7	55.8	43.3	43.4
Na	44.57	175.5	55.00	6.54	238
K	3.66	3.75	2.85	1.45	12.69
Al	0.003	nd	nd	nd	0.009
Fe	nd	nd	nd	0.261	0.194
Mn	nd	nd	0.003	0.026	0.092
Sr	0.107	0.112	0.083	0.091	0.095
Ba	0.0761	0.0882	0.0890	0.0372	0.0602
Si	13.43	12.92	10.14	6.07	7.39
Anions (in ppm)					
Alk. (as $CaCO_3$)	375	378	372	324	427
Cl	116.3	426.7	125.4	12.1	377.5
Br	0.027	0.190	0.063	0.023	0.139
NO_3-N	0.947	5.524	4.582	0.012	0.048
NO_2-N	<0.002	<0.004	<0.002	<0.002	<0.004
SO_4	34.63	46.68	39.99	34.26	37.56
PO_4-P	0.065	0.043	0.011	<0.006	2.15
Total P	0.067	0.036	0.007	0.004	2.49
F	0.277	0.070	0.083	0.078	0.810
Acetate	<0.011	<0.020	<0.011	<0.011	<0.020
Formate	<0.011	<0.020	<0.011	<0.011	<0.020
Oxalate	<0.011	<0.020	<0.011	<0.011	0.166
Charge Balance					
Cations (meq/kg)	11.83	21.11	12.45	7.64	18.13
Anions (meq/kg)	11.56	20.96	12.13	7.52	19.97
% difference	1.17	0.35	1.31	0.79	-4.84
Cl/Br (wt)	4,307	2,246	1,991	525	2,715

Name	MW-A	MW-B	MW-C	WWTP
Date	16-May-12	16-May-12	16-May-12	17-May-12
pH	7.13	7.02	7.17	7.0
Conductivity (µS/cm @ 25°C)	1133	2250	1174	1350
Cations (in ppm)				
Ca	108.8	142.9	107.9	80.0
Mg	52.0	73.4	55.9	44.6
Na	44.78	170.3	53.80	230
K	4.12	3.91	2.75	13.37
Al	0.003	0.005	nd	0.025
Fe	nd	nd	nd	0.235
Mn	nd	nd	0.004	0.132
Sr	0.111	0.118	0.089	0.104
Ba	0.0772	0.0892	0.0888	0.0863
Si	13.53	12.95	10.10	7.53
Anions (in ppm)				
Alk. (as $CaCO_3$)	361	364	358	415
Cl	115.1	428.8	123.4	377.2
Br	0.027	0.195	0.065	0.013
NO_3-N	0.904	5.445	4.521	0.044
NO_2-N	<0.002	<0.004	<0.002	<0.004
SO_4	33.97	46.44	39.97	40.83
PO_4-P	0.077	0.056	0.014	2.23
Total P	0.069	0.039	0.009	2.44
F	0.280	0.077	0.084	0.813
Acetate	<0.011	<0.020	<0.011	<0.020
Formate	<0.011	<0.020	<0.011	<0.020
Oxalate	<0.011	<0.020	<0.011	0.135
Charge Balance				
Cations (meq/kg)	11.77	20.69	12.39	18.01
Anions (meq/kg)	11.23	20.73	11.78	19.78
% difference	2.33	-0.10	2.54	-4.68
Cl/Br (wt)	4,263	2,199	1,898	29,012